Transactions of the I·R·E

Professional Group on Antennas and Propagation

VOLUME AP-2 NUMBER 2 APRIL 1954

Published Quarterly

The Institute of Radio Engineers

TRANSACTIONS OF THE I•R•E® PGAP IS A QUARTERLY PUBLICATION DEVOTED TO EXPERIMENTAL AND THEORETICAL PAPERS ON ANTENNAS AND WIRELESS PROPAGATION OF ELECTROMAGNETIC WAVES

MANUSCRIPTS should be submitted to John B. Smyth, Editor, U. S. Navy Electronics Laboratory, San Diego, California. Manuscripts should be original typewritten copy, double spaced, plus one carbon copy. References should appear as footnotes and include author's name, title, journal, volume, initial and final page numbers, and date. Each paper must have an abstract of not more than 200 words. News items concerning PGAP members and group activities should be sent to the News Editor, Mr. H. A. Finke, Polytechnic Research and Development Company, 55 Johnson Street, Brooklyn, New York.

ILLUSTRATIONS should be submitted as follows: All line drawings (graphs, charts, block diagrams, cutaways, etc.) should be inked uniformly and ready for reproduction. If commercially printed grids are used in graph drawings, author should be sure printer's ink is of a color that will reproduce. All half-tone illustrations (photographs, wash, airbrush, or pencil renderings, etc.) should be clean and ready to reproduce. Photographs should be glossy prints. Call-outs or labels should be marked on a registered tissue overlay, not on the illustration itself. No illustration should be larger than 8 x 10 inches.

Copies can be purchased from

THE INSTITUTE OF RADIO ENGINEERS

1 East 79 St., New York 21, N.Y.

PRICE PER COPY: members of the Professional Group on Antennas and Propagation $2.00; members of the IRE $3.00; nonmembers $6.00.

Application has been made for second class entry, at the post office at Menasha, Wisconsin, under the act of March 3, 1879. Acceptance for mailing at a special rate of postage is provided for in the act of February 28, 1925, embodied in Paragraph 4, Section 412, P. L. & R., authorized October 26, 1927.

Why Transactions?

ERNST WEBER
Microwave Research Institute, Brooklyn, N. Y.

With the growth of professional organizations, the publications program becomes inevitably a serious problem. IRE has been no exception in this respect and publication policies have been the center of many subjective and objective discussions. Subjectively, each member would like to see the main organ of IRE carry important news and readable articles covering fully his own particular field of interest. Objectively, the Editorial Department has endeavored to satisfy the necessarily widely divergent individual desires while also trying to maintain the very high standard of papers within rigidly confining space limits. It should be obvious that any ideal solution is unattainable through the PROCEEDINGS alone.

With the initiation of the professional group system, a solution of the difficult publication problem appears to be at hand in a most natural manner. Each professional group may publish in its transactions almost at a moment's notice any paper or group of papers of interest to its circles, without long formal reviews, painful surgeries, and unhappy feelings of authors. Moreover, transactions are destined to become the repository for outstanding papers in the particular field of each professional group, contributing collected papers on specific subject matter! Surely, it is now the responsibility of the professional groups to maintain the standard of the papers by effective use of their own editorial prerogatives. What was manifestly an impossible task for the PROCEEDINGS has become possible by delegation to 22 professional groups; a full, efficient, rapid, up-to-date reporting of scientific and technological developments to each interested sector of the IRE membership!

There might be a feeling on the part of some authors that the circulation of his contribution might be restricted by publication in the TRANSACTIONS as compared with publication in the PROCEEDINGS. This is not justified on at least two counts: unless the contribution is of such wide membership interest that it warrants full distribution to all members, it will not be published at all in the PROCEEDINGS; and the PROCEEDINGS will carry abstracts of all TRANSACTIONS papers and, in addition, will include their authors and titles in the annual TRANSACTIONS index. Actually, therefore, the TRANSACTIONS will constitute specialized "sections" of the over-all Institute publications and thus rank with the PROCEEDINGS from the professional point of view. Indeed, the PROCEEDINGS will now be able to concentrate upon a single objective, namely to publish matters of wide interest, and preferably of interest to most members of IRE.

Just what the division of subject matter between the PROCEEDINGS and between the TRANSACTIONS of the Professional Groups might be, whether, indeed, a clear-cut division should be made, is yet an open question. Much will depend upon the use that Professional Groups will make of this unparalleled opportunity for self-expression. One possibility might be that the PROCEEDINGS include tutorial, informational, and basic scientific papers of high quality and of fundamental interest to a large majority of IRE members, granting the authors ample space for the full development of their ideas and thus making the papers valuable and lasting reference material. Most of the more specialized technical papers would then go automatically to the TRANSACTIONS which might, of course, also carry news of plans and activities of the particular Professional Group and its chapters.

Surely a publication policy which can achieve satisfaction of the unifying membership interests in the PROCEEDINGS and of the divergent membership interests in the TRANSACTIONS of the Professional Groups is as close to an ideal solution of the intricate publication problem as we should hope for. Its success must, of course, depend upon the wholehearted support of each and every member of IRE and particularly upon the hard work of the laboring authors and of the editorial staffs. "By their deeds ye shall know them" . . . I feel sure the proper deeds will be forthcoming in the interest of the members, who after all constitute IRE, no more and no less.

news and views

The Much Abused "Decibel"

DISCUSSION revolving around the terms "decilog" and "logit" has been going on for some time, and seems to be coming to a head. Despite the efforts of some stalwart purists, engineers have persistently used the "decibel" loosely, thereby causing painful errors.

E. I. Green, Chairman of the American Standards Association subcommittee concerned with communication terms, has proposed a new unit for logarithmic ratios to replace the overworked decibel. His thinking on this problem is incorporated in the ensuing article of his writing.

A New Unit for Logarithmic Ratios

The use of a simple logarithmic unit based on power ratio for the distortionless measurement of telephone transmission was first proposed by R. V. L. Hartley. Such a unit, with the name of "transmission unit," was adopted in 1924 by the Bell System in place of the previous " mile of standard cable." Four years later the International Advisory Committee on Long Distance Telephony in Europe adopted the "bel" and the "neper" as alternative units for transmission measurement and the transmission unit was rechristened the "decibel." While the bel was the unit officially selected, the decibel has proved so much more convenient in size that the bel is now all but forgotten. The definition of the decibel is simple, the number of decibels corresponding to the ratio of any two powers P_1 and P_2 being equal to $10 \log_{10} P_1/P_2$.

Through the years the decibel has found wide utility in communication and allied fields. The logarithmic expression is handy because it saves explanatory words and because for large ratios it requires a minimum of figures. It is simpler to say that two powers differ by 50 db than either to say that they bear a ratio of 100,000 to 1, or to employ the exponential expression that one is 10^5 times the other. More important than this, it is far easier to add and subtract db's than to multiply or divide the corresponding ratios.

So useful has the db proved that scientists have been lured into extending its meaning, in some instances with a degree of reason, but in others improperly, in ways not conforming to the original definition. It was rather natural to extend the decibel to quantities related to power, for example, voltage squared or current squared. Thus the number of decibels corresponding to a scaler current ratio I_1/I_2 or a scaler voltage ratio V_1/V_2 was taken as $20 \log_{10} V_1/V_2$, respectively. Initially the db was applied to voltage or current ratios only in cases where these ratios were the square roots of the corresponding power ratios, but it was gradually extended to voltage and current ratios where this was not the case, a practice which has received the sanction of defining bodies, provided specific statement of conditions is given. The decibel has also been extended, with approval of defining bodies, to ratios of sound intensity (using $10 \times \log_{10}$) and ratios of sound pressure and sound particle velocity (using $20 \times \log_{10}$).

While even this extension of usage tended to introduce a certain amount of confusion, the confusion has in recent years become more confounded as engineers have discovered that a logarithmic unit is convenient for expressing ratios of quantities entirely unrelated to power, and in default of an accepted unit for this purpose have pirated the db. A number of people are beginning to use the db as a yardstick for ratios of values of length, or size, or frequency, or ohms, or permeability, or dollars, or whatnot. Usually they ignore the basic difficulty which arises from the fact that db's are equal to 10 times the logarithm of the ratio when applied to powers and 20 times the logarithm of the ratio when applied to voltages or current. Hence in using the db for other kinds of ratios, some people have made it always equal to 10 times the logarithm, some 20 times, and some have used either 10 or 20 times according to whatever similarity they found or fancied to exist between the quantity under consideration and either power or voltage.

This extension of the db to magnitude ratios of any kind has been a matter of growing concern to defining bodies and others. Vigilance and deprecation, however, have only partially arrested the trend. To illustrate the

chaotic state of affairs which now exists, the writer, as Chairman of the ASA C42 Subcommittee on Definitions of Communication Terms, has been bombarded with letters divided about equally between pleas for extension of the db to new kinds of ratios and pleas for strict limitation of its meaning. Like any group of lexicographers, the subcommittee has tried neither to walk too far ahead of usage nor to lag too far behind. It is apparent, however, that a more positive approach is needed.

There have been several proposals for taking care of this situation. M. W. Baldwin, Jr. and R. E. Graham, in an unpublished memorandum dated March 24, 1947, suggested that the name "decilu" (derived from decilogarithmic unit), with abbreviation dl, be employed to express the ratio between two values of any quantity, the number of decilus being equal to 10 times the common logarithm of the ratio. While many persons subscribed in principle to this proposal, the decilu has not caught on. Subsequently J. W. Horton, in an excellent treatment of this problem suggested that the name "logit" (an abbreviation of logarithmic unit) be used in the same way, i.e. the number of logits being equal to 10 times the logarithm of the ratio of two magnitudes of any quantity. The suggested abbreviation for the logit was "lgt." Despite the fact that this proposal received strong encouragement from the Standards Committee of the I.R.E., the name logit has not taken hold. Others have proposed that the "brigg" be defined as equal to the common logarithm of any magnitude ratio, with the "decibrigg" equal to 10 times the common logarithm of the ratio. Still others have suggested that the name "decade" be employed in the same sense as proposed above for brigg. These latter proposals have met the same fate as their predecessors. The best available terminology today would seem to be the rather cumbersome and imprecise expression that two values which bear a ratio of about 10 to 1 differ by an order of magnitude.

There seems to be rather widespread agreement that a new logarithmic unit for expressing the ratio of two values of any kind of quantity is needed. Many people would agree, too, that the preferred magnitude for the new unit is $10^{0.1}$ or, in other words, that the number of units should equal 10 times the common logarithm of the ratio. Why then have none of the proposals to date gained currency? The answer seems to be that defining bodies are reluctant to accept a new term until it has achieved fairly general usage, while in the case of anything as fundamental as a unit of measurement, most people want the stamp of authority before accepting something new. The solution obviously lies in the same procedure which has been used in the past for many kinds of units, namely, official authentication by national and preferably international authorities as a warrant for general use. While defining bodies are usually best advised to let usage develop naturally, new units are an important exception since early standardizing action can prevent imprecise and inconsistent usage.

It seems clear, then, that a new unit is needed to represent the ratio of two values of any quantity. The size of the unit should be $10^{0.1}$, which is to say that the number of units should equal 10 times the common logarithm of the ratio. There remains the choice of a name for the new unit. The name "logit," which has enjoyed the greatest publicity, is open to certain objections. If pronounced with a hard *g* it is not euphonious, nor is it etymologically correct since logit logically should have a soft *g*. In addition, the proposed three-letter abbreviation "lgt" is less desirable for both spoken and written use than a two-letter abbreviation analogous to db. The name "decilu" is good but the abbreviation "dl" is awkward since the same symbol on the typwriter denotes a lower case letter l and the numeral 1. Brigg would bring with it the decibrigg, together with its abbreviation "db" which is untenable because the same abbreviation stands for decibel. Decade, which is inconsistent with the present accepted usage of this word, would be a most unfortunate choice.

In view of the nonacceptance of names thus far proposed, it seems better to try a new one. The name should be reasonably euphonious and should lend itself to a simple and unmistakable two-letter abbreviation. Search of various possibilities leads to the suggestion of the name "decilog" (meaning one tenth of the logarithm) and the abbreviation "dg."[1] The similarity of the name and the abbreviation to decibel and db, respectively, should facilitate understanding and acceptance. The use of the initial and final letters to form an abbreviation is analogous to stock ticker practice where SY stands for Sperry Corporation, AN for Air Reduction Co., and so forth. The theoretical and practical considerations which have been so ably advanced by J. W. Horton in his article on the use of relative magnitudes are all applicable to this proposed new unit.

Closely related to the matter of a logarithmic unit for expressing magnitude ratios is the need for a logarithmic way of expressing the ratio of a magnitude to some standard magnitude of the same quantity, or in other words, expressing the level of a quantity with respect to some reference level. In the case of the decibel certain abbreviations have become current for this purpose. Thus dbm expresses the power level in decibels referred to 1 milliwatt and dbw the power level in decibels referred to 1 watt. While such abbreviations are convenient, the application of the new term "decilog" to many different quantities will make it difficult to find suitable abbreviations. It is proposed, therefore, that levels be designated by writing the reference level in parentheses immediately after the abbreviation dg. Thus 40 db (1 gauss) would signify a level of magnetic flux density 40 dg above 1 gauss, i.e. 10,000 gausses.

In summary, it is proposed to request the approval of standardizing bodies for the definition of a new term as follows:

[1] Since writing the above, the writer has learned that A. G. Fox in 1951 proposed the same unit, to be named "decilog" with abbreviation "dl." This coincidence suggests that the name is a happy choice.

DECILOG (dg)

The decilog, abbreviated dg, is a dimensionless unit for expressing the ratio of two values of any quantity, the number of decilogs being 10 times the logarithm to base 10 of the ratio.

The magnitude or level of a quantity may be stated in dg, expressing the ratio to a reference value. Thus N dg (1 gauss) signifies a level of magnetic flux density N dg above 1 gauss.

PGAP

As of December 31, 1953 there were 1,219 paid members of the Group. After a canvass, all unpaid members have been removed from the enrollment list.

Welcome to our newest chapter: Albuquerque—Los Alamos! R. B. Jacques is Chairman.

Local Chapters

The Chicago Section of the PGAP, under the general Chairmanship of G. P. Kearse and Papers Chairman L. Krahe, have had an active year of meetings. The following meeting and talks have been held in the past months:

Oct. 16, 1953—"Graphical Integration of Patterns for Antenna Gain Measurements," by Dr. R. R. H. Yang, Andrew Corporation.

Dr. Yang discussed the basic theory involved in determining antenna gain by pattern integration methods. The mathematical formulas were derived and used in the construction of a special type of graph paper. Dr. Yang described the method of using this paper to eliminate many of the mathematical computations involved. A question and answer period followed.

Nov. 20, 1953—"UHF TV Receiving, Antenna Measuring Techniques," by Dr. R. M. Soria, American Phenolic Corporation.

Dr. Soria presented a slide film showing propagation characteristics of vhf and uhf TV signals and comparing the performance characteristics of standard vhf and uhf TV receiving antennas. The film was followed by a brief description of vhf and uhf test equipment and measuring techniques. A question and answer period followed.

Dec. 18, 1953—(Joint Meeting with Microwave Theory and Technique Group)—"Waveguide Coupled Circuits," by Mr. Tore N. Anderson, Airtron, Inc.

Mr. Anderson covered the theoretical and experimental aspects of all basic types of directional couplers including the Bethe Hole Couplers, Moreno Couplers, Crossed Guide Couplers, and Multi-Hole Couplers. Mr. Anderson explained the limitations, uses, relative advantages, and gave demonstrations of each type.

March 19, 1954—"UHF TV Propagation Problems," by Mr. H. N. Frihart, Motorola.

Meetings

The Los Angeles Chapter of the PGAP is organizing three sessions of technical papers on antennas and propagation at the August 1954 Western Electronics Convention in Los Angeles.

Our Professional Group is sponsoring a Spring Technical Meeting jointly with the USA National Committee of the International Scientific Radio Union (URSI). This meeting will be held at the National Bureau of Standards, Washington, D. C. on May 3, 4, 5, and 6, 1954.

A meeting of the USA National Committee and meetings of participating commissions will be held on Monday, May 3. The technical sessions will be held on Tuesday, Wednesday, and Thursday, May 4, 5, and 6.

The participating Commissions and their chairmen are:

Commission 1: Radio Measurement Methods and Standards
Chairman: Dr. Rufus G. Fellers,
Bldg. 3, PH, Radio 1,
Naval Research Laboratory,
Washington 20, D. C.

Commission 2: Tropospheric Radio Propagation
Chairman: Dr. Henry G. Booker,
School of Electrical Engineering,
Cornell University
Ithaca, N. Y.

Commission 3: Ionospheric Radio Propagation
Chairman: Dr. L. V. Berkner,
Associated Universities, Inc., Room 6920,
350 Fifth Ave.,
New York 1, N. Y.

Commission 4: Torrestrial Radio Noise
Chairman: Mr. Frederic H. Dickson,
Communications Liaison Branch OCSigO,
Room 2D276, National Defense Building,
Washington 25, D. C.

Commission 5: Radio Astronomy
Chairman: Dr. John P. Hagan,
Naval Research Laboratory,
Washington 20, D. C.

Commission 6: Radio Waves and Circuits, Including General Theory and Antennas
Chairman: Prof. E. C. Jordan,
Department of Electrical Engineering,
University of Illinois,
Urbana, Ill.

Commission 7: Electronics
Chairman: Prof. W. G. Shapherd,
Institute of Technology,
University of Minnesota,
Minneapolis 14, Minn.

The success of these meetings depends upon the whole-hearted co-operation of the individuals participating in them and a continuation of the enthusiastic response we have had in previous years.

Advance registration forms and details of the meeting will have been sent to you on or about April 1, 1954, together with the preliminary program of titles.

Your co-operation in making these URSI-IRE meetings a success in the past and your continued effort anticipated in similarly producing a worthwhile meeting this Spring are greatly appreciated. It is hoped that you and other members of your organization will be able to attend and participate in the meetings.

Correspondence

The editors of the PGAP Transactions have recently received a letter from W. E. Gordon of Cornell University surveying the IRE and the Professional Group System in general and the PGAP in particular. The letter is reproduced in its entirety for the information of the membership.

"A professional society should provide its members with (*a*) a meeting place for the presentation and discussion of original contributions to the science, (*b*) a journal for the publication of these contributions, and (*c*) a publication devoted to reviews and news.

"The Institute of Radio Engineers because of the diversified interests of its 37,000 members is not a professional society but should be considered as a collection of professional societies. The professional group movement is evidence of this. The professional groups must assume the status of professional societies with strong assistance from the Institute. The assistance should be substantial judging from the current financial statement of the Institute.

"If the PGAP is to become a professional society it must fulfill the three requirements set forth in the first paragraph. PGAP is providing the meeting place through joint sponsorship of URSI meetings, although membership in PGAP is not required of persons attending the joint meetings. The Transactions of the IRE PGAP does not constitute the journal and, it seems to me cannot, for two reasons. First, the scientific scope is limited. No member of PGAP limits his radio interests to the narrow field of antennas and propagation, and hence the Transactions do not cover the interests of the membership. The scope should be broadened to include what might be called radio physics embracing radio waves in the atmosphere, both troposphere and upper atmosphere, the physical problems associated with radio waves in the atmosphere, and radio waves from extra-terrestrial sources. I realize that to broaden the scope of the Transactions requires broadening the scope of PGAP, but feel that this is required not only for the reason just cited but, secondly to enlarge the membership of the Group so that a first class journal will be economically feasible.

"The Proceedings could serve a useful purpose to the Group and all other members by expanding its review and tutorial paper policy, and disseminating news of interest, thus fulfilling requirement (*c*).

"In becoming a journal, the Transactions of the Institute of Radio Engineers Professional Group on Antennas and Propagation must change its name to something less awkward and something that will be referenced more usefully in libraries. Radio Physics or Radio Waves seems more appropriate.

"Since the Transactions is just starting I feel strongly that now is the time to make the change in a direction which more satisfactorily serves the interests of the members and which promotes survival both on a scientific and economic basis. To this end the editor with the approval of the Professional Group should formulate a policy regarding the scope and format and specifically invite papers representative of the new scope of the journal and the Professional Group should secure the support of the Institute."

contributions

An Experimental Investigation of the Single-Wire Transmission Line*

T. E. ROBERTS, JR.†, ASSOCIATE, IRE

Summary—**The results of some measurements made on a dielectric coated wire are presented and compared with theoretical results. These measurements indicate that the single-wire line can be considered as a simple transmission line provided account is taken of the "end-effect."**

INTRODUCTION

SINCE THE INTRODUCTION of the dielectric coated wire as a practical means of transmitting high-frequency radio waves,[1] there has been considerable speculation as to whether transmission-line concepts were really applicable to such a structure. It has recently been shown[2,3] that the structure can be treated as a transmission line whenever its length is sufficiently great.

The purposes of the present research have been to perform some rather fundamental experiments that clarify the theoretical results, and also to develop measuring techniques applicable to the single-wire line.

The physical quantities of most interest are:

1. attenuation and phase velocity of the principal mode,
2. equivalent circuits for the transition from a coaxial line to the single-wire line,
3. current and charge distributions,
4. radiation-field patterns.

The first three quantities can all be measured with the same equipment. Measurement of the field pattern, however, requires entirely different equipment, and involves a considerable project. For this reason, and because our primary interest is in the transmission qualities of the single-wire line, it was decided not to make measurements of the field patterns.

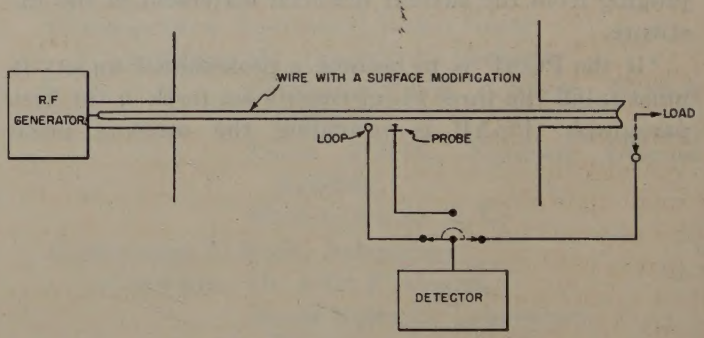

Fig. 1—Block diagram of the system.

The required equipment is quite simple. It consists of a stable radio-frequency generator,[4] detecting equipment, and a straight wire supported at each end, with a traveling probe or loop to measure the magnitudes of the electric and magnetic fields. A block diagram of the system is shown in Fig. 1, and a photograph of the experimental arrangement is shown in Fig. 2.

A wavelength of 3.2 cm was chosen for the radio-frequency signal. This appeared to effect a reasonable

* Manuscript received by PGAP, March 22, 1953. Part of a thesis submitted in partial fulfillment of the requirements for the degree of Doctor of Philosophy. This research was made possible by support extended Cruft Laboratory, Harvard University, under contract N5ori-76, T.O. 1.

† Formerly, Harvard University; now, American Machine and Foundry Co., Greenwich, Conn.

[1] G. Goubau, "Surface waves and their application to transmission lines," *Jour. Appl. Phys.* vol. 21, p. 1119; 1950.

[2] G. Goubau, "On the excitation of surface waves," PROC. I.R.E., vol. 40, p. 865; 1952.

[3] T. E. Roberts, Jr., "Theory of the single-wire transmission line," *Jour. Appl. Phys.*, vol. 24, p. 57; 1953.

[4] T. E. Roberts, Jr., "A stable amplitude-modulated microwave generator," PROC. I.R.E., vol. 40, p. 1125; 1952.

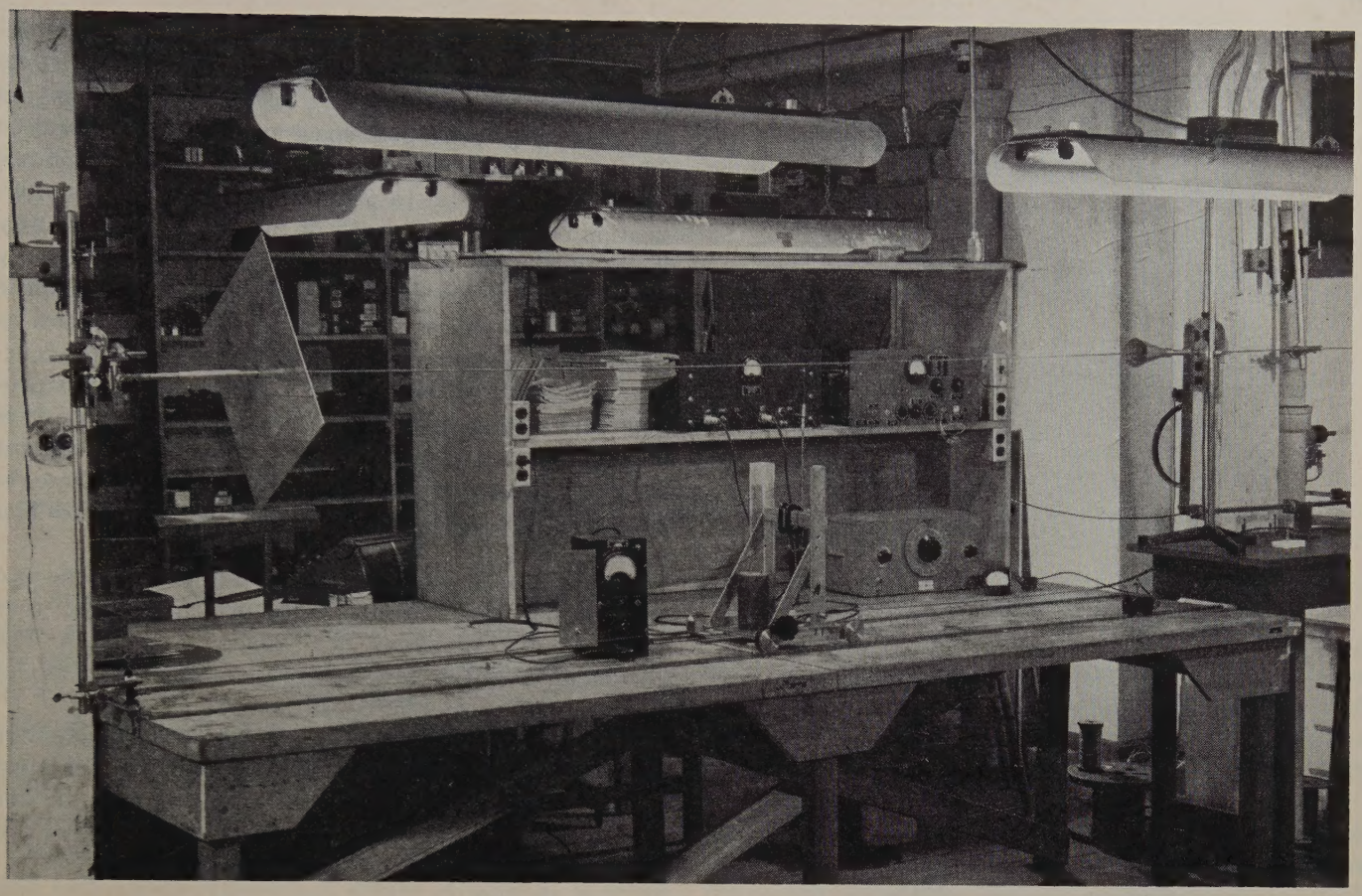

Fig. 2—The experimental arrangement.

compromise between accuracy and over-all size, making it possible to obtain a probe-travel over the entire length of line (about 80λ). An over-all length of 80λ is sufficient for making measurements on wires that are of practical interest, although all properties of *unmodified* wires (excepting wires of small radius) cannot be measured.

Accurate methods of measuring charge and current distributions on cylindrical structures, developed by Morita,[5] make use of small probes and shielded loops extending from a slotted tube. This method cannot conveniently be applied in the present case because of the small dimensions involved. Also, the use of long slotted tubes would greatly reduce the possible choice of wires that could be investigated. It was therefore decided to use probes and loops that were supported from the outside by the smallest coaxial line available (1/32 inch o.d.) and to accept the consequent errors.

A photograph of the probe and shielded loop is shown in Fig. 3. It will be noticed that neither of these units is really small compared to the wavelength, but it can be shown that the error introduced by their size is of consequence only near the ends of the wire. A rather serious error of another type, commonly referred to as "probe-loading," is introduced by the supporting coaxial line and the loop (or probe) considered as a unit. This unit affects the charge and current on the line—that is, it acts as a load (predominantly reactive in this case). This second error cannot be completely eliminated in the measurement of current and charge, although it can be reduced somewhat by using loose coupling. If the loop is spaced any great distance from the wire there will be a considerable error introduced near the ends. In the case of a long wire there can be a rather large spacing between the measuring loop (or probe) and the wire, without introducing an appreciable error in the distributions *except* near the ends. In this way the "probe-loading" effect is made negligible for measurements made away from the ends. In making measurements near the ends the coupling is increased, and there may be some error from "probe-loading." Measurements can be made by making use of this "probe-loading" effect in a scheme developed by Goubau.[6] The method is similar to the method of measuring field strengths in resonant cavities. It is not used in this work, however.

The purpose of the circular plate on the charge probe (Fig. 3, p. 48) is to isolate the probe from the supporting structure. Without such a plate the response of the probe was inconsistent and a number of errors were introduced. The small cap on the tip of the probe increases the coupling to the wire and appears to give a slightly better measure of the radial electric field close to the wire. The loop pick-up is shielded and symmetrical; a plate below the loop would serve no use.

[5] T. Morita, "Measurement of Current and Charge Distributions on Cylindrical Antennas," Cruft Laboratory Technical Report No. 66, Harvard University; February, 1949.

[6] G. Goubau, "Zur ausmessung elektromagnetischer felder nuttels testkörper," *Hochfreq. und Elektroak.*, vol. 62, p. 73; 1943.

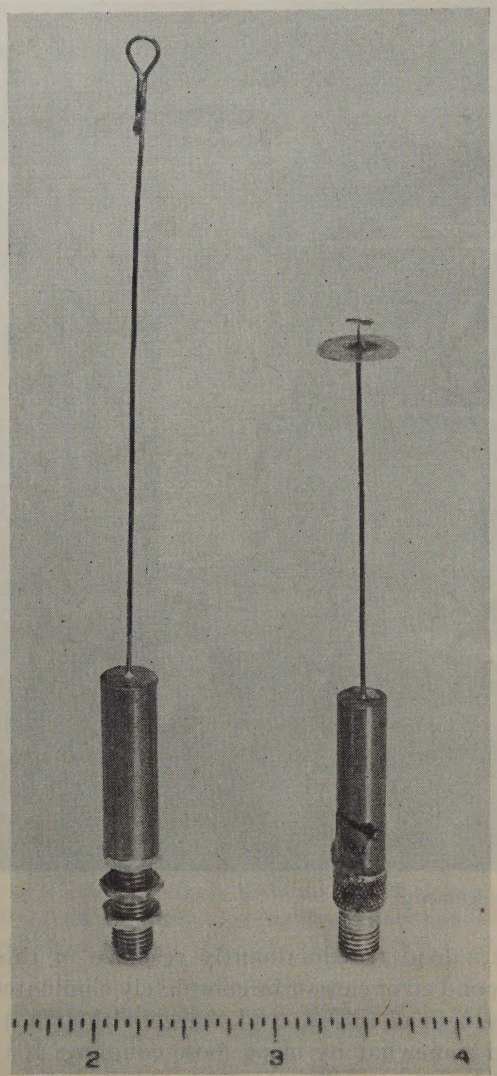

Fig. 3—The current loop and charge probe.

The probe carriage is mounted on a steel track by means of four flanged (railroad-type) wheels. The position of the probe is indicated in centimeters by a steel tape. For accurate distance measurements over short intervals a vernier is mounted on a small magnet that may be placed anywhere along the steel track without danger of slipping. The carriage is shown with the other equipment in Fig. 2.

In some of the measurements coaxial horns were used to make the transitions from the single-wire to the coaxial lines. Two identical horns were constructed from sections of 30-degree cones of 0.003-inch brass stock. The cones tapered out from a diameter of 0.556 inch to a diameter of 3.1 inches. At the point where the cone joins the coaxial line of the same diameter there is a sharp junction which probably gives considerable reflection.

Summary of Theoretical Results

The specific structure of interest here (see Fig. 4) consists of a finite length of wire (with a modified surface) connected to a flanged coaxial line at each end. A number of theoretical results for this structure were reported earlier,[3] and a brief summary of them is given below.

The total axial current in the wire $I(z)$ may be represented as a sum of two components, $I_0(z)+I'(z)$. $I_0(z)$ is a "transmission-line current" with a propagation constant $\zeta_0>\beta$ (β is the free-space propagation constant). The auxiliary component of current $I'(z)$ is a complicated function of z. In general, however, some simplification occurs if the length of the line L is sufficiently large. In this case the current $I'(z)$ is of significance only near the ends of the wire. This auxiliary current is quite large at each flange and decreases to small values at points some distance from the flange. The auxiliary current is a result of the voltage V in the gap and is proportional to this voltage. For the case where the gap is small, numerical values of the component of current $I(z)$ were computed for two specific cases[3] and these results used to compare with the experimental values in a later section.

It was also shown that the coupling between the two coaxial lines was by means of the principal mode,[7] that is, the equivalent circuit is that shown in Fig. 4. The parameter G_1 is the radiation conductance; efficiency of coupling is directly related to the ratio G_1/G_0.

The apparent admittance terminating the single-wire line is indicated by the standing-wave ratio, which must be measured at some distance from the ends of the line in order to be a measure of the propagating mode only.

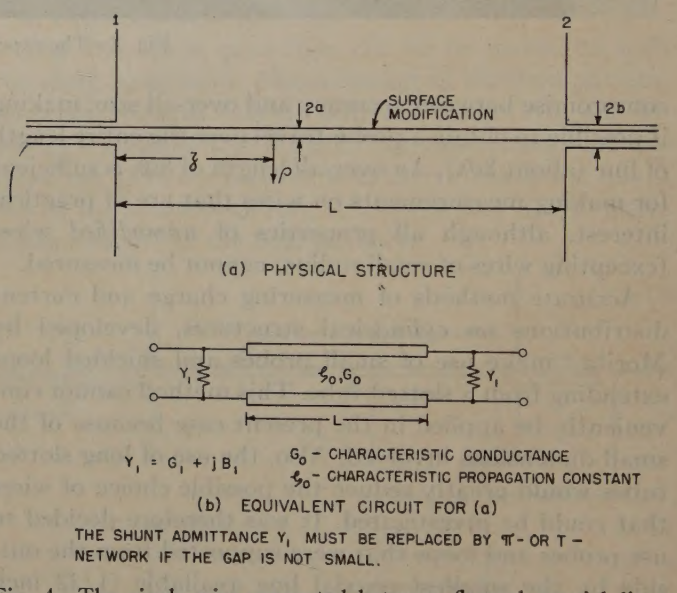

Fig. 4—The single wire connected between flanged coaxial lines.

Since a coaxial-horn feed introduces a smaller auxiliary current than the sharp transition of the flange, this type of feed is often used at the transmitter end to excite the line. If the voltage at the receiving end is zero (i.e., a short circuit), no auxiliary current is introduced at that end. Then the attenuation and phase velocity of the wire can be determined by measuring the parameters $A_s+jF_s=j\zeta_0 s+\rho_s+j\Phi_s$, at a distance s from the short-circuited end. $\zeta_0 s$ represents the attenuation and phase shift of the line; ρ_s and Φ_s are the terminal functions.[8]

[7] This is true only for large L.

[8] Ronald King, "Transmission-line theory and its application," *Jour. Appl. Phys.*, vol. 14, p. 577; 1943.

Physical Properties of the Experimental Lines

Most of the measurements presented here were made on two dielectric-coated wires, No. 1 and No. 2, having the characteristics given in Table I. A few measurements were made on wire No. 3, also described here.

TABLE I

Physical Properties of Dielectric Coated Wires

Wire No. 1		*Wire No. 2*		*Wire No. 3*	
a'	0.159 cm	a'	0.0572 cm	a'	0.0318 cm
a	0.203 cm	a	0.0610 cm	a	0.0279 cm
ϵ_i/ϵ	2.25 } measured	ϵ_i/ϵ	2.50 } (M.I.T. Tables)		
$\tan\delta$	0.0010 } measured	$\tan\delta$	0.011 } (M.I.T. Tables)		
σ	1.5×10^7 mhos (Brass)	σ	5.65×10^7 mhos (hard-drawn copper)		
Dielectric Material Vinyl Plastic "Spaghetti"		Dielectric Material—Formvar (a trade name, General Electric Company)			

The properties of the dielectric coating of wire No. 1 were measured at the operating wavelength of 3.2 cm by placing a short piece of hollow "spaghetti" coating in a rectangular cavity and observing the shift in the resonant frequency and the change in the Q of the cavity. From these measurements the values of the relative dielectric constant, ϵ_i/ϵ_0, and the loss tangent, $\tan\delta$, are easily calculated.

Since the dielectric coating on wire No. 2 is very thin and not readily removed, it would be difficult to measure accurately its dielectric constant. Previous measurements have been made on a block of this material, which has the trade name of Formvar, by the M.I.T. Laboratory for Insulation Research, and the data given above were taken from their report.[9] It is not certain that the dielectric coating used here is identical with the sample tested at M.I.T., but no other data on this material are available. If there is any slight variation in the materials, one usually expects the loss tangent to be quite different and the dielectric constant to be relatively unchanged.

Current and Charge Distributions

It has been shown elsewhere[3] that a finite wire of sufficient length can be terminated so that it behaves as a flat line except near the ends. Under terminated conditions the current and charge distribution near the driving end of this finite line should be the same as for the infinitely long wire.

An experiment was arranged with the transmitter connected as shown in the insert of Fig. 5. A horn was connected at the receiving end, and the load tuned until a minimum standing wave was indicated by the traveling probe near the center of the line. The probe was then moved to the receiving end and the line appeared almost flat (swr <1.05) except in a small region near the receiving horn. Near the generator the current rises sharply as expected from the theory. The result of the measurement on wire No. 1 is shown in Fig. 5 together with a theoretical curve. (The theoretical curve was obtained by adding the two components of current $I_0(z)$ and $I'(z)$. Curves of $I'(z)$ for wires No. 1 and No. 2 have been given elsewhere.[10])

TABLE II

Transmission Line Properties of Dielectric Coated Wires

wire	$\lambda_0'a$	βa	G_0 mhos	G_1 mhos	G_1/G_0	α die db/m	α cu db/m	α Total db/m	λ_g† cm	
No. 1	0.092	0.40	0.0079	0.0062	0.784	0.43	0.17	0.60	3.120	Theoretical
					0.79			0.53	3.115	Experimental
No. 2	0.010	0.12	0.0039	0.0040	1.02	0.06	0.125	0.185	3.185	Theoretical
					1.00			0.24	3.19	Experimental

† Guide wavelength.

Table II contains a summary of the most basic data related to these two wires. The experimental values for both wires are seen to be in rather good agreement with the theory. One should expect somewhat closer agreement between the measured and theoretical values of the attenuation of wire No. 2, but, as mentioned above, the value of the loss tangent of the dielectric coating may be in error in this case. Before discussing the methods used in arriving at the experimental values of Table II, it is convenient to discuss some of the other measurements. This discussion leads to the procedures used to obtain the above data.

The theoretical current-distribution curve of wire No. 1 is interesting in that there is a slightly dip below the final constant value. This dip can be interpreted as interference between the two components of current I_0 and I', since I_0 has a propagation constant of ζ_0 and I' has an "average propatation constant" of β, the free-space value.

[9] "Tables of Dielectric Material," Report V, M.I.T. Laboratory for Insulation Research; February, 1944.

[10] Roberts, "Theory of the single-wire transmission line," *ibid.*, Figs. 5 and 6.

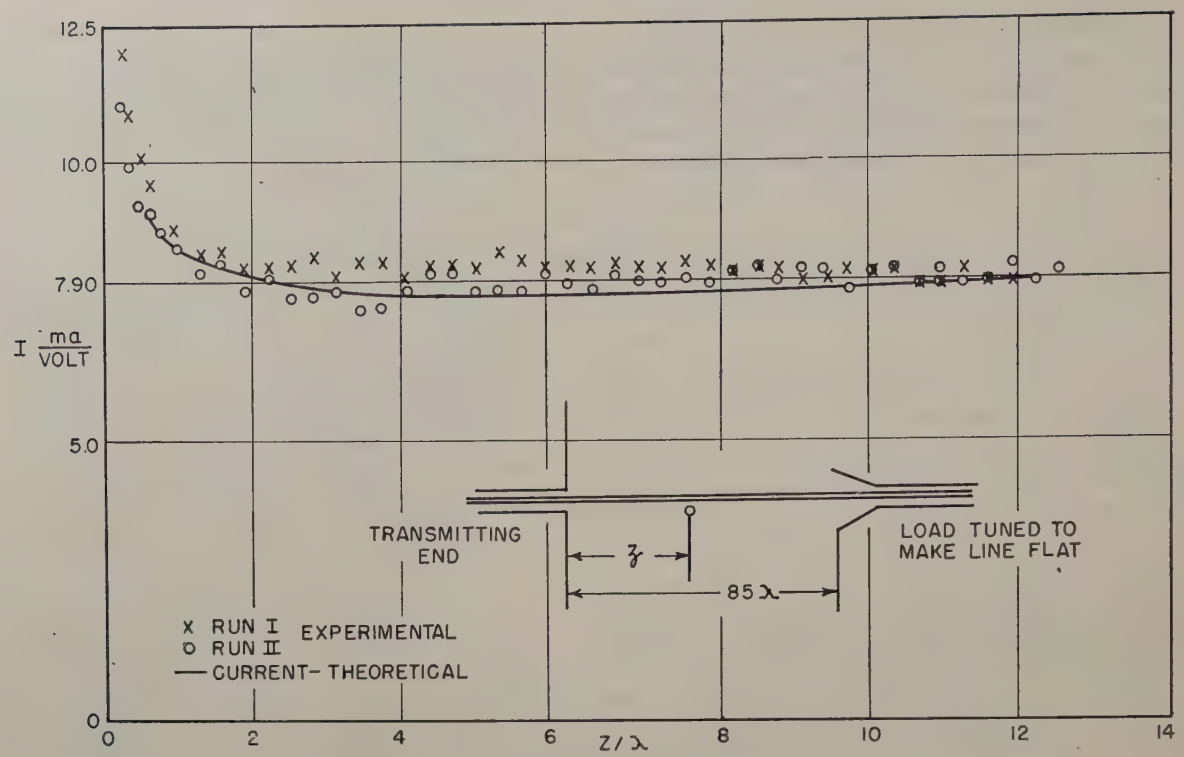

Fig. 5—The current on a terminated single wire, wire No. 1.

The accuracy of the measured curve of Fig. 5 is rather poor because the result depends directly on the probe-to-line spacing. Moreover, some error is introduced by the small residual standing wave and by probe loading. Considerable improvement was made by supporting the line with polyfoam so that the unsupported span was only about 50 cm. Even so, it cannot be concluded from the measurements that the dip exists.

The lack of accuracy can be reduced by measuring the distribution in a somewhat indirect manner. Let the positions of the generator and load be interchanged. The current near the receiving end (flanges in this case) is closely related to the current near the generator on an infinitely long wire, as is seen from the following.

If a load, Y_L, is connected to terminals 11 such that $Y_L+Y_1=G_0$, there will be no reflected transmission-line current, in other words, the wire is terminated. There will be a standing wave near the flange caused by a current of type $I'(z)$. The total current will be $I(z)=I_0e^{-i\beta_0 z}+I'(z)$. Except for the reversal of the propagation direction of the current $I_0(z)$, this expression is identical to the current on an infinite line. The two components of current interfere and produce a standing wave, as shown in Figs. 6 and 7. The agreement between experiment and theory is seen to be quite good. The maximum discrepancy occurs for small values of z. The theoretical curves are expected to be more accurate than the experimental values because of possible probe-loading effects. It seems, however, that the relative magnitude of $I(z)$ can be determined to a reasonable accuracy from such an experiment. Any variation in probe coupling can be easily corrected because the current distribution must be symmetrical about a horizontal line.[11]

The curve of Fig. 6 does not show a slow interference beat as occurs in the theoretical curve of Fig. 5 because there is no reflected transmission-line current $I_0(z)=I_0e^{i\beta_0 z}$. Such a beat is detected if the load is tuned to some value other than $Y_L=G_0-Y_1$. The distribution on wire No. 1 for $Y_L=-jB_1$ is shown in Fig. 8, p. 52, where interference between the reflected components of current $I_0e^{i\beta_0 z}$ and $I'(z)$ is quite evident. The measured distributions on wire No. 1 for a larger gap, $b=0.22$, with $Y_L=jB$ are given in Fig. 9, p. 53. Note that the final standing-wave ratio is much greater for the large than for the small gap. This is to be expected since the radiation conductance, G_1 is less for the large gap; that is, there is a stronger coupling between the coaxial line and the single-wire line.

The above measurements are in quantitative agreement with the theory and are a good illustration of the advantage gained by separating the current into two components.

Measurement of Attenuation and Phase Velocity

The experimental measurements given above verify the theoretical result that the single-wire line, if it is sufficiently long, may be treated as a transmission line. An idea of its required length has also been obtained in the two specific cases considered. It would appear, therefore, that the transmission-line techniques of measurement may be applied provided care is taken in application that ranges of validity are not exceeded.

[11] In the measurements presented here a correction curve was determined by short-circuiting the gap and measuring the magnitudes of the maximum of the resulting high standing wave. From these data the probe was calibrated.

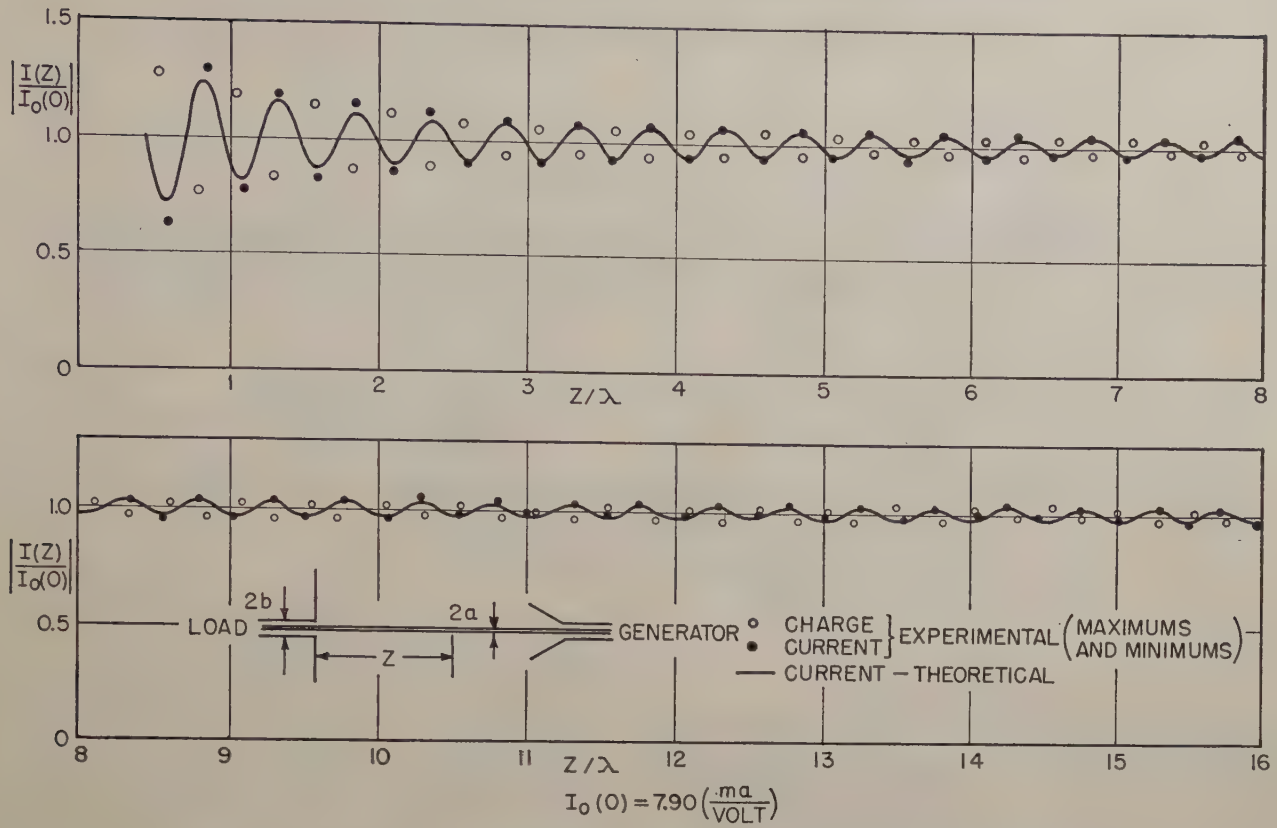

Fig. 6—Current and charge distribution, wire No. 1, $Y_L = G_0 - Y_1$ (line terminated); $b = a$.

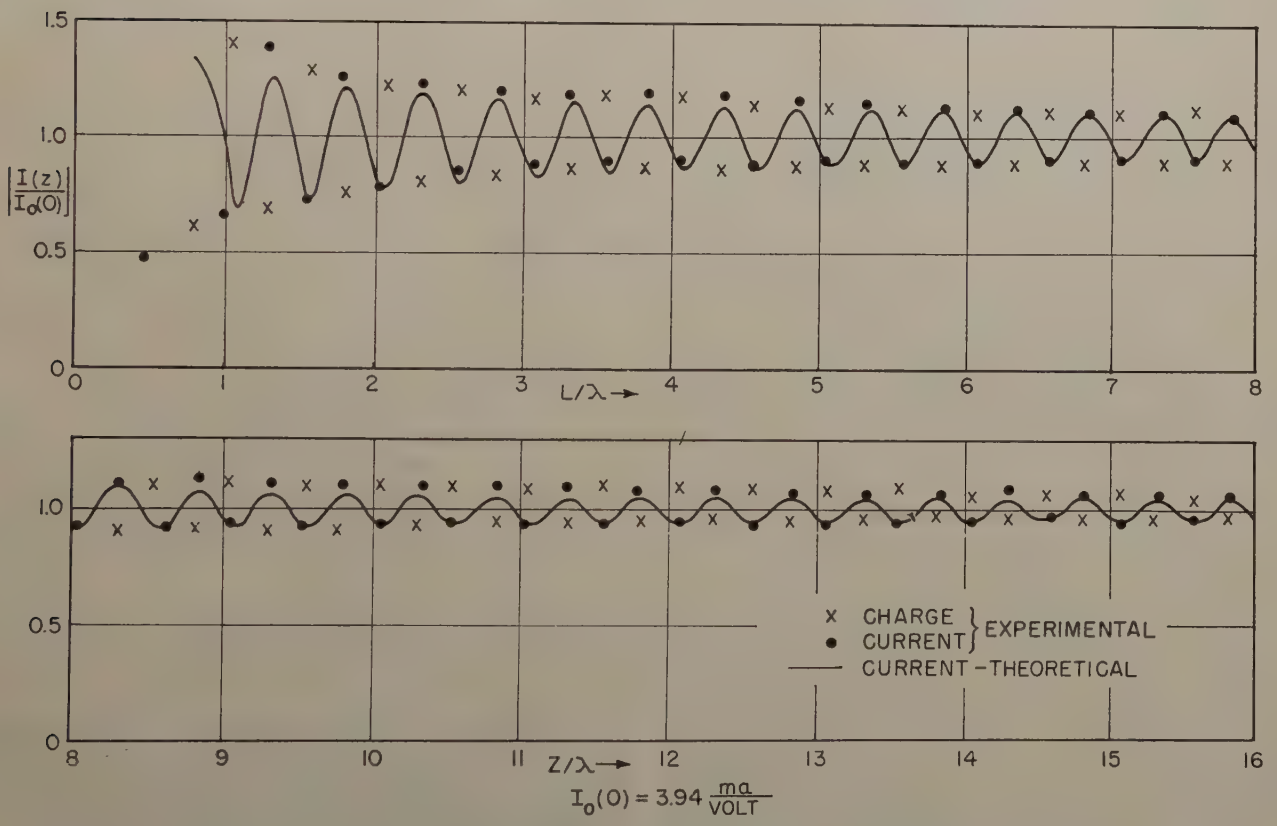

Fig. 7—Current and charge distribution, wire No. 2, $Y_L = G_0 - Y$; (line terminated) $b = a$.

One of the most accurate methods of measuring small attenuation is to measure the standing-wave ratio on a short-circuited line. In the present work, the wire was terminated in a large rectangular flange ($11.2 \times 14.4\lambda$) which was expected to represent a good short circuit, and a coaxial horn was used to couple to the transmitter. The standing-wave ratio was determined at points about two meters from the short circuit by measuring the "width" of the minimum. The relation between attenuation and the above "width measurements" is

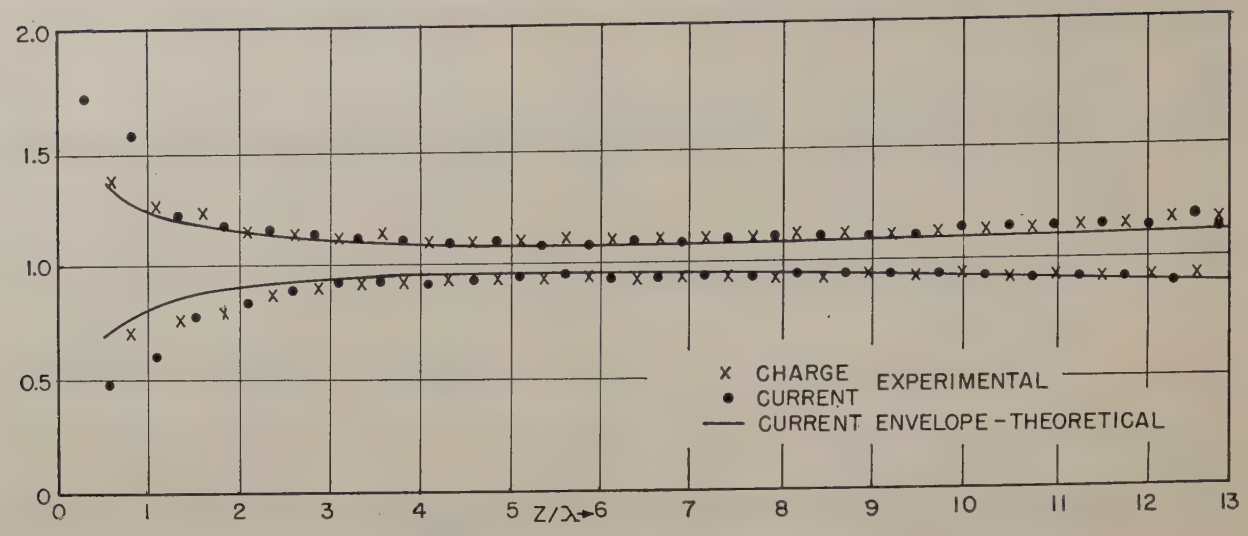

Fig. 8—Current and charge distribution, wire No. 1, $Y=-jB$; $b=a$.

given by

$$\sqrt{p^2-1}\sinh \alpha s = \sin \beta\delta,$$

where p is the ratio of the current (charge) at a distance δ from the minimum to the current (charge) at the minimum. Since a horn was used to couple into the line and the measuring probe was located near the center of the line, the current $I'(z)$ may be considered negligible, and the results should be an accurate measure of the attenuation. The guide wavelength (equivalent to phase velocity) was determined from the distance between minima. These results are given in Table II.

Another method of measuring the attenuation yielded results that are substantially in agreement with the measurements just discussed. Here, two horns are connected to the line and the received signal is measured as a function of the horn separation, L. The final slopes of the curves of received signal vs separation should be equal to the attenuation. These curves are plotted in Figs. 9 and 10 and the attenuation measured by the two methods is indicated. Some deviation from a straight line for small spacing is of course to be expected since the fields are quite complicated near each horn.

It is interesting to compare the data of wires No. 1 and No. 2 with data taken for similar wires with no dielectric coating. It is seen in Figs. 9 and 10 that in the case of no dielectric coating the horns are not sufficiently far apart for the attenuation of the received signal to approach a simple linear function of the distance. The measured curve is expected to approach an asymptote of the slope indicated by the theoretical attenuation curves. The length of wire is not sufficiently long to show this. Thus it can be stated that the uncoated wires *of the length used here* cannot be classified as transmission lines but the coated wires can be so classified. This comparison of the coated and uncoated wires clearly displays the guiding properties of a thin dielectric coating. (The dielectric coating was only 0.015 inch thick for wire No. 2.)

The Radiation Conductance G_1

The transition from a flanged coaxial line to a single-wire line may be represented by a four-terminal network. If the gap is sufficiently small, so that the radial electric and magnetic field distributions in the gap are the same whether the circuit is driven from the coaxial line or from the single-wire line, then the general four-terminal network reduces to a simple shunt circuit. This shunt circuit is located at the flange and may be represented by an admittance $Y_1=G_1+jB_1$ plus an auxiliary transformer.

Suppose the network is represented by a simple shunt circuit. The most important parameter is G_1, since the susceptance B and the transformation ratio n can be changed by tuning adjustments made *inside* the coaxial line. These tuning adjustments (by use of lossless elements) do not change the value of G_1. The relative conductance G_1/G_0 (where G_0 is the characteristic conductance of the single-wire line) is a measure of the efficiency of coupling between the two lines.[12]

The radiation conductances (G_1) of wires No. 1 and No. 2 were determined by the Weissfloch[13–15] method by placing a movable short circuit inside the coaxial line and measuring the input admittance to the single-wire line at a point about two meters from the junction. (The radio-frequency excitation, $\lambda=3.2$ cm, was coupled into the single-wire line by means of a horn.) The measured input admittance was transformed to the reference plane at the junction of the two lines by subtracting out the attenuation of the length of line used. The re-

[12] For example, the efficiency of coupling (on a power basis) from a coaxial line to a *terminated single-wire line* is $1/(1+G_1/G_0)$, and the efficiency of coupling from a single-wire line to a coaxial line which *terminates the single-wire line* is $(1-G_1/G_0)$.

[13] A. Weissfloch, "Ein transformation über verlustose vierpole und seine anwendung," *Hochfreq. Electroak.*, vol. 60; 1942.

[14] N. Marcuvitz, "On the representation and measurement of waveguide discontinuities," Proc. I.R.E., vol. 36, p. 728; June, 1948.

[15] A. A. Oliner and H. Kurss, "The Precision Measurements of the Equivalent Circuit Parameters of Dissipative Microwave Structures," Paper No. 78, I.R.E. National Convention, New York, N. Y.; 1951

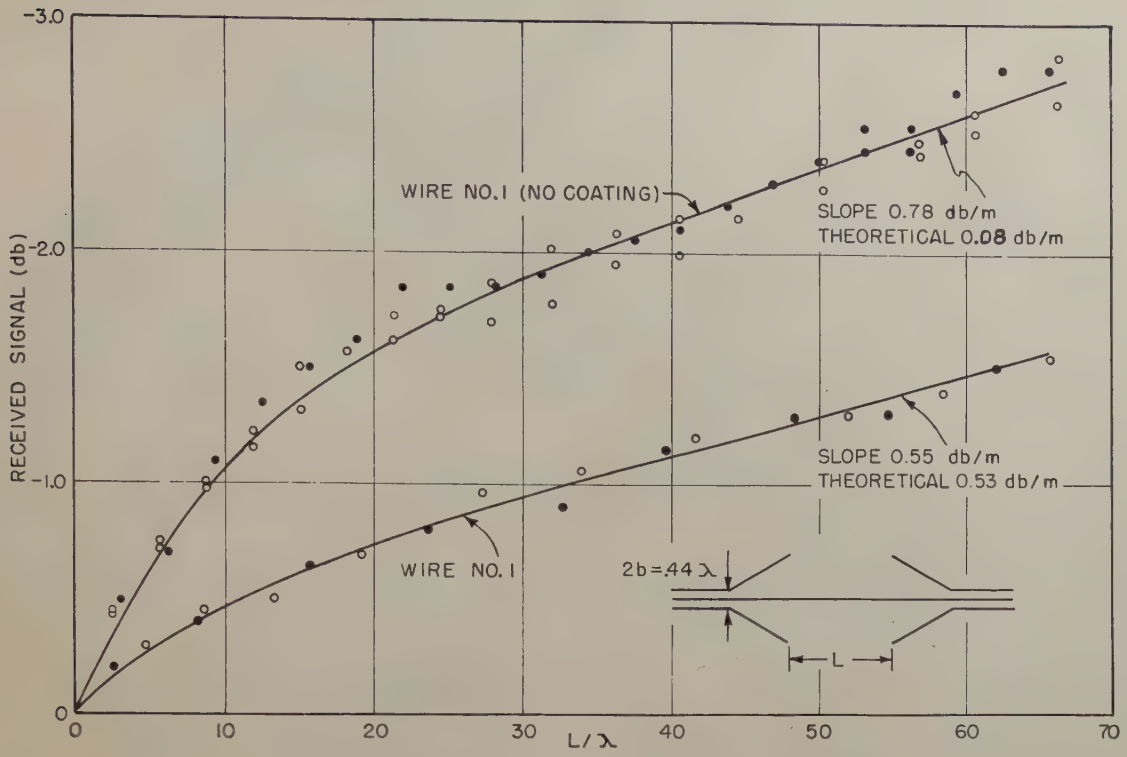

Fig. 9—Received signal as a function of separation, L, wire no. 1.

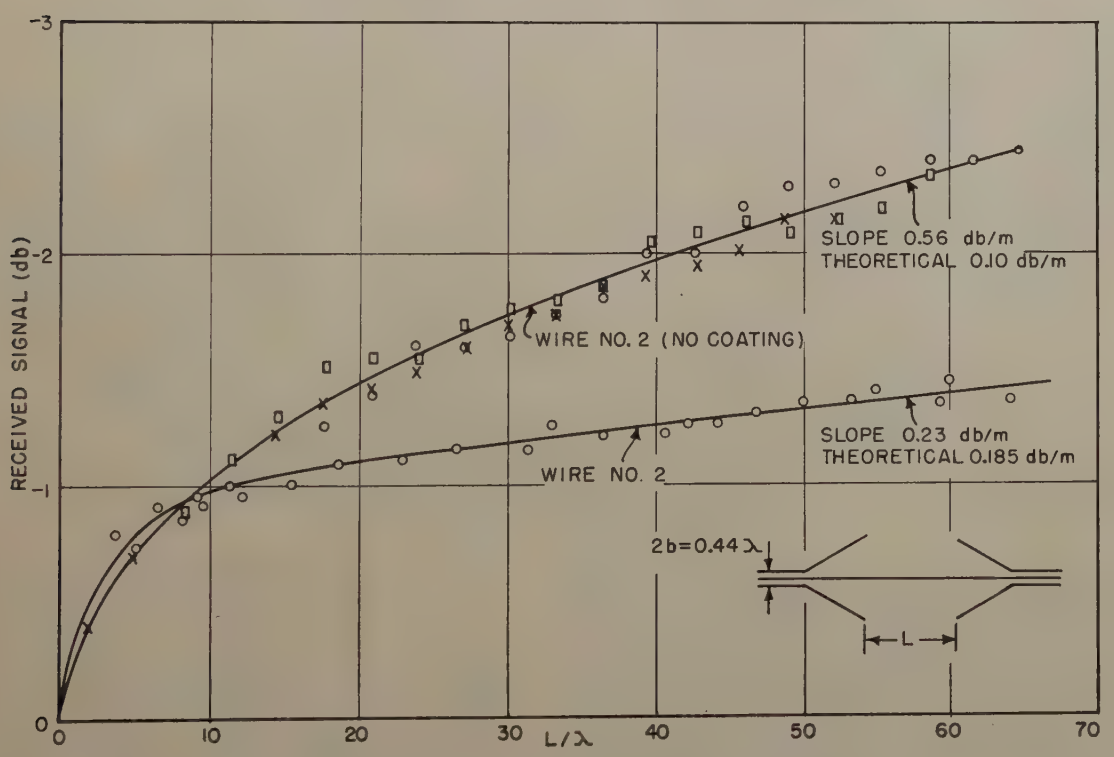

Fig. 10.—Received signal as a function of separation, L, wire no. 2.

sulting input-admittance measurements were then plotted on the Smith chart and the parameters G_a and G_b were determined from the best circle. The value of G_b was zero (within the experimental accuracy) for all diameters of the coaxial line used. G_a, therefore, represents G_1 directly. An example of the data for wire no. 1 is given in Fig. 11, p. 54.

In this way values of G_1 were determined for a number of gap radii, b; these results are in Fig. 12, p. 54. A curve is drawn through the measured points, then extrapolated to the value at zero gap, which value it approaches at zero slope.

Measurements made for very small gaps are not accurate because of the losses in the coaxial line. The ef-

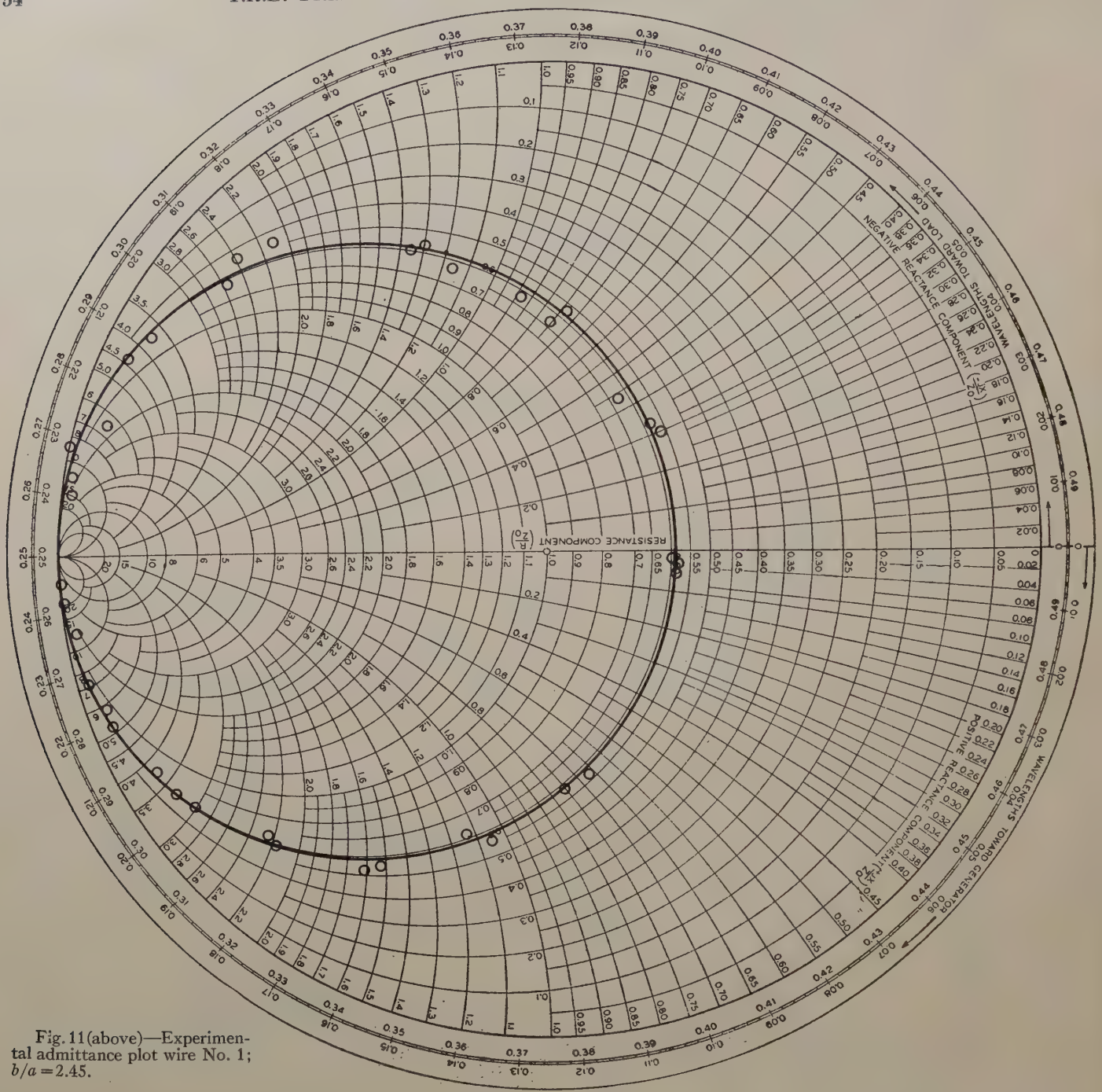

Fig. 11(above)—Experimental admittance plot wire No. 1; $b/a = 2.45$.

fect of these losses is easily determined by changing the length of the coaxial line by several half-wavelengths and repeating the measurement. If the losses in the coaxial line are appreciable, the measured values will be different in the two cases.[16] These losses were quite noticeable for gaps of about half the smallest size indicated in Fig. 12. However, no such "loading effect" was detectable for the values given in these figures.

The results of the above extrapolation are tabulated with the theoretical values in Table II. The agreement is very close. It is, in fact, somewhat better than is expected from an inspection of the experimental data of Fig. 11.

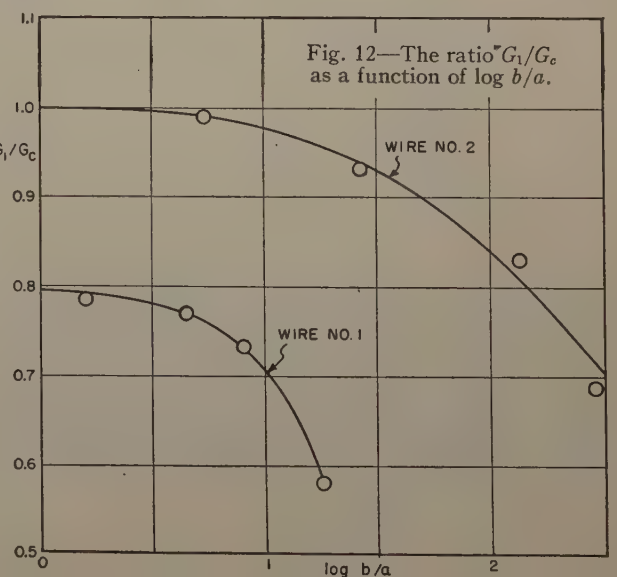

Fig. 12—The ratio G_i/G_c as a function of log b/a.

[16] Montgomery, Dicke, and Purcell, "Principles of Microwave Circuits," M.I.T. Radiation Laboratory Series, vol. 8, McGraw-Hill Book Co., New York, N. Y., p. 231; 1948.

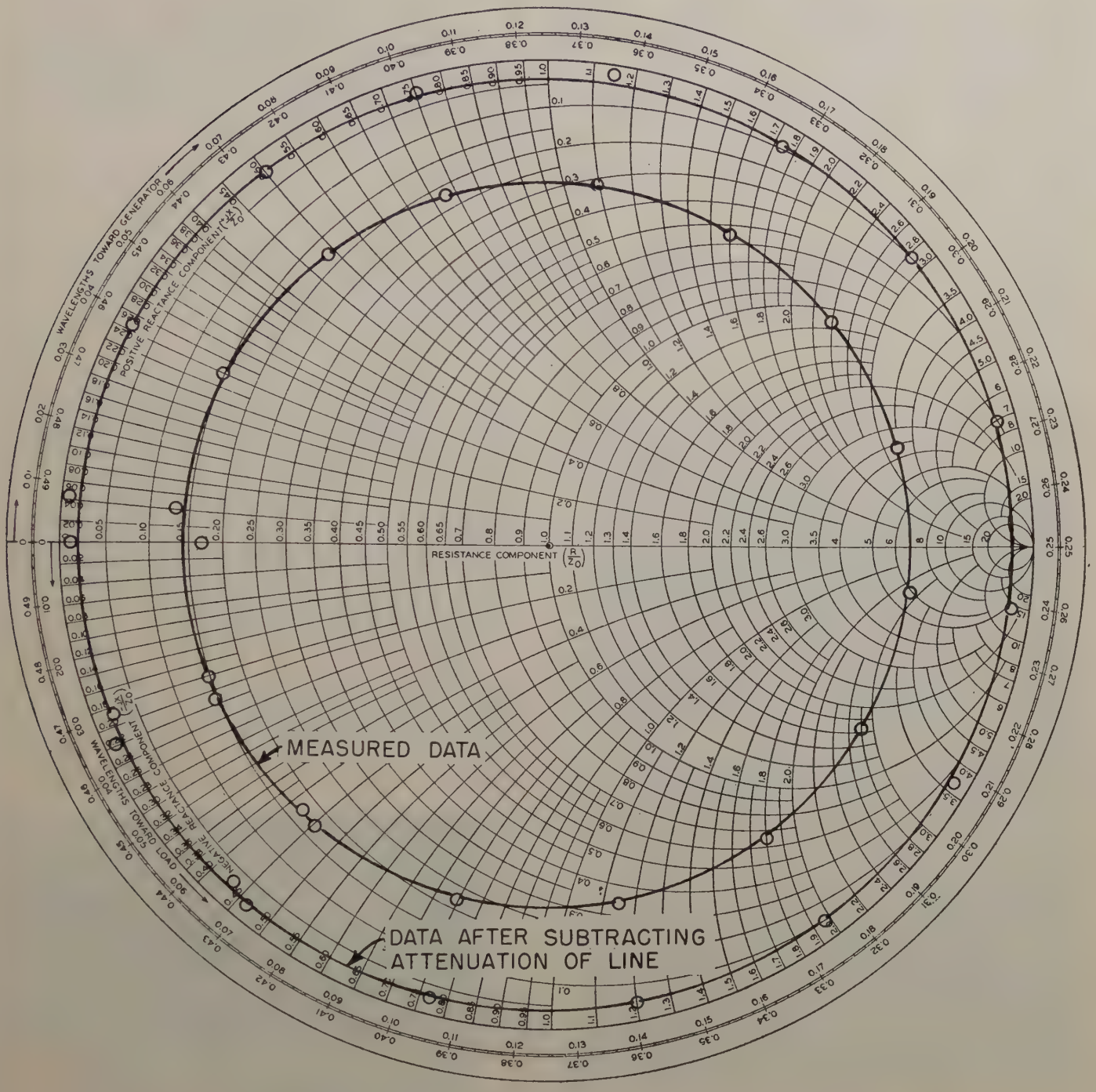

Fig. 13—Data for determining the insertion loss of the coaxial horn; wire no. 1.

The Measured Efficiency of the Coaxial Horns

As a point of practical interest, the efficiency of the coaxial horn was determined experimentally. The horn was connected to wire no. 1 at the receiving end in place of the flange, and the measurement was carried out as in the previous section. The data are given in Fig. 13. The results of the measurement are: insertion loss, 0.17 db—or efficiency, 96 per cent.

Since, for this specific case, the center of the measured admittance circle lies at the center of the Smith chart, the equivalent circuit can be represented by an attenuation of 0.17 db, plus a properly located transformer. After carrying out the complete procedure the transformation ratio was found to be $n=1.05$. Thus the 30-degree, 6-inch-diameter coaxial horn is a reasonably efficient device with very low insertion and reflection losses.

The measurement was also made in the reverse sense, i.e., by connecting the short circuit, a large conducting plate, to the single-wire line and measuring the admittance seen by the coaxial line. Of course, the measured admittance circle was not centered at the center of the Smith chart, but the data were in agreement with the equivalent circuit found above.

In general, more accurate data are obtained by making the measurements in the reverse sense noted above,

although there is additional graphical work involved in subtracting out the attenuation of the single-wire line in this case.[17]

[17] The single-wire line must be rather long (usually causing appreciable attenuation) in either case, in order to avoid the auxiliary current effects.

ACKNOWLEDGMENTS

The author wishes to acknowledge the encouragement and guidance of Professor R. W. P. King and the valuable suggestions of Dr. T. Morita and others of the Cruft Laboratory.

Sweep Frequency Backscatter—Some Observations and Deductions*

RICHARD SILBERSTEIN†

Summary—**Sweep-frequency backscatter records have proved to be of great value in identifying the sources of backscatter seen on a fixed frequency by demonstrating the development of the echo as frequency and range increase. The most commonly observed scatter is ground scatter propagated via the F2 layer, but it is also evident that the other layers propagate ground scatter and that scatter from the distant *E* region may at times be important.**

In one group of observations over an 1,150-km path on three undisturbed days, the values of F2-layer maximum usable frequency scaled from midpoint vertical-incidence ionospheric records and those determined by backscatter delay assuming ground scatter agreed almost within experimental error. In another three-day group characterized by a low-latitude ionospheric disturbance with low geomagnetic *K* indexes but considerable sporadic *E* activity, values of muf determined from scatter were much too high under the ground-scatter assumption, errors of about 30% being not uncommon.

INTRODUCTION

USE of sweep-frequency equipment to observe characteristics of scatter energy received back at the site of a high-frequency radio transmitter represents a new approach to the study of the ionosphere.

Early in 1951 a Model C3 ionosphere recorder[1] was modified for a 3- to 25-mc linear 12-minute sweep and connected to two rhombic antennas at the Sterling, Virginia laboratory of the National Bureau of Standards. These antennas were pointed westward for observation of oblique-incidence pulse transmissions over the 1,150-km path from Sterling to a site near St. Louis, Missouri. An ionosphere recorder was installed at Batavia, Ohio, the path midpoint, for obtaining vertical-incidence data from which calculations of maximum usable frequency and travel time were to be made and checked against oblique-incidence results.[2]

As early as July, 1951, photographs were made by E. E. Ferguson on the Sterling equipment showing backscatter starting locally and running out to about 3,500 km. Results then were rather poor because of the low power, about 30 kw peak, with a 50-microsecond pulse, and a receiver bandwidth of 70 kc.

* Original manuscript received by PGAP, October 5, 1953; revised manuscript received January 19, 1954.

† National Bureau of Standards, Washington, D. C.

[1] J. M. Carroll, "Automatic ionosphere recorder," *Electronics*, vol. 25, pp. 128–131; May, 1952.

[2] E. E. Ferguson and P. G. Sulzer, "Sweep-frequency oblique-incidence ionosphere measurements over an 1,150-km path," PROC. I.R.E., vol. 40, p. 1124; September, 1952.

It was later found that, for the specific job of scatter studies, a relatively slow rise time and considerable pulse elongation could be tolerated, so that a bandwidth near the theoretical value for maximum signal-to-noise ratio in the presence of white noise (1.2 divided by the pulse duration) would be used. Values of 100 μsec for the pulse duration and 11 kc for the bandwidth were finally adopted. In recording the marginal scatter signals, base-line shift due to strong interfering signals was troublesome. In overcoming this difficulty it was necessary to apply more video clamping to the oscilloscope circuit than was used in the standard Model C3 recorder. Also all short time-constant differentiation was eliminated since it contributed to base-line shift and also caused gaps following the trace produced by a strong echo, which obscured subsequent weak echoes.

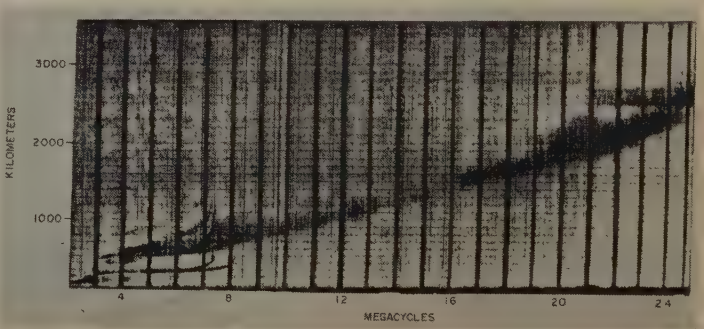

Fig. 1—Multifrequency sweep for December 15, 1952, at 1257 EST, showing backscatter.

Fig. 1 is a photograph of a typical normal-day, sweep-frequency back-scatter record taken on December 15, 1952 at 1257 EST. Perpendicular to the horizontal axis are frequency markers at 1-mc intervals running from 3 mc on the left to 25 mc on the right. The vertical scale is height or slant range in hundreds of kilometers, running to 4,000 km at the top, the first visible marker above the ground pulse at the bottom being for 100 km. At the lower left-hand corner is seen the well-known vertical-incidence $h'-f$ trace, which could be obtained because some energy does escape from the rhombic antenna in a vertical direction. Starting at the second-order reflection and increasing in range as frequency increases is the trace of the scatter echoes presumably

coming from the distant ground and propagated via the F2 layer.[3] Starting at 21 mc behind the regular line of echoes is an echo at a constant range of 2,500 km. Relatively fixed echoes (i.e. echoes not sensitive to frequency) appear at about the same slant range at the higher frequencies on practically all sweeps in which the range to the frequency-sensitive scatter is shorter at these frequencies. This slant range is correct for the Rocky Mountains. The higher frequencies appear to work best because of low absorption and favorable low-angle antenna characteristics.

Sweep-frequency "scatter sounding" has several advantages over the fixed-frequency type in the study of ionospheric phenomena and in the practical evaluation of the use of scatter echoes for skip-distance determination. By sweeping the frequency it is possible to obtain information as to the source or type of scatter by the manner in which the echoes "grow" as the frequency is increased. Again for the test of any premise, a large number of samples are afforded (*a*) at different frequencies in any one sweep, and (*b*) under different diurnal conditions. For instance, in skip-distance determination over a fixed path there are, in general, only two times of day when a fixed frequency skips. With sweep-frequency techniques it is likely that there will be some frequency which will just skip on the particular path at any time of day.

Present results were limited mainly to daytime hours. With the present power and rhombic antenna, the main lobes are too high at the relatively low frequencies, which have long F2-layer skip ranges at night with low-angle requirements.

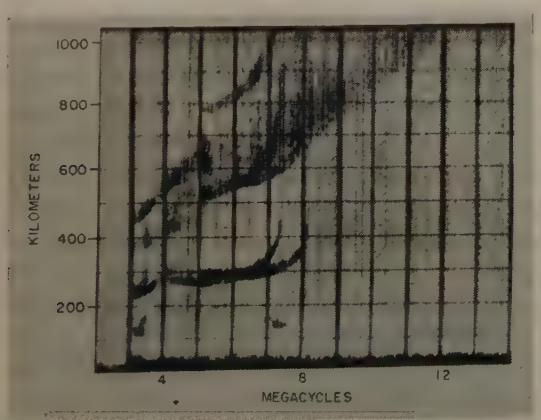

Fig. 2—Multifrequency sweep for December 15, 1952, at 1309 EST, with expanded height scale.

Fig. 2 shows a similar sweep made 12 minutes later using a 1,000-km height scale. More detail is visible on the manner in which the backscatter develops from the second-order F2 echo. The separation in the scatter trace which is most prominent at 700 to 800 km and 8.2 to 9.2 mc seems to be associated with the extraordinary wave.[3,4] It is often visible under quiet conditions. The frequency separation of these scatter echoes at near vertical incidence is often less than the well-known frequency separation of ordinary and extraordinary wave echoes at vertical incidence.

[3] W. Dieminger, "Origin of ionospheric scattering," *Proc. Conference on Ionospheric Physics*, vol. II, 1950, The Pennsylvania State College and the Air Force Cambridge Research Laboratories.

[4] Dieminger, "The scattering of radio waves," *Proc. Phys. Soc. B*, (London, Eng.) vol. 64, 374B, pp. 142–158; February, 1951.

A Detailed Study of Two Different Periods

Analyses were made of records taken during two periods which differed radically in ionospheric characteristics but were both geomagnetically quiet. The period January 21–23, 1953 was a quiet period both geomagnetically and ionospherically and was marked by a very low incidence of sporadic-*E* reflections. On the other hand, the period December 17–19, 1952, although quiet geomagnetically, was characterized by rapid changes of critical frequency throughout the day (characteristic of a low-latitude type disturbance) and by a high incidence of sporadic-*E* reflection. The quiet period will be considered first.

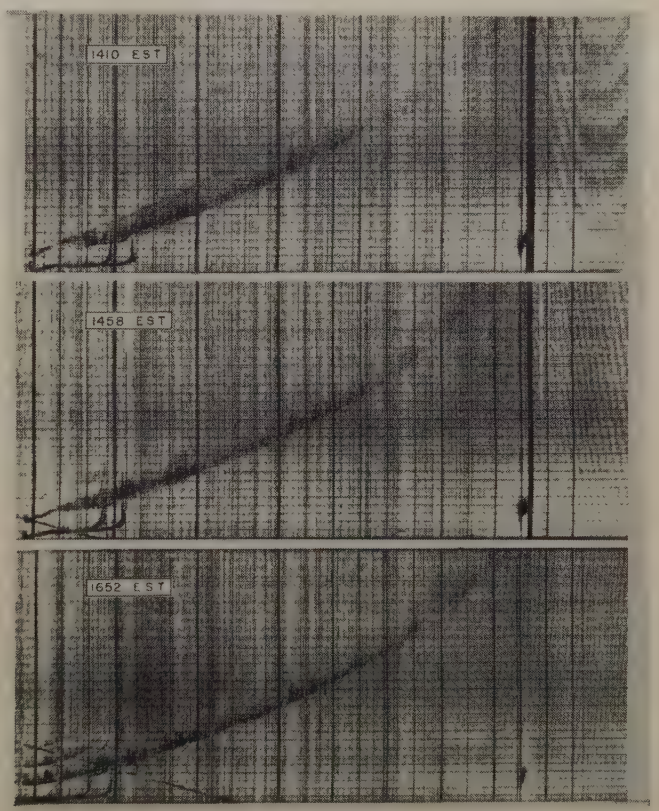

Fig. 3—Sweeps for January 22, 1953.

Fig. 3 shows a sequence of three sweeps made on January 22, 1953. The range scale begins at 200 km in each of these. The first sweep at 1410 EST shows a fairly regular scatter trace which originates at the second-order F2 vertical-incidence trace and exhibits the separation discussed above. There is another fine line of scatter echoes coming off the second-order F1 vertical-incidence trace which has been demonstrated to be ground scatter propagated by the F1 layer. In the next sweep at 1458 the F1 layer is starting to disappear and the scatter propagated by it is weaker. In the last sweep at 1652 the F1 layer and the scatter associated with it have disappeared,—also the apparent

skip ranges for F2-propagated scatter are noticeably longer than in the previous sweeps, because of the lateness of the hour.

A method of determining the source of scatter propagated back to the receiver via any layer was first shown by Dieminger.[3,4] The simple proof of the technique appears in a paper by Peterson.[5] If the ordinary wave sweep is plotted on linear co-ordinates, a line from the origin (zero frequency and zero height) tangent to the second-order trace marks the locus along which the minimum-time-delay backscatter echoes of the ordinary wave will fall as the frequency increases, if these echoes are from the ground. If they are from the distant E layer they should lie along a line starting at a point about the E-layer virtual height below the tangent point. The technique is correct for essentially transverse propagation.

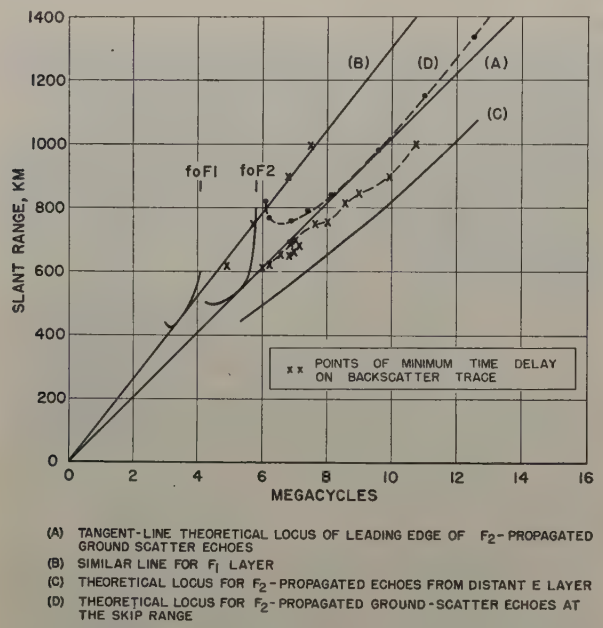

Fig. 4—Analysis of multifrequency backscatter echoes following second-order F1 and F2 reflections at Sterling, Virginia, January 23, 1953, 1124 EST.

Fig. 4, for January 23, 1953 at 1154 EST which is similar in principle to figures shown by Dieminger and Peterson, is presented as an illustration of the technique. The solid curved lines are a plot of the second-order F1 and F2 layer ordinary-wave traces, and the crosses are a plot of the leading edge of the backscatter echoes. A straight line (A) drawn from the origin tangent to the F2 ordinary-wave second-order trace falls close to the line of the backscatter echoes at the outset. The line of echoes represented by the three lowest crosses illustrate the separation often seen and appears, as mentioned above, to be associated with the extraordinary wave. The crosses at 7.6 and 8.0 mc represent a jog often seen in this type of trace and could represent a region at which resolution of the two separated echo lines ceases to exist. Similar but larger jogs sometimes seen on disturbed days are likely to be due to steep horizontal gradients in the ionosphere.

Another straight line (B) from the origin tangent to the F1 layer ordinary-wave second-order trace falls very close to the points of the type identified with F1 propagated ground scatter in the discussion of Fig. 3.

The isolated slant line (C) below the F2 tangent line is the line along which the F2-layer-propagated scatter echoes would be expected to fall if they were scattered back from an E layer at a virtual height of 105 km above the ground, and it certainly appears here that the scatter does not come from the E layer, especially at the start. The line of scatter echoes approaches nearer to the E-layer line at greater distances, but here it must be remembered that ionization at the reflection point is not the same as overhead ionization and the more distant scatter could have been propagated by a region of greater ion density.

Peterson[5] introduced the concept of "time-delay focus" and demonstrated that it causes the amplitude of a scatter echo to rise rapidly after the minimum-time-delay echo, which represents waves scattered from a greater distance than the skip distance, to a maximum at a delay time still short of the skip-distance delay time. In Fig. 4 the dashed line (D) above the minimum-time-delay line marks the delay time for the skip-distance ray, calculated by the use of N. Smith's transmission curves for the curved earth and curved ionosphere.[6] It will be noted that the difference between the minimum-time-delay ray and the skip ray begins to become negligible at about 800-km slant range. Beyond 950 km the separation apparently widens again. However this is the case only because the minimum-time-delay tangent line was drawn on the flat-earth, flat-ionosphere hypothesis and actually should curve upward and approach the skip ray asymptotically. The upward curvature is caused by the fact that a given apex half angle, angle ϕ_0 on the ray trajectory, is associated with a greater slant range in the curved-earth case than in the flat-earth case, the relative increase becoming greater as distance increases.

Out of a dozen sweeps for the period under consideration which were analyzed in this way, only one yielded a disposition of points which might be considered to be in disagreement with the proposition that the short-range F2-propagated scatter comes from the ground.

Considering the disturbed period, Fig. 5 shows a sequence of eight records for December 17 beginning just after local noon. The records are characterized by high absorption of the lower frequency echoes and great distortion of the traces with distant echo traces

[5] A. M. Peterson, "The mechanism of F-layer propagated backscatter echoes," *Jour. Geophys. Res.*, vol. 56, pp. 221–237; June, 1951.

[6] N. Smith, "The relation of radio sky-wave transmission to ionosphere measurements," Proc. I.R.E., vol. 27, pp. 332–347; May, 1939.

splitting in odd ways, the entire configuration of the sweep changing rapidly from sweep to sweep. Nearly horizontal traces with sharp jogs and straight-line inclined traces in a regular pattern are due to pulse interference.

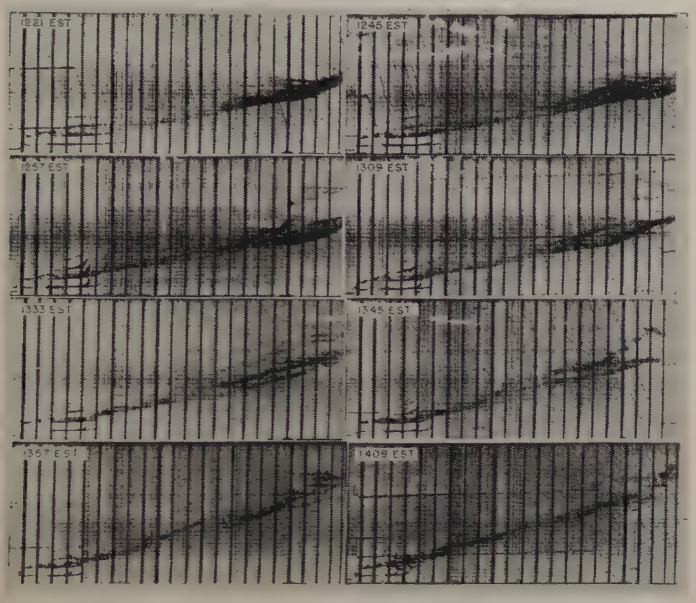

Fig. 5—Sweeps for December 17, 1952.

Although few vertical-incidence sporadic-*E* reflections are seen on this set of records, many were seen on vertical-incidence records made at the same time at nearby Ft. Belvoir, Virginia. The Sterling records for the following day, December 18, showed a great deal of sporadic-*E* reflection. These records will be discussed below under sporadic-*E* phenomena.

In an analysis of a dozen of the records for this period by the tangent-line method, six left no doubt but that the backscatter near vertical incidence was from the ground. The other six were somewhat doubtful but only one of the six gave a distinct impression that the scatter might be coming from the *E* region.

To test the merit of using such backscatter records for determination of the maximum usable frequency over a fixed distance and in particular to test the validity of the assumption that backscatter takes place at the ground rather than at the *E* layer or other ionospheric region, use was made of vertical incidence records obtained during these same two periods at the ionosphere station at Batavia, Ohio, the midpoint of the 1,150-km path between Sterling and St. Louis. As mentioned previously the backscatter records were obtained using rhombic antennas pointed toward St. Louis.

Unfortunately the transmitting operations near St. Louis had been terminated when data-taking was begun in this experiment; however, close agreement between the observed delay times and muf for oblique transmission over the path and the delay times and muf derived from the midpoint records had already been well established. Vertical-incidence sweeps made at Batavia every three minutes were scaled by use of 1,150-km transmission curves to obtain the muf and the virtual height. Using these virtual heights, path-delay times were obtained from geometrical calculations under the assumption that the scatter was from the ground, and then the apparent muf was scaled at these delay times on the 12-minute backscatter sweeps, appropriate sweep-time corrections being made. In the few cases where the scatter records had two branches at the correct delay time, scalings from both were plotted. However, in the subsequent analysis of results only the lower branch was considered, unless the upper branch showed evidence of being a much stronger echo, in which case it alone was considered.

Use of the geometric method, to calculate the delay time for the equivalent triangular path, was justified by previous results of analyses of round-trip travel time for the 1,150-km path which indicated that the geometric method gave travel times agreeing with experiment within about 2 per cent, or almost within experimental error. It should be noted that our "slant range" is really a virtual slant range, since it applies to the equivalent triangular path.

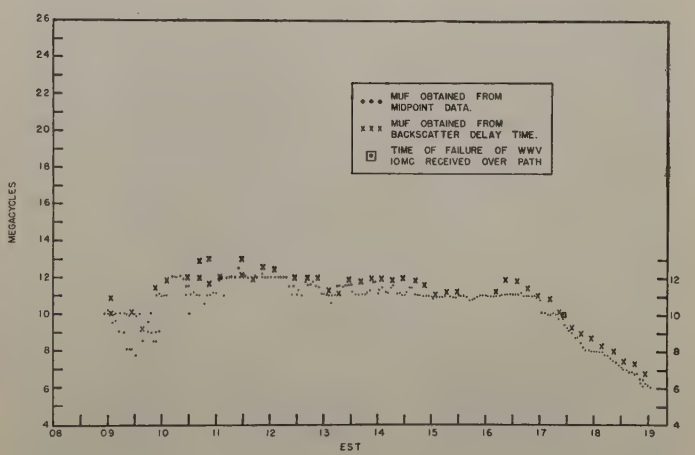

Fig. 6—January 22, 1953; 1,150-km path, assuming ground scatter.

Fig. 6 is for one day of the quiet period, January 22, 1953, dots indicating the path muf computed from the midpoint data and crosses indicating the path muf computed from the backscatter. It is evident that the two sets of muf usually agree to within a few per cent and there is no doubt but that the scatter originates at the ground. The small systematic difference is consistent with results obtained in the oblique incidence experiment between Sterling and St. Louis mentioned previously. As a further check, the small rectangle at 1726 EST indicates the failure of 10-mc transmissions from Station WWV, at Beltsville, Maryland, observed at St. Louis. It is seen that this falls right on the graph of the scatter data. A similar result was obtained on January 23.

Fig. 7 is for one day of the disturbed period December 18, 1952, the dots and crosses having the same meaning as before. The results here are vastly different from those for the previous period. The muf derived from the backscatter sweeps, assuming the ground to be the origin, have much larger values than those derived from the midpoint data.

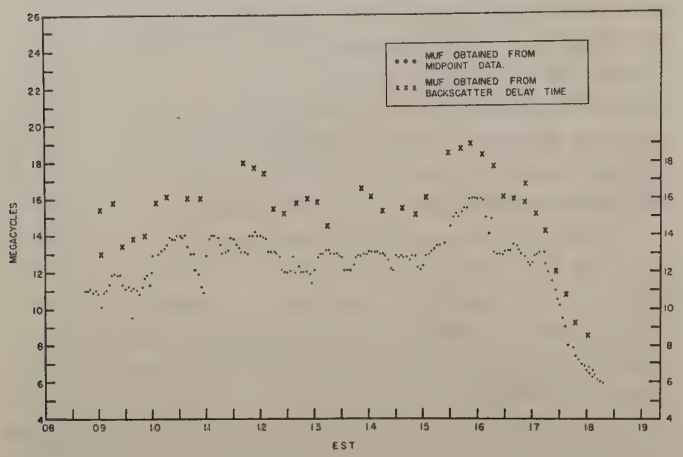

Fig. 7—December 18, 1952; 1,150-km path, assuming ground scatter.

When these results were noted the next logical step appeared to be to assume that the distant E layer was the source of backscatter. A height of 105 km was assumed for the E layer and to simplify calculations, a constant F2-layer virtual height of 300 km was used.

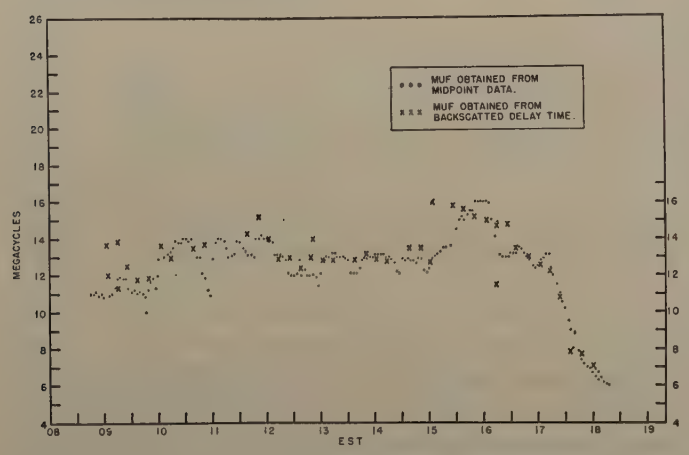

Fig. 8—December 18, 1952; 1,150-km path, assuming E-layer scatter.

The amount by which all slant ranges calculated for ground scatter should be diminished for this case is approximately 240 km. Typical results are shown in Fig. 8. Here it is evident that although there is considerable variation in the difference between the midpoint and backscatter results, the agreement on the whole is very close.

Frequency diagrams of number of observations vs per cent difference (backscatter frequency minus midpoint frequency), (*a*) for the January period assuming ground scatter, (*b*) for the December period assuming ground scatter and (*c*) for the December period assuming E scatter, appear in Fig. 9. Results are expressed in Table I.

TABLE I

Period	Assumed Scatter Source	Number of Observations	Median Difference Per cent	Per cent Difference Exceeded in	
				95% of cases	5% of cases
January 21–33, 1953	ground	73	4.4	−0.8	11
December 17–19, 1952	ground	73	22.9	13.7	39.3
December 17–19, 1952	E layer	95	1.8	−3.2	21.2

The median value of 4.4 per cent by which the values of muf for January 21–23, 1953 determined from the backscatter, assuming ground scatter, exceed those determined from the midpoint data, should be compared with results of the oblique-incidence, two-way pulse experiment previously conducted over the same path in which the median value of the per cent difference between the muf of the actual transmitted pulses and the muf derived from the midpoint data for daytime in January 1952 was 3 per cent. Thus it would appear that for the conditions of January 21–23, 1953 the backscatter assumed to be from the ground was an indicator of muf to within 1 or 2 per cent error.

The median value of 22.9 per cent by which the values of muf for December 17–19, 1952 determined from backscatter, assuming ground scatter, exceed those determined from the midpoint data makes the ground-scatter hypothesis seem invalid. However, when the backscatter muf is based upon assumed scattering from an E layer about 105 km high, a median difference of only 1.8 per cent results, suggesting that scatter by the distant E layer was the source of most of the echoes and that perhaps the correction should be smaller, as would be the case for a slightly lower height of the E layer.

Also, in Fig. 9 the similarity between the distributions for the January 21–23 period, assuming ground scatter, and the December 17–19 period, assuming E scatter, is noted. The wide spread of differences of a small number of points in the December period is probably due to the fact that this period was characterized by stratifications and turbulence. Violent fluctuations of F2 layer muf with time like those on December 17 indicate space fluctuations of a similar magnitude, which would enable the relatively broad-beamed antennas used in this experiment to find paths of equivalent delay time having substantially higher muf than that over Batavia.

One is led to believe by the comparison with the Batavia records that the scatter in the December period was returned from the distant E layer,—yet the scatter trace at lower frequencies merges with the second-order F2 vertical incidence reflection indicating that short distance scatter was from the ground! It is conceivable that there could have been an E layer struc-

ture from which the scattering was much more prominent at oblique incidence than at vertical incidence; but if this were the case, the transition from ground scatter to E-layer scatter should appear on the December 17–19 records, both being visible on some part of a sweep. No clear-cut transition is visible on any of the records. Jogs in the scatter trace like that of Fig. 4 at 7.8 mc could be construed to indicate a mode change, but the effect of F2-layer turbulence may also have played a dominant role. The latter, by producing irregular slant range records could probably mask any transition effects.

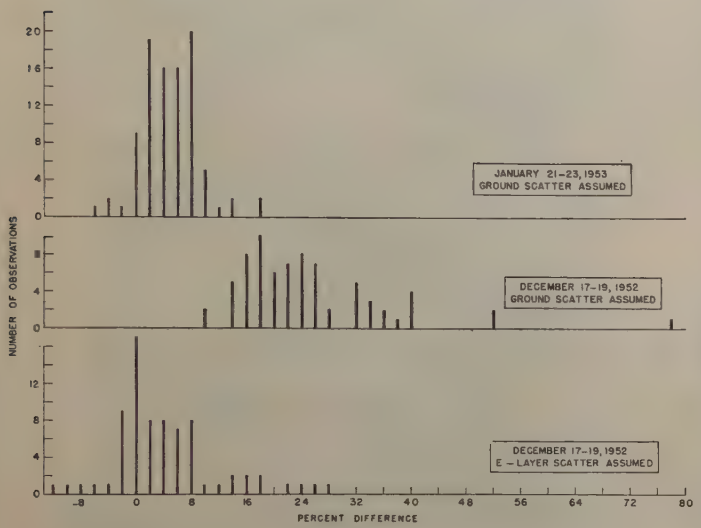

Fig. 9—Distribution of muf differences.

Direct Oblique Reflections from Sporadic E and Ground Scatter Propagated via Sporadic E

The sweep-frequency records tend to bear out conclusions previously reached in studies of range-time records at a fixed frequency that certain echoes represent direct, oblique reflections from sporadic-E regions while others represent ground scatter propagated by sporadic E.[7]

The first of two sweeps in Fig. 10 for December 19, 1952 at 0450 was chosen for examination, first, because at that hour the F2-propagated ground scatter is not seen and, second, because the F2-layer first echo is in a position where it is not mixed with the sporadic-E 2nd echo and the ground scatter propagated by sporadic E. In this sweep the first F2 ordinary-wave echo can be seen faintly in the lower left-hand corner with a minimum virtual height of about 320 km and critical frequency of 3.2 mc. Below it at a little over 100 km is seen the first-order sporadic E reflection terminating at about 4.2 mc.

Above the regular sporadic E reflection is clearly seen the diffuse second-order reflection. Out of this is seen to develop a very dense echo which recedes to 800 km at 19 mc. A fainter echo group finally fades out at 21 mc and 1,150 km. The strong echo appears to be ground scatter propagated via sporadic E ionization since it grows out of the second-order echo. It is also evident that, since the sporadic-E distance factor for an 800-km slant range is about 2.8, the maximum frequency value at this distance would have to be associated with a sporadic E region at a control point where the maximum frequency value, assuming power dependence is not important, is of the order of 7 mc. Below the dense echoes there are weak echoes running out to about 13 mc at 300 km which could be due to oblique reflections directly from a localized sporadic E region.

In the sweep for 0514 on the same day the F2 reflections are not seen. Here the apparent direct reflections from sporadic E go out beyond 18 mc at about 400 km. The dense, longer-range echo again appears to be ground scatter propagated via sporadic E.

An oblique echo which exhibits a fixed range with increasing frequency such as the sharp one at 1,150 km in the sweep for 0450 probably represents reflection or scattering off a small dense region of sporadic E or ground scatter propagated by such a region.

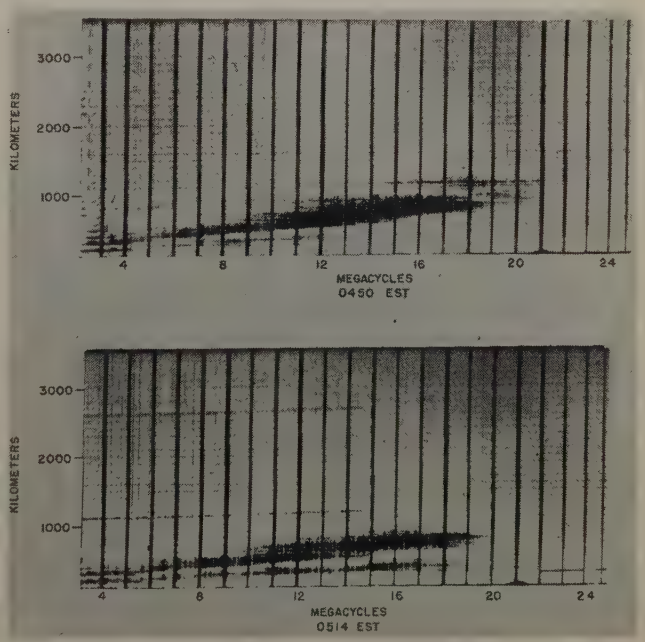

Fig. 10—Sweeps for December 19, 1952.

Fig. 11 is a series of three daytime sweeps made on December 18, 1952, which illustrates phenomena associated with sporadic E in addition to the regular scatter traces. In the sweep for 1155 EST direct sporadic E scattering from an obliquely situated region is evident out to nearly 11 mc at 200 km. Another heavy sporadic E trace appears to grow out of the second-order sporadic-E echo and blots out the first-order F2 reflections, finally terminating at 13 or 14 mc and 500 km. This appears to be the ground-scatter type because of its receding range and association with second-order spo-

[7] W. L. Hartsfield and R. Silberstein, "A comparison of cw field intensity and backscatter delay," Proc. I.R.E., vol. 40, pp. 1700–1076; December, 1952.

radic E. The sweep for 1231 shows a similar effect apparently with direct reflections from many small clouds and stratifications of sporadic E at short ranges.

In the sweep for 1307 the scatter appearing after the first-order F2 reflection upon casual inspection might be interpreted as direct scatter from the F2 layer since the dense part starts after the F2 ordinary-wave critical frequency, continuing to 9 mc, and since a similar appearing and equally dense trace occurs at about twice the delay time, apparently superimposed on the regular scatter trace emanating from the second-order F2 trace. A few other sweeps around this time had similar features, but there seems to be no definite reason why direct F2 scatter should have appeared.

Questions arising out of study of the record for 1307 led to a determination of how a particular mode, the "1F" mode proposed by Eckersley[8] would appear. This mode is the case of the wave being reflected at the F2 region, striking a distant scattering source in the E layer and returning directly to the transmitter. The reverse passage of the wave would be equally possible. Results

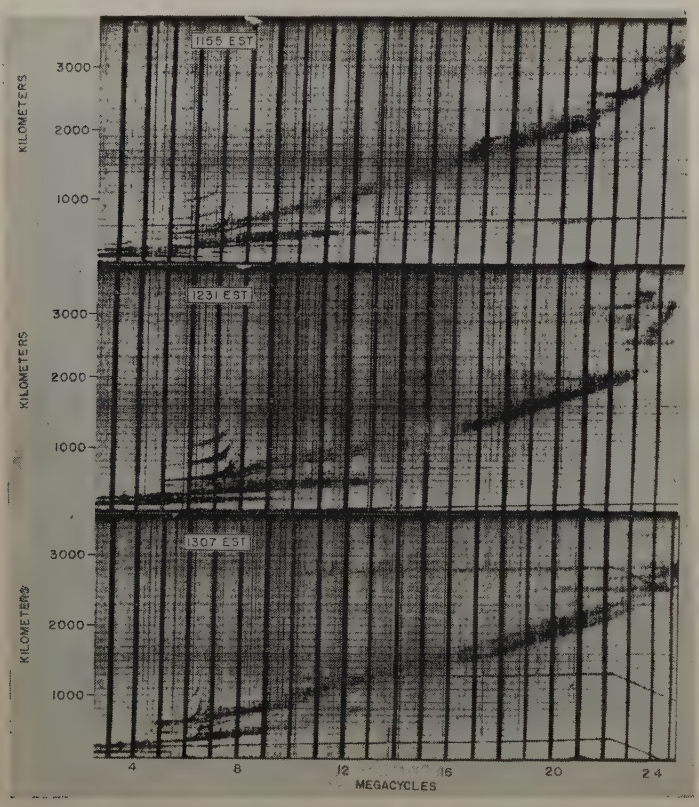

Fig. 11—Sweeps for December 18, 1952.

of an analysis indicate that the mode grows out of the first-order F2 reflection a little below the critical frequency. It should go to higher virtual heights than the heavy scatter emanating from the first F2 echo in any of the sweeps in Fig. 11. The thin steep trace going from about 6.6 mc at 470 km to 7.8 mc at 600 km in the record for 1307 was thought possibly to be such a trace, but does not agree well with the calculated curve. Because of the low angle, the phenomenon, if seen, should be chiefly for fairly short distances, and it might be deduced from the records so far examined that the mode does not play a very important role.

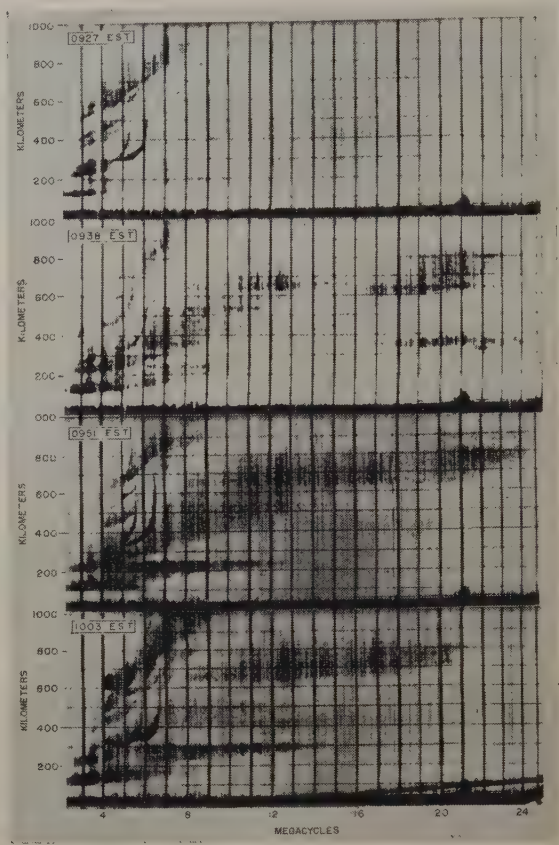

Fig. 12—Sweeps for December 24, 1952.

Fig. 12 is a sequence of four sweeps for December 24 with a 1,000-km range scale illustrating more sporadic-E phenomena in addition to the regular scatter growing out of the second-order F2 modes. Echoes appear which have the properties of direct and oblique reflections from sporadic-E regions and ground scatter propagated by sporadic E in rapidly changing configurations. "M" reflections are also seen.

Conclusion

Sweep-frequency backscatter records, by introducing the frequency parameter into scatter-sounding techniques, make it possible to obtain a large number of samples for study of phenomena on a given frequency or at a given distance in any one day. Also the development of echoes as frequency increases gives strong clues as to their origin and as to the relative quietness or disturbance of the ionosphere in the period under study.

Under certain quiet ionospheric conditions the measurement of maximum usable frequency and therefore of skip distance, from backscatter records under the assumption that scattering is from the ground yields excellent results; however, it was demonstrated that the same assumption yields very erroneous results during a period of intense sporadic E reflection. Under these latter conditions the distant scatter appears to originate

[8] T. L. Eckersley, "Analysis of the effect of scattering in radio transmissions," *Jour. IEE*, vol. 86, pp. 548–563, disc. 563–567, Fig. 23b, p. 559; June, 1940.

at the E layer, although nearby scatter still appears to originate at the ground. To date no clear transition between the two sources has been observed on any one sweep and not enough data have been taken to afford observations on the change between the type of ionospheric conditions where distant scatter appears to come from the E layer and the type where it appears to come from the ground.

Relative to the effectiveness of backscatter measurements in skip distance indication it can be said that a single frequency technique may fail during a low-latitude disturbance, which is not forecast at present by forecasting agencies; yet during such disturbances signal behavior is erratic and skip-distance information would be desirable. It is noteworthy[9] that commercial equipment for skip-distance determination permitting measurements on several frequencies has recently been described in the literature.

The sweep-frequency technique tends to confirm the presence of direct scatter from discrete regions ("clouds") producing sporadic-E reflections and of ground scatter propagated by sporadic E but the echo patterns are frequently so complex as to make a positive statement about any one very difficult.

The sensitivity of the records to varying conditions of the ionosphere indicates that disturbance tracking and forecasting by its means may be possible.[7,10]

The use of high power with very high-gain, narrow-beam antennas should make a study of night F2-layer propagated backscatter echoes possible, thus affording information on propagation of the lower, high frequencies during the hours of darkness.

[9] L. C. Edwards, COZI—Communications Zone Indicator, *Electronics* vol. 28, pp. 152–155; August, 1953.

[10] R. S. Lawrence, "Continental maps of four ionospheric disturbances," *Jour. Geophys. Res.*, vol. 58, p. 219; 1953.

Some Stochastic Problems in Wave Propagation—Part II*

JOSEPH FEINSTEIN†

Summary—**In part I some of the properties of wave energy reflected from surfaces subject to random height variations were investigated in the previous issue.**

Here we ascertain the effects of refractive index fluctuations within a volume upon the properties of waves traversing the medium. The results are applied to problems encountered in tropospheric and ionospheric wave propagation.

Volume Problems

Tropospheric Applications

RECENT WORK[1] on the effects of refractive index fluctuations upon wave propagation has been based upon the primary scattering produced by the dipoles equivalent to the medium fluctuations. An alternative viewpoint, developed here, considers the phase incoherence introduced into the wave fronts by these refractive index fluctuations. This approach takes account of multiple scattering which, although it may play an important role in the ionosphere is not likely to be of significance in the troposphere. While the two methods are equivalent when only single scattering enters, the phase incoherence approach leads in a natural way to a diffraction phenomenon which has thus far been overlooked in the scattering theory treatment of propagation beyond the horizon. In addition, the determination of the fluctuation characteristics of wave energy within line of sight seems better adapted to the methods of this paper.

Phase Fluctuations Produced by a Finite Thickness Screen: We consider the field produced at plane Q, a distance D_2 from a slab of medium of thickness R, illuminated by a transmitter at a distance D_1 (Fig. 1). Employing usual second-order phase approximation,

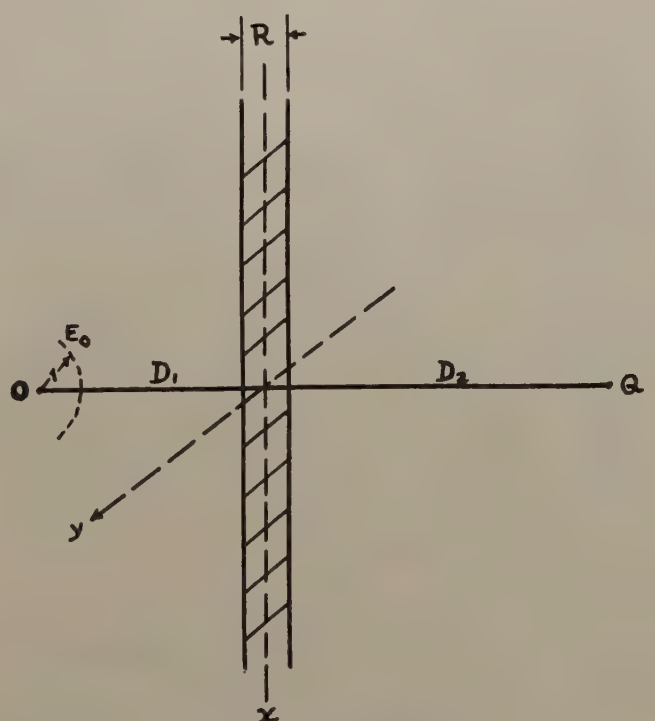

Fig. 1—Single slab geometry.

$$E_Q(x_0, y_0, t) = \frac{kE_0 e^{-i\omega_0 t}}{2\pi D_1 D_2} \int\int_{-\infty}^{\infty} \cdot e^{ik\left\{\frac{x^2+y^2}{2D_1}+\frac{(x+x_0)^2+(y+y_0)^2}{2D_2}\right\}+i\Delta\phi(x,y,t)}\, dxdy \qquad (1)$$

* Revised manuscript received by PGAP, January 18, 1954.

† Bell Telephone Labs., Murray Hill, N. J.

[1] H. G. Booker and W. E. Gordon, "A theory of radio scattering in the troposphere," Proc. I.R.E., vol. 38, p. 401; April, 1950.

for $R \ll D_{1,2}$ where x_0, y_0 are co-ordinates in the xy plane of Fig. 1, the origin being taken as the intersection with the xy plane of a perpendicular from the transmitter; $\Delta\phi$ is the phase departure from its mean value introduced by the fluctuations in the slab. The association of this phase with a single point in a plane carries with it the implication of phase integration through the slab, $\Delta\phi = k\int_R \Delta\mu(r_1, t)dr_1$, each trajectory being specified by its point of intersection with the reference plane. For simplicity, $\Delta\mu$ will be taken as real, thus neglecting absorption. We are interested in obtaining the correlation pattern at Q, defined as:

$$\overline{C}_Q(x_0, y_0; s, v) = \lim_{T\to\infty} \frac{1}{2T}\int_{-T}^{T} dt \cdot E_Q(x_0, y_0, t)\cdot E_Q^*(x_0+s, y_0+v, t). \quad (2)$$

Using (1), and interchanging order of integration:

$$\overline{C}_Q(x_0, y_0; s, v) = \left(\frac{E_0 k}{2\pi D_1 D_2}\right)^2 \int\int_{-\infty}^{\infty}\int\int dx dx' dy dy' \cdot e^{\frac{ik}{D}(x^2-x'^2+y^2-y'^2)} \cdot e^{\frac{ik}{D_2}\left\{s(x+x_0)+v(y+y_0)+x_0(x-x')+y_0(y-y')-\frac{s^2}{2}-\frac{v^2}{2}\right\}} \cdot \frac{1}{2T}\int_{-T}^{T} dt \cdot e^{i[\Delta\phi(x,y,t)-\Delta\phi(x',y',t)]}. \quad (3)$$

To proceed further, the statistical properties of $\Delta\phi$ must be specified,—in particular the probability distribution of "$\Delta\phi(x, y, t)-\Delta\phi(x', y', t)$." Since each $\Delta\phi$ is composed of a large number of random contributions as a result of the integration of $(\Delta\mu)$ over each trajectory, we may invoke the central limit theorem to justify the assumption of a bivariate normal joint distribution. Then the difference of the $\Delta\phi$'s is also normally distributed with variance $\overline{(\Delta\phi)^2}(x-x', y-y')$, a function only of the difference of the coordinates if the fluctuations are homogeneous. Average over time may now be replaced by average over the probability distribution:

$$\frac{1}{2T}\int_{-T}^{T} dt \cdot e^{i[\Delta\phi(x,y,t)-\Delta\phi(x',y',t)]} = \int_{-\infty}^{\infty} \frac{e^{-\frac{(\delta\phi)^2}{2\overline{(\Delta\phi)^2}_{x-x',y-y'}}}}{\sqrt{2\pi\overline{(\Delta\phi)^2}_{x-x',y-y'}}} \cdot e^{i\delta\phi} \cdot d(\delta\phi) = e^{-\frac{1}{2}\overline{(\Delta\phi)^2}(x-x', y-y')}. \quad (4)$$

Making the transformations $\xi = x-x'$, $\eta = y-y'$ in (3), and utilizing the Fourier integral theorem:

$$\overline{C}_Q(x_0, y_0; s, v) = \left(\frac{E_0}{D_1+D_2}\right)^2 \cdot e^{-\frac{1}{2}\overline{(\Delta\phi)^2}\left(\frac{sD_1}{D_1+D_2}, \frac{vD_1}{D_1+D_2}\right)} \cdot e^{\frac{ik}{D_1+D_2}\left(sx_0+vy_0-\frac{s^2}{2}-\frac{v^2}{2}\right)}. \quad (5)$$

For a plane wave ($D_1 \simeq \infty$) at normal incidence ($x_0 = y_0 = 0$) we continue to obtain the field correlation pattern at the slab, over all parallel planes. This result has been obtained previously for a one-dimensional screen.[2] In the more general case, a scale factor enters, and an oscillating phase factor is superimposed upon the pattern. We next determine the mean square difference of phase along two trajectories, 1 and 2.

$$\overline{(\Delta\phi)_{1,2}}^2 = \frac{k^2}{2T}\int_{-T}^{T} dt \left\{\int_0^{R_1} \Delta\mu(r_1, t)dr_1 - \int_0^{R_2} \Delta\mu(r_2, t)dr_2\right\}^2 \quad (6)$$

$$= \frac{k^2}{2T}\int_{-T}^{T} dt \left\{\int_0^{R_1}\int_0^{R_1} \Delta\mu(r_1, t)\Delta\mu(r_1', t)dr_1 dr_1' + \int_0^{R_2}\int_0^{R_2} \Delta\mu(r_2, t)\Delta\mu(r_2', t)dr_2 dr_2' - \int_0^{R_2}\int_0^{R_1} \Delta\mu(r_1, t)\Delta\mu(r_2^1, t)dr_1 dr_2' - \int_0^{R_1}\int_0^{R_2} \Delta\mu(r_2, t)\Delta\mu(r_1', t)dr_2 dr_1'\right\}. \quad (6a)$$

If we define a correlation function in the medium by:

$$\frac{1}{2T}\int_{-T}^{T} dt \cdot \Delta\mu(\underline{r}, t)\cdot\Delta\mu(\underline{r}', t) = \overline{(\Delta\mu)^2}\rho(\underline{r}, \underline{r}') \quad (7)$$

then for parallel trajectories with perpendicular spacing "q," (6a) becomes:

$$\overline{(\Delta\phi)_q}^2 = 2k^2\overline{(\Delta\mu)^2}\left\{\int_0^{R_1} dr_1 \int_{r_1}^{-R_1+r_1} \rho(s)ds - \int_0^{R_1} dr_1 \int_{r_1}^{-R_1+r_1} \rho(s, q)ds\right\} \quad (8)$$

$$= 2k^2\overline{(\Delta\mu)^2}\left\{\int_{-R}^{R} (R-s)\rho(s)ds - \int_{-R}^{R} (R-s)\rho(s, q)ds\right\} \quad (8a)$$

where the transformation $s = r_1 - r_1' = r_2 - r_2'$ has been made; for isotropic turbulence, $\rho(s, q) = \rho(\sqrt{s^2+q^2})$. If the slab thickness, R_1 is several times the scale of turbulence, limits of $\pm\infty$ may be employed on the integrals involving ρ, and $(R-s) \simeq R$. Finally then, for a correlation function of the form $\rho(u) = e^{-u^2/l^2}$, one obtains:

$$\overline{(\Delta\phi)_q}^2 = 2k^2\overline{(\Delta\mu)^2}\cdot R\cdot l\cdot\sqrt{\pi}(1-e^{-q^2/l^2}) \quad (9a)$$

while with $\rho(u) = e^{-|u|/l}$

$$\overline{(\Delta\phi)_q}^2 = 4k^2\overline{(\Delta\mu)^2}\cdot R\cdot l\cdot\left[1-\frac{|q|}{l}K_1\left(\frac{|q|}{l}\right)\right] \quad (9b)$$

where K_1 is the Bessel function of the second kind for imaginary argument. For substitution in (4) and (5) one of course sets $q = \sqrt{(x-x')^2+(y-y')^2}$.

The technique of phase integration is essentially a geometric optical one. Consequently diffraction effects are neglected over the thickness of the slab, which is re-

[2] H. G. Booker, J. A. Ratcliffe, D. H. Shinn, "Diffraction from an irregular screen," *Phil. Trans. Roy. Soc. A*, vol. 242, p. 579; Sept., 1950.

quired to have a value a few times the scale of coherence in virtue of the assumptions above. This is analogous to neglecting diffraction over a distance of a few slit widths in front of a slit, an approximation which does not appear serious.

Extension to multiple screens: To consider the effect of a series of slabs upon the wave, we take the field incident upon slab n at distance z_n from the source as that which has emerged from slab $(n-1)$ at z_{n-1}, and evaluate the additional phase incoherence introduced on a plane at z_{n+1}.

$$E_{z_{n+1}}(x_0, y_0, t) \sim \iint_{-\infty}^{\infty} E_{z_n}(x, y, t) \cdot e^{\frac{ik}{2(z_{n+1}-z_n)}[(x+x_0)^2+(y+y_0)^2]+i\Delta\phi_n(x,y,t)}\, dxdy. \tag{10}$$

The correlation pattern at this position is then:

$$\overline{C}_{z_{n+1}}(x_0, y_0; s, v) = \frac{1}{2T}\int_{-T}^{T} dt \cdot \iiiint_{-\infty}^{\infty} E_{z_n}(x, y, t)\cdot E_{z_n}{}^*(x', y', t) \cdot e^{i\{\Delta\phi_n(x,y,t)-\Delta\phi_n(x',y',t)\}} \cdot dxdx'dydy' \cdot e^{\frac{ik}{2(z_{n+1}-z_n)}[(x+x_0)^2+(y+y_0)^2-(x'+x_0+s)^2-(y'+y_0+v)^2]} \tag{11}$$

After transforming variables through $\xi = x - x'$, $\eta = y - y'$, the time average of the product of the fields at z_n may be replaced by the correlation pattern (5), after setting $x_0 = x$, $y_0 = y$, $s = \xi$, $v = \eta$, $D_1 = z_{n-1}$, $D_2 = z_n - z_{n-1}$ in this pattern. The time average over the phase fluctuations introduced by the nth screen is taken separately, since events on this screen are not correlated with the incident wave. This yields an expression analogous to (4). The x dependence in (11) has the form

$$\frac{ik}{e^{z_{n+1}-z_n}} x\left(\frac{z_{n+1}}{z_n}\xi - s\right),$$

so that integration over x yields a delta function of argument $[(zn+1/zn)\xi - s]$. Integration over ξ then amounts to setting $\xi = sz_n/(z_{n+1})$. (This procedure is identical with employing the Fourier integral theorem, as was done in deriving (5)). Analogous results follow for y and η, so that (11) yields:

$$\overline{C}_{z_{n+1}}(x_0, y_0; s, v) = \left(\frac{E_0}{z_{n+1}}\right)^2 \cdot e^{-\frac{1}{2}\overline{(\Delta\phi)^2}_{n-1}\left(s\frac{z_{n-1}}{z_{n+1}},\, v\frac{z_{n-1}}{z_{n+1}}\right)} \cdot e^{-\frac{1}{2}\overline{(\Delta\phi)^2}_n\left(\frac{sz_n}{z_{n+1}}, \frac{vz_n}{z_{n+1}}\right)} \cdot e^{\frac{ik}{z_{n+1}}\left(sx_0+vy_0-\frac{s^2}{2}-\frac{v^2}{2}\right)}. \tag{12}$$

For a group of m discrete slabs positioned at distances z_m from the source, the correlation pattern at distance D, is given by:

$$\overline{C}_D(x_0, y_0; s, v) = \left(\frac{E_0}{D}\right)^2 \cdot e^{\frac{ik}{D}\left(sx_0+vy_0-\frac{s^2}{2}-\frac{v^2}{2}\right)} \cdot \prod_{m=1}^{M} e^{-\frac{1}{2}\overline{(\Delta\phi)_m{}^2}\left(\frac{sz_m}{D}, \frac{vz_m}{D}\right)}. \tag{13}$$

This result is subject to a rather simple interpretation. Since the product of a group of exponentials is equivalent to a sum of exponents the phase incoherence effects introduced by the slabs, each modified by a scale factor in accordance with the ratio of source-slab to source-receiver distance, add at the receiver plane. Precisely this result would follow from the geometric optical method of integrating the phase along the total path of each ray from source to receiver. There is this difference, however. The solution obtained here by the methods of physical optics is a consequence of the infinite limits on the various integrals taken over the $x-y$ plane, i.e., each slab of medium was taken to be infinite in the transverse directions. Geometric optics does not impose this requirement. So long as diffraction effects are unimportant over the entire path length a one-to-one correspondence exists between points on the wave-front at difference z, rendering the concepts of geometric optics valid. This is the situation for $l/\lambda \to \infty$. Once diffraction enters however, it is an area on a given wave front which contributes to the field at a point on a succeeding wave front. The significance of (13) lies in its statement that the scattering of energy out of the direct ray under these conditions is exactly compensated by the diffracted energy from adjacent portions of the wave front. It should be noted that if the angular range over which significant diffraction occurs becomes sufficiently large to make it necessary to take account of the variation of the distance attenuation and obliquity factors assumed constant in (l), these results no longer hold. For the usual values of "1" encountered in the troposphere this condition appears unlikely.

We should now like to generalize (13) to continuous media. To this end we may visualize the distance D divided into sections R, each at least several times the scale of turbulence, l, so that the coherence between sections is negligible compared to that within a section. Then provided $D \gg R$ so that the scale factor remains essentially constant within a section and neglecting for the moment the apparent failure of the second order phase approximation as the distance between slabs becomes small, we may substitute an integration of the exponent in (13) for the discrete set of product factors. Neglecting phase factor (we may take $x_0 = y_0 = 0$; the Fresnel zone argument $k(s^2+v^2)/2D$ is generally slowly varying compared to correlation pattern amplitude), we obtain for gaussian correlation function:

$$\overline{C}_D(s, v) = e^{-\int_0^D k^2\overline{(\Delta\mu)^2}l\sqrt{\pi}\left[1-e^{-(z/D)^2(s^2+v^2/l^2)}\right]dz} \tag{14a}$$

while utilizing (9b), the exponential correlation function yields:

$$\overline{C}_D(s, v) = e^{-\int_0^D 2k^2\overline{(\Delta\mu)^2}l\left[1-\frac{z\sqrt{s^2+v^2}}{lD}K_1\left(\frac{z\sqrt{s^2+v^2}}{lD}\right)\right]dz}. \tag{14b}$$

For homogeneous turbulence, $\overline{(\Delta\mu)^2}$ and l may be removed from the integral, so that (14a) reduces to:

$$\overline{C}_D(s, v) = e^{-\sqrt{\pi}k^2\overline{(\Delta\mu)^2}lD\left[1-\frac{l}{\sqrt{s^2+v^2}}\cdot\frac{\sqrt{\pi}}{2}\,\mathrm{erf}\left(\frac{\sqrt{s^2+v^2}}{l}\right)\right]} \quad (15a)$$

while (14b) becomes:

$$\overline{C}_D(s, v) = e^{-2k^2\overline{(\Delta\mu)^2}lD\left[1+K_0\left(\frac{\sqrt{s^2+v^2}}{l}\right)-\frac{}{\sqrt{s^2+v^2}}\int_0^{\sqrt{s^2+v^2}/l}K_0(u)du\right]}. \quad (15b)$$

We must now consider the significance of these expressions in the light of the fact that the second order phase approximation upon which they are based is valid only for energy transmission from section to section within cones of small angle; except for cases wherein geometric optics is applicable, this condition would appear to be violated as the continuous limit is approached. A quantitative error criterion may be obtained from a power series expansion of the exponential in (15). The terms in such an expansion may be interpreted as the various orders of scattering; the contribution of single scattering, for example, is given by the linear term and represents the sum of the scattered waves produced by all the slabs, the effect of each being calculated in the absence of all the others. It is apparent that our phase approximation is valid for this term, except possibly for a few slabs at each end of the path. Similarly the quadratic term gives the second order interactions which number $n(n-1)/2$ for n slabs, of which only n are between adjacent slabs. For $D \gg l$, consequently, the approximation will break down only at quite high orders of scattering, and under conditions such that these high orders are of importance, several of our other approximations will fail. For the usual conditions encountered in tropospheric propagation only single scattering is of importance so that the expansions of (15a, b) need be carried only through the linear terms.

Information may be obtained about the frequency power spectrum of the received signal, by forming the temporal (auto-) correlation:

$$\overline{P}_D(\tau) = \frac{1}{2T}\int_{-T}^{T} dt\cdot E_D(t)\cdot E_D^*(t+\tau) \quad (16)$$

$$\overline{P}_D(\tau) \sim e^{i\omega_0\tau}\iiiint_{-\infty}^{\infty} e^{\frac{ik}{2D}(x^2-x'^2+y^2-y'^2)}\cdot dx\,dx'\,dy\,dy' \cdot\frac{1}{2T}\int_{-T}^{T} dt\cdot e^{i[\Delta\phi(x,y,t)-\Delta\phi(x',y',t+\tau)]}. \quad (16a)$$

To proceed through steps analogous to (6), (7), and (8) we must define a new type of correlation function:

$$\frac{1}{2T}\int_{-T}^{T} dt\cdot\Delta\mu(\underline{r}, t)\cdot\Delta\mu(\underline{r}', t+\tau) = \overline{(\Delta\mu)^2}C(\underline{r}-\underline{r}', \tau). \quad (17)$$

If it is assumed that "$\Delta\phi(x, y, t)$ and $\Delta\phi(x', y', t+\tau)$" continue to have a bivariate normal distribution then (4) is applicable. Finally we must make some assumption regarding the space-time correlation function in (17). If we write

$$C(\underline{r}-\underline{r}', \tau) = \rho(\underline{r}-\underline{r}')\cdot p(\tau) \quad (18)$$

then (16a) becomes:

$$\overline{P}_D(\tau) \simeq e^{-a[1-p(\tau)]}\cdot e^{i\omega_0\tau} \quad (19)$$

where $a = bk^2\overline{(\Delta\mu)^2}lD$. "$b$" having the value $\sqrt{\pi}$ for a gaussian "ρ," and 2 for a brownian "ρ."

The power spectrum is now obtained as the transform of the autocorrelation function:

$$\overline{P}(\omega) = \int_{-\infty}^{\infty} e^{i\omega\tau}\cdot\overline{P}_D(\tau)\cdot d\tau. \quad (20)$$

For $p(\tau) = e^{-\tau^2/2T_0^2}$, we obtain

$$\overline{P}(\omega) = e^{-a}\left\{\delta(\omega-\omega_0)+\frac{T_0}{\sqrt{2\pi}}\sum_{n=1}^{\infty}\frac{a^n}{n!\sqrt{n}}\cdot e^{-\frac{(\omega-\omega_0)^2}{2n}T_0^2}\right\}. \quad (20a)$$

Diffraction Beyond the Horizon Produced by Phase Incoherence: In this section we consider the effect of phase incoherence due to turbulence in modifying the diffraction field which results from earth curvature. Fig. 2

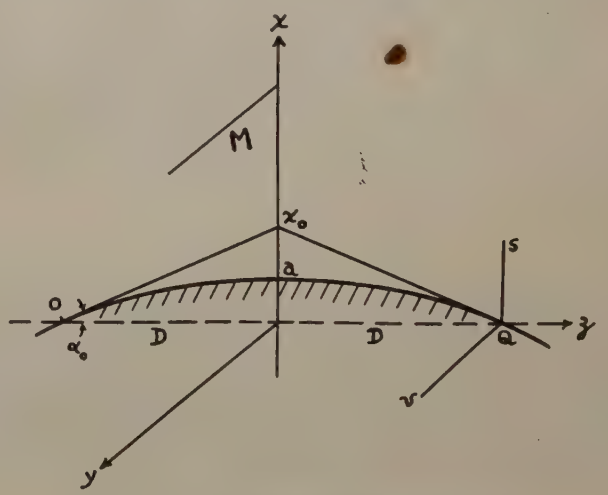

Fig. 2—Diffraction beyond the horizon.

illustrates the physical situation. The new element here is the fact that the point of stationary phase in the x-co-ordinate, $x=0$, no longer lies in the volume of integration. We obtain the field at Q by summing the contributions which arise from the field on the mid-plane M, each with its proper phase.

$$E_Q = \frac{k}{\pi D}\int_{-\infty}^{\infty} dy\int_{a}^{\infty} dx\cdot E_M(x, y, t)\cdot e^{\frac{ik}{2D}(x^2+y^2)+i\Delta\phi(x,y,t)} \quad (21)$$

where normalization with respect to the free space field has been introduced; $\Delta\phi$ is the phase variation introduced into the wave in going from M to Q. The average power received at Q is then:

$$\overline{P}_Q = \left(\frac{k}{\pi D}\right)^2 \cdot \frac{1}{2T} \int_{-T}^{T} dt \cdot \iiiint_{x,x'=a,y,y'=-\infty}^{\infty} E_M(x, y, t) \cdot E_M^*(x', y', t) \cdot e^{i[\Delta\phi(x,y,t) - \Delta\phi(x',y',t)]_{MQ}} \cdot e^{\frac{ik}{2D}(x^2 - x'^2 + y^2 - y'^2)} \cdot dx dx' dy dy'. \quad (22)$$

After usual change of variable $\xi = x - x'$, $n = y - y'$, correlation pattern given by (13) with amplitude as in (14b) is substituted for $\overline{E_M E_M}^*$; argument $(x_0, y_0; s, v)$ of the latter is of course replaced by $(x, y; \xi, \eta)$. For the time average of the difference of the $(\Delta\phi)$'s is (22) we gain employ (4), (9b), and finally (14b):

$$\overline{P}_Q = \left(\frac{k}{\pi D}\right)^2 \int_a^\infty dx \int_{-\infty}^{\infty} dy \int_{-\infty}^{\infty} d\xi \int_{-\infty}^{\infty} d\eta \cdot F^2(x) \cdot e^{\frac{ik}{D}(2x\xi + 2y\eta - \xi^2 - \eta^2)} \cdot e^{-2\int_0^D 2k^2 l \overline{(\Delta\mu)^2} \left[1 - \frac{z\sqrt{\xi^2+\eta^2}}{lD} K_1\left(\frac{z\sqrt{\xi^2+\eta^2}}{lD}\right)\right] dz}. \quad (23)$$

The integration over y yields $(\pi D/k)/\delta(\eta)$, so that integration over η merely consists of setting $\eta = 0$. The factor $F^2(x)$ has been introduced to connote the fact that between $x = a$, the surface of the earth, and $x = x_0$, the horizon, the field increases gradually from a very small value to its free space value. Since $4k^2\overline{(\Delta\mu)^2} lD \ll 1$ for the usual tropospheric case, we may employ the first two terms of the exponential expansion:

$$\overline{P}_Q = \frac{k}{\pi D} \int_a^\infty dx \int_{-\infty}^{\infty} d\xi \cdot F^2(x) \cdot e^{-\frac{ik}{D}\xi^2} \cdot e^{\frac{2ik}{D}x\xi} \cdot \left[1 - 4k^2\overline{(\Delta\mu)^2} lD \left(1 - \int_0^D \frac{\xi z}{lD} K_1\left(\frac{\xi z}{lD}\right) \cdot dz\right)\right], \quad (24)$$

where homogeneous turbulence has been assumed. For $\overline{(\Delta\mu)^2} = 0$ over the whole path the integration of (24) would give rise to the small diffracted field at Q characteristic of propagation over a spherical earth. Since we are interested in the contribution which results from phase incoherence we shall neglect this first term and begin the X-integration from x_0. In addition we may neglect the phase variation produced by exp $(-ik\xi^2/D)$ compared to exp $(2ikx\xi/D)$ provided the vertical dimension (x) of the effective contributing volume is much greater than "l," the scale of coherence (which determines the effective limits of ξ). With these changes

$$\overline{P}_Q \simeq \frac{k}{\pi D} (4k^2\overline{(\Delta\mu)^2} lD) \int_{x_0}^{\infty} dx \int_{-\infty}^{\infty} d\xi \cdot e^{\frac{2ik}{D}x\xi} \cdot \int_0^D dz \frac{\xi z}{lD^2} K_1\left(\frac{\xi z}{lD}\right) \quad (25)$$

$$\simeq k^2\overline{(\Delta\mu)^2} lD \left[1 - g \log\left(\frac{1}{g} + \sqrt{1 + \frac{1}{g^2}}\right)\right] \quad (25a)$$

where $g = 2klx_0/D$. For $g \gg 1$, corresponding to large scale turbulence, there results:

$$\overline{P}_Q \simeq \frac{1}{24} \frac{R_e^2 \overline{(\Delta\mu)^2}}{lD} \quad (26)$$

where R_e is the radius of the earth. It is interesting to compare this value with the contribution made by direct scatter from turbulence lying within line of sight. For the exponential type correlation function used above, an expression for the average power per unit volume has been given in reference (6). For large "g," integration of this expression over the trough shaped region above line of sight yields precisely the same dependence upon the parameters as does (26); the magnitude is virtually identical with that of (26) for the same $\overline{(\Delta\mu)^2}/l$. In practice furthermore one would expect this turbulence parameter to decrease with increasing altitude. Since (23) indicates that it is a weighted mean of this parameter over the total path which is to be employed in (26), whereas only its value above line of sight is to be used in evaluating the direct scatter, the contribution of (26) can be expected to strongly dominate over the direct scatter at large distances. From the point of view which treats the effects of medium fluctuations as scattering, the field contribution derived here represents the diffraction of forward scatter.

To obtain correlation pattern over a vertical plane at the receiver, we add a displacement (s, v) to (x, y) in phase term of (22). Integration over y then leads to $\delta[\eta - (v/2)]$, so that we set $\eta = v/2$ to integrate over η. Integration over ξ can be performed next, leaving:

$$\overline{C}_Q(s, v) = \int_{x_0}^{\infty} dx \cdot e^{\frac{iks}{D}x} \int_0^D dz \cdot \frac{1}{D}\left(\frac{z}{lD}\right)^2 \cdot e^{-\frac{v}{2}\left[\left(\frac{2kx}{D}\right)^2 + \left(\frac{z}{lD}\right)^2\right]^{1/2}} \cdot \left\{\frac{1 + \frac{v}{2}\left[\left(\frac{2kx}{D}\right)^2 + \left(\frac{z}{lD}\right)^2\right]^{1/2}}{2\left[\left(\frac{2kx}{D}\right)^2 + \left(\frac{z}{lD}\right)^2\right]^{3/2}}\right\}. \quad (27)$$

This expression can be evaluated for $g \gg 1$.

For the special cases where s or v equal zero, we obtain for the normalized correlation amplitudes:

$$\frac{\overline{C}_Q(s, 0)}{\overline{P}_Q} \cong \frac{\sin ks\alpha_0}{ks\alpha_0}; \qquad \frac{\overline{C}_Q(0, v)}{\overline{P}_Q} \cong e^{-kv\alpha_0} \quad (28)$$

where $\alpha_0 = x_0/D$. Corresponding expressions for direct scatter are similar, although not identical, but the differences do not seem sufficient to admit of an experimental discrimination. What experimental evidence there is seems to be in agreement with forms such as (28).

Too, these correlation expressions prove of value when effect of objects adjacent to source or receiver can be represented by means of images. Example: If effect of ground reflection upon transmitter and receiver antenna fields can be represented by images at positions separated in height by h_T and h_R respectively (distances above ground of $\frac{1}{2}h_T$ and $\frac{1}{2}h_R$), results of (28) and similar developments lead to formula below for average power:

$$\overline{P}(h_T, h_R) - \overline{P}_Q[4 - 4C_V(h_T)\cos kh_T - 4C_V(h_R)\cos kh_R + 2C_V(h_T - h_R)\cos k(h_T + h_R) + 2C_V(h_T + h_R)\cos k(h_T - h_R)].$$

where $\overline{P}_Q$ is given by (26) and C_V is the normalized correlation amplitude in the vertical direction.

Ionospheric Applications

This class of problems is characterized by the dependence of the degree of inhomogeneity upon the mean value of refractive index when the state of turbulence is specified in terms of electron density fluctuations, the physically significant variable. In addition, it differs from problems of the type considered in section (a) because of the large variation in mean refractive index encountered by a wave, leading generally to total reflection at some level.

Formulation of Ionospheric Fluctuations: The phase integral representation of a field reflected from an inhomogeneous medium is given by[3]

$$E_{x_0} \sim \int d\theta \cdot e^{ikx_0 \sin\theta + 2ik\int_0^{z_m}\sqrt{\mu^2-\sin^2\theta}\,dz} \tag{29}$$

where x_0 is the total horizontal distance between transmitter and receiver, μ is the refractive index with mean value a function of height z, $\mu(z_m) = \sin\theta$, and θ is the angle made with the normal by a given trajectory at take-off.

We set $\mu = \mu_0 + \Delta\mu$, and expand the phase to first order in $(\Delta\mu)$:

$$\int_0^{z_m}\sqrt{\mu^2-\sin^2\theta}\,dz = \int_0^{z_m}\sqrt{\mu_0^2(z)-\sin^2\theta}\,dz + \int_0^{z_m}\frac{(\Delta\mu)dz}{\sqrt{\mu_0^2(z)-\sin^2\theta}}. \tag{30}$$

The method of stationary phase is now applied to the mean terms, to find the trajectory angle θ_0, which corresponds to a given range x_0.

$$\frac{\partial}{\partial\theta}\left[kx_0\sin\theta + 2k\int_0^{z_m}\sqrt{\mu_0^2-\sin^2\theta}\,dz\right] = 0 \tag{31}$$

$$x_0 = 2\sin\theta_0\int_0^{z_m}\frac{dz}{\sqrt{\mu_0^2(z)-\sin^2\theta_0}}. \tag{31a}$$

Utilizing the second order approximation to the phase, (29) can now be written:

$$E_{x_0} \sim \int d\theta\cdot e^{\frac{i\phi''(\theta_0)}{2}(\theta-\theta_0)^2 + 2ik\int_0^{z_m}\frac{(\Delta\mu)dz}{\sqrt{\mu_0^2-\sin^2\theta}}} \tag{32}$$

where

$$\phi''(\theta_0) = 2k\cos\theta_0\left[\frac{\partial}{\partial\theta}\int_0^{z_m(\theta)}\frac{dz}{\sqrt{\mu_0^2(z)-\sin^2\theta}}\right]_{\theta_0}. \tag{33}$$

The average power takes the form:

$$\overline{P}_{x_0} = \iint d\theta\cdot d\theta'\cdot e^{\frac{i\phi''(\theta_0)}{2}[(\theta-\theta_0)^2-(\theta'-\theta_0)^2]} \cdot\frac{1}{2T}\int_{-T}^{T}dt\cdot e^{2ik\left\{\int_0^{z_m}\frac{(\Delta\mu)_\theta dz}{\sqrt{\mu_0^2-\sin^2\theta}} - \int_0^{z_m}\frac{(\Delta\mu)_{\theta'}dz}{\sqrt{\mu_0^2-\sin^2\theta'}}\right\}}. \tag{34}$$

We now make our usual assumption that the difference of the two random phase fluctuations is normally distributed. Some justification for this assumption exists in this case regardless of the distribution of $(\Delta\mu)$ at any given point, in virtue of the central limit theorem, since each integrated random phase is the resultant of a large number of independent contributions. We proceed to determine the variance of this phase difference:

$$\overline{(\Delta\phi)^2_{\theta-\theta'}} = 2k^2\cdot\frac{1}{2T}\int_{-T}^{T}dt \cdot\left\{\int_0^{z_m}\int_0^{z_m}\frac{(\Delta\mu)_\theta(\Delta\mu)_{\theta'}dzdz'}{\sqrt{[(\mu_0^2(z)-\sin^2\theta][\mu_0^2(z')-\sin^2\theta]}} - \int_0^{z_m(\theta)}\int_0^{z_m(\theta')}\frac{(\Delta\mu)_\theta\cdot(\Delta\mu)'_{\theta'}dzdz'}{\sqrt{[\mu_0^2(z)-\sin^2\theta][\mu_0^2(z')-\sin^2\theta']}}\right\} \tag{35}$$

It is now desirable to introduce the physical variable, electron density, related to μ through:

$$\mu = \sqrt{1 - Ne^2/m\omega^2} \tag{36}$$

so that

$$\Delta\mu = \frac{\mu^2-1}{2\mu}\left(\frac{\Delta N}{N}\right). \tag{36a}$$

Setting

$$\frac{1}{2T}\int_{-T}^{T}dt\cdot\frac{\Delta N}{N}(\underline{r},t)\cdot\frac{\Delta N}{N}(\underline{r}',t) = \overline{\left(\frac{\Delta N}{N}\right)^2}\rho(\underline{r}-\underline{r}') \tag{37}$$

and replacing linear distance in the argument of the correlation function by Δs, arc length along the trajectory, an approximation which is justified provided the radius of curvature of the trajectory is large compared to the scale of coherence, (35) becomes:

$$\overline{(\Delta\phi)^2_{\theta-\theta'}} = 2\overline{\left(\frac{\Delta N}{N}\right)^2}\int_0^{z_m}\left(\frac{\mu_0^2-1}{2\mu_0}\right)^2\cdot\frac{dz}{\mu_0^2-\sin^2\theta} \cdot\int_{-z_m}^{z_m}d\zeta\left\{\rho(\Delta s) - \rho\left(\sqrt{\xi^2+(\Delta s)^2+2\xi(\Delta s)\frac{\sin\theta}{\mu}}\right)\right\} \tag{38}$$

[3] H. Bremmer, "Terrestrial Radio Waves," Elsevier Publishing Co., New York, N. Y., p. 165; 1949.

where the transformation $\zeta = z - z'$ has been effected, and z has been set equal to z' except in the correlation function; ξ is the lateral displacement of trajectories specified by θ and θ' at height z, so that the argument of the second correlation function is the distance between points at height z on trajectory θ, and z' on θ'. We now determine (Δs) and ξ is terms of z:

$$\frac{ds}{dz} = \frac{1}{\cos\phi}; \qquad \sin\theta = \mu_0(z)\sin\phi \tag{39}$$

by Snell's law, so that

$$\Delta s = \frac{\zeta \cdot \mu_0}{\sqrt{\mu_0^2 - \sin^2\theta}} \tag{40}$$

$$\frac{dx}{dz} = \tan\phi = \frac{\sin\theta}{\sqrt{\mu_0^2 - \sin^2\theta}};$$

$$x\theta(z) = \int_0^z \frac{\sin\theta\, dz}{\sqrt{\mu_0^2(z) - \sin^2\theta}} \tag{41}$$

$$\xi = x\theta(z) - x_{\theta'}(z) \cong (\theta - \theta')\cdot\frac{\partial x\theta(z)}{\partial\theta} = \beta F(\theta, z) \tag{42}$$

where we have set $\beta = \theta - \theta'$, $F = \partial x/\partial\theta$.

Returning to (38), for a correlation function of the form $\rho(u) = e^{-u^2/l^2}$, the integral over ζ becomes:

$$\int_{-\infty}^{\infty} d\zeta \left\{ e^{-\frac{\zeta^2\mu_0^2}{l^2(\mu_0^2 - \sin^2\theta)}} - e^{-\frac{1}{l^2}\left[\xi^2 + \frac{\zeta^2\mu_0^2}{\mu_0^2 - \sin^2\theta} + \frac{2\xi\zeta\sin\theta}{\sqrt{\mu_0^2 - \sin^2\theta}}\right]} \right\}$$

$$= \sqrt{\pi}\, l \frac{\sqrt{\mu_0^2 - \sin^2\theta}}{\mu_0} \left\{ 1 - e^{-\frac{\xi^2}{l^2}\left(1 - \frac{\sin^2\theta}{\mu_0^2}\right)} \right\} \tag{43}$$

where infinite limits have been employed, since the thickness of the ionosphere is much greater than the scale of coherence.

$$\overline{(\Delta\phi)_\beta^2} = \frac{k^2 l\sqrt{\pi}}{2}\cdot\overline{\left(\frac{\Delta N}{N}\right)^2}\int_0^{z_m} \frac{(\mu_0^2 - 1)^2}{\mu_0^3\cdot\sqrt{\mu_0^2 - \sin^2\theta}} \cdot\left\{1 - e^{-\frac{\beta^2 F^2}{l^2}(\theta, z)\left(1 - \frac{\sin^2\theta}{\mu_0^2}\right)}\right\} dz. \tag{44}$$

The average power takes the form:

$$\overline{P}_{\theta_0} = \iint d\theta\cdot d\beta\cdot e^{\frac{i\phi''(\theta_0)}{2}(2\theta\beta - 2\theta_0\beta - \beta^2)}\cdot e^{-2\overline{(\Delta\phi)_\beta^2}}. \tag{45}$$

To obtain the correlation pattern on the ground, we add a displacement s to x_0. This has the effect of altering θ_0 by an amount, $\Delta\theta_0$ given by:

$$s = \Delta x_0 = \Delta\theta_0 \frac{d}{d\theta_0}\left[2\sin\theta_0 \int_0^{z_m} \frac{dz}{\sqrt{\mu_0^2(z) - \sin^2\theta}}\right] \tag{46}$$

which we may write as $s = (\Delta\theta_0)\cdot g(\theta_0)$, where $g(\theta_0)$ is the derivative on the right hand side. The change in $\phi''(\theta_0)$ is of second order, so that the phase term in (34) takes the form

$$\frac{\phi''(\theta_0)}{2}\left[(\theta - \theta_0)^2 - \left(\theta' - \theta_0 - \frac{s}{g}\right)^2\right].$$

This gives rise to additional terms

$$\phi''(\theta_0)\left[\frac{\theta s}{g} + \frac{1}{2}\left(\frac{s}{g}\right)^2 + \frac{\theta_0 s}{g}\right].$$

Then

$$\overline{P}_{\theta_0}(s) = \iint d\theta\cdot d\beta \cdot e^{i\phi''(\theta_0)\left[\theta\left(\beta - \frac{s}{g}\right) - \theta_0\left(\beta - \frac{s}{g}\right) + \frac{1}{2}\left(\frac{s}{g}\right)^2 - \frac{1}{2}\beta^2\right]} \cdot e^{-2\overline{(\Delta\phi)^2\beta}}. \tag{47}$$

Provided the θ variation of $(\Delta\phi)^2_\beta$ is slow compared to the oscillations produced by θ in the phase term, we may replace θ by θ_0 in the variance; integration over θ then yields $\delta(\beta)$, and $\delta[\beta - (s/g)]$ in (45) and (47) respectively. Integration over β then gives a unity reflection coefficient and a ground correlation pattern amplitude

$$e^{-2\overline{(\Delta\phi)^2\beta}} = s/g.$$

To proceed farther we must adopt a specific form for $\mu_0(z)$. We assume a linear profile of electron density, beginning at height H above the ground. Then $\mu_0 = \sqrt{1 - kz}$, and performing the indicated integrations:

$$F(\theta, z) = H\sec^2\theta + \frac{2}{K}\left(\cos^2\theta - \sin^2\theta - \cos\theta\sqrt{\cos^2\theta - Kz} + \frac{\sin^2\theta\cdot\cos\theta}{\sqrt{\cos^2\theta - Kz}}\right) \tag{42a}$$

$$g(\theta_0) = 2H\sec^2\theta_0 + \frac{4}{K}\cos 2\theta_0 \tag{46a}$$

while the variance becomes:

$$\overline{(\Delta\phi)_\beta^2} = \frac{k^2}{2}\overline{\left(\frac{\Delta N}{N}\right)^2} l\sqrt{\pi}\int_0^{z_m = \cos^2\theta/K} \frac{K^2 z^2}{(1 - Kz)^{3/2}} \cdot\frac{dz}{\sqrt{\cos^2\theta - Kz}}\left[1 - e^{-\frac{\beta^2 F^2(\theta, z)}{l^2}\cdot\frac{\cos^2\theta - Kz}{1 - Kz}}\right]. \tag{44a}$$

Evaluation of Phase Incoherence: In general this integral may be evaluated only in certain special cases, several of which we now consider.

At vertical incidence, $\theta_0 = 0$,

$$F^2(\theta, z) = \frac{4z}{K} - \sqrt{1 - Kz}\left(\frac{8}{K^2} + \frac{4H}{K}\right) + H^2 + \frac{4H}{K}\cdot \tag{42b}$$

If the integration in (44a) is carried to $z = 1/K$, a divergence occurs because $\mu_0 = 0$ at this point. Since the first order relation (36a), for $\Delta\mu$ does not hold in this case, but instead $\mu \simeq \sqrt{\Delta N/N}$, we may proceed by integrating to

$$z = \frac{1}{K}\left(1 - \left|\frac{\overline{\Delta N}}{N}\right|\right),$$

and then adding the contribution of the remaining segment,

$$\Delta z = \frac{1}{K}\left|\frac{\overline{\Delta N}}{N}\right|,$$

to the level of reflection. Since it is apparent that the major contribution comes from the region $Kz \sim 1$, we may set $z = 1/K$ in (42b).

$$\overline{(\Delta\phi)^2}_{\beta,\theta_0=0} = \frac{k^2}{2}\left(\overline{\frac{\Delta N}{N}}\right)^2 \cdot l\sqrt{\pi}\left[1 - e^{-\frac{\beta^2}{l^2}\left(H+\frac{2}{K}\right)^2}\right] \cdot \left\{\int_0^{z=1/K(1-|\overline{\Delta N/N}|)} \frac{dz}{(1-Kz)^2} + \int_{z=1/K(1-|\overline{\Delta N/N}|)}^{z=1/K} \frac{dz}{\left|\frac{\overline{\Delta N}}{N}\right|^{3/2}\sqrt{1-Kz}}\right\}$$

$$= \frac{3\sqrt{\pi}\, k^2 l}{2K}\left|\frac{\overline{\Delta N}}{N}\right|\left\{1 - e^{-\frac{\beta^2}{l^2}\left(H+\frac{2}{K}\right)^2}\right\}. \quad (44b)$$

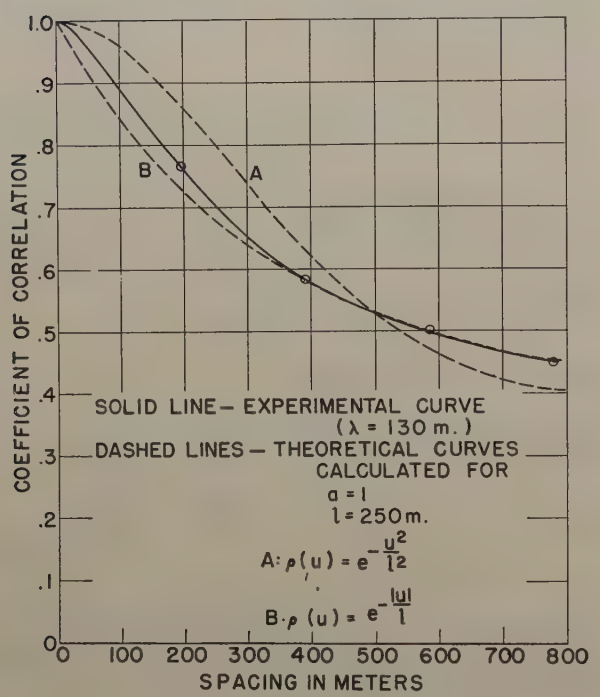

Fig. 3—Ground correlation pattern of ionospherically reflected signal.

Since $g(0) = 2[H + (2/K)]$, the scale factor in the ground correlation pattern is $\frac{1}{2}$, as we might expect. For a nonlinear profile, the electron density gradient at the level of reflection should be employed to determine K, since the major portion of the phase incoherence is introduced at this point. Fig. 3 shows a typical pattern deduced from experimental measurements on ionospheric winds by utilizing a space-time conversion under conditions of small structure change. Since it is the signal envelope rather than the rf which has been correlated here, a modification of the above theory is required which in the worst case, a Rayleigh distribution, would require squaring the theoretical pattern. Gaussian and exponential types of correlation patterns are shown for comparison. The best fit corresponds to parametric values of $l \simeq 250$ meters and $|\overline{\Delta N/N}| \simeq 10^{-4}$. The half power points of the angular spectrum occur at $\beta = \pm 5°$.

For highly oblique incidence, $\theta_0 \gg 0$, $1 - Kz \geqq \sin 2\theta_0 \sim 1$, the leading terms in

$$F^2(\theta, z) \simeq \frac{4}{K^2}\,\frac{\sin^4\theta_0 \cos^2\theta_0}{\cos^2\theta_0 - Kz} + H^2 \sec^4\theta_0$$

so that

$$\overline{(\Delta\phi)^2}_{\beta,\theta_0\neq 0} \simeq \frac{k^2 l\sqrt{\pi}}{2}\left(\overline{\frac{\Delta N}{N}}\right)^2 \int_0^{z=\cos^2\theta/K} \frac{K^2 z^2 dz}{\sqrt{\cos^2\theta_0 - Kz}} \cdot \left\{1 - e^{-\frac{\beta^2}{l^2}\left[\frac{4}{K^2}\sin^4\theta_0\cos^2\theta_0 + H^2\sec^4\theta_0(\cos^2\theta_0 - Kz)\right]}\right\} \quad (42c)$$

$$= \frac{8\sqrt{\pi}\, k^2 l}{15K}\left(\overline{\frac{\Delta N}{N}}\right)^2 \cos^5\theta_0 \cdot \left[1 - \left\{\frac{135}{64}\,\frac{l\sqrt{\pi}}{\beta H\sec\theta_0}\,\mathrm{erf}\left(\frac{\beta H\sec\theta_0}{l}\right) - \left(\frac{75}{32} + \frac{15}{4}\cos^2\theta_0\right)e^{-\beta^2\frac{H^2}{l^2}\sec^2\theta_0}\right\} \cdot e^{-\frac{4\beta^2\sin^4\theta_0}{l^2K^2}\cos^2\theta_0}\right] \quad (44c)$$

It is apparent that far less phase incoherence is present at oblique incidence than at vertical incidence.

Finally, we consider the case of turbulence present in a lower layer, in which the mean refractive index does not differ very much from unity, i.e, we take $(\overline{\Delta N/N})^2$ as different from zero over a thickness (Δz), at μ_0. Then:

$$\overline{(\Delta\phi)^2}_{\beta,\theta_0,\Delta z} = \frac{k^2 l\sqrt{\pi}}{2}\cdot\frac{(\Delta z)}{\cos\theta_0}\cdot\left(\overline{\frac{\Delta N}{N}}\right)^2(1-\mu_0^2)^2 \cdot\left[1 - e^{-\frac{\beta^2 H^2}{l^2}\sec^2\theta_0}\right]. \quad (44d)$$

The correlation pattern in this case consists of a product of two exponentials, corresponding to the phase incoherence introduced in the upgoing and downcoming waves. For the turbulent layer at height H', and a total virtual height of reflection D, the scale factors have the values $(2D - H')/2D$ and $H'/2D$ respectively.

In all cases the frequency power spectrum may be obtained from the results of section 4 with "a" set equal to $(\overline{\Delta\phi})^2_{\beta=\infty}$, provided the assumption is made that the space-time correlation function of $(\Delta N/N)$ can be written as a product of functions of space and time individually. This requirement arises from the integration along a trajectory necessary to evaluate "a" in volume-type problems.

On the Theory of Corrugated Plane Surfaces*

R. S. ELLIOTT†

Summary—An analysis is given of an electromagnetic system composed of a rectangular waveguide in tandem with a corrugated waveguide which feeds a flat, corrugated surface of arbitrary length terminated by a ground plane, whose length is also arbitrary. An improved procedure of field determination is used which combines Floquet's theorem and the variational principle, thus revealing an additional requirement on the corrugation geometry. Factors influencing a match at the feed mouth, and satisfactory launching of the surface wave are discussed. The degree of suppression of the feed radiation is given in db as a function of the geometry of the system. Approximate radiation patterns are derived for two cases, (a) when the system is terminated by an infinite ground plane, and (b) when the system is terminated by a finite ground plane. For the latter case, an upper bound on the tilt angle of the main beam and a lower bound on its beamwidth result from an approximate theory. For both cases, the Hansen-Woodyard endfire relation is found to provide beam sharpening even when the feed radiation is considered. The presence of higher order surface modes, their effect, and their elimination are discussed. Comparison of the theory with experiment is reasonably good.

Introduction

THE THEORY OF electromagnetic waves supported by corrugated conductors has been treated by many authors. In 1941 Slater[1] derived an approximate theory for wave propagation between parallel conducting plates of infinite extent, the interior surface of one of the plates being corrugated in the transverse dimension. Goldstein[2,3] extended this analysis to rectangular waveguide and Walkinshaw[4,5] applied the technique to circular waveguide. Cutler[6] appears to have been the first to demonstrate that surface waves can exist *exterior* to a single corrugated conductor. By assuming that only the dominant surface mode was present, and by matching its average surface impedance to that of the TEM modes assumed to exist between the corrugations, he succeeded in deriving approximate expressions for the phase velocity on flat and circular corrugated surfaces. By making a better approximation for the field distribution across the gaps between corrugations, Rotman[7] obtained a slight modification of Cutler's formulas.

All of these analyses were based on Floquet's theorem.[8] In 1950, Goubau[9] reviewed the work of Sommerfeld[10] pertaining to axial surface waves on cylinders and extended it to conductors with dielectric coats. Assuming a quasi-stationary field, he also showed that a conductor with a modified surface (e.g., a threaded conductor) could support an axial surface mode. Lucke[11] used a novel approach to determine the propagation constant over a single, flat corrugated surface. By considering a finite length of surface terminated by vertical conducting walls (which thus formed a resonator), he was able to get two expressions for the propagation characteristic—one in terms of the unknown electric field and the other in terms of the unknown magnetic field. The advantage of this method is that both formulations must be satisfied by the true field, so that the degree of approximation of any trial function may be gauged. The resonator method unfortunately requires the consideration of many corrugations, which makes the analysis cumbersome. By applying Floquet's theorem to Lucke's method, the analysis can be confined to a single corrugation, meanwhile retaining the desirable feature of alternative formulations.

In the next section this modified procedure is applied to a corrugated rectangular waveguide to obtain the propagation characteristics of the allowable mode configurations. The analysis is extended to a corrugated parallel plate transmission line (by letting the side walls recede to infinity) and to a single, flat corrugated surface (by then letting the top wall also recede to infinity). This affords an insight into the matching characteristics of a corrugated waveguide feeding a corrugated surface.

Radiation patterns of corrugated surfaces have been measured by the Stanford group[12] and by Ehrlich and Newkirk.[13] Discrepancies between theoretical and experimental patterns led Ehrlich to an experimental demonstration that feed radiation was contaminating the patterns and he was successful in devising techniques for reducing the effect of the feed. Theoretical support for this viewpoint will be given, together with curves of feed suppression as a function of the system geometry. It is demonstrated that by suitable design, the feed radiation can be reduced to reasonable propor-

* Revised manuscript received by PGAP, January 21, 1954. Work reported here was performed at Hughes Aircraft Company, sponsored by Air Force Cambridge Research Laboratory, Cambridge, Mass., under Contract AF 19(604)-262, and was described in Hughes Aircraft Company Technical Memorandum No. 317.

† Hughes Research and Development Labs., Culver City, Calif.

[1] J. C. Slater, "Theory of the Magnetron Oscillator," MIT Radiation Lab. Report V-5S, pp. 1–32; August, 1941.

[2] H. Goldstein, "Cavity Resonators and Waveguides Containing Periodic Elements," Ph.D. Thesis, MIT; 1943.

[3] H. Goldstein, "The Theory of Corrugated Transmission Lines and Waveguides," MIT Radiation Lab. Report 494, pp. 1–17; April, 1944.

[4] W. Walkinshaw, "Theory of Circular Corrugated Waveguide for Linear Accelerator," British TRE Report T2037; August, 1946.

[5] W. Walkinshaw, "Theoretical Design of Linear Accelerator for Electrons," *British Proc. Phys. Soc.*, vol. 345; September, 1948.

[6] C. C. Cutler, "Electromagnetic Waves Guided by Corrugated Conducting Surfaces," Bell Telephone Labs. Report MM-44-160-218; October, 1944.

[7] W. Rotman, "A study of single surface corrugated guides," PROC. I.R.E., vol. 39, pp. 952–959; August, 1951.

[8] For a discussion of Floquet's theorem the reader is referred to J. C. Slater, "Microwave Electronics," pp. 169–177, D. Van Nostrand Co., Inc., New York, N. Y.; 1950.

[9] G. Goubau, "Surface waves and their application to transmission lines," *Jour. Appl. Phys.*, vol. 21, pp. 1119–28; November, 1950.

[10] A discussion of Sommerfeld's analysis may be found in J. A. Stratton, "Electromagnetic Theory," pp. 524–537, McGraw-Hill Book Co., Inc., New York, N. Y.; 1941.

[11] Second Quarterly Progress Report, "Ridge and Corrugated Antenna Studies," Stanford Research Inst.; January, 1950.

[12] Quarterly Progress Reports 2 through 6, "Ridge and Corrugated Antenna Studies," Stanford Research Inst.; October 1949 to January 1951.

[13] M. J. Ehrlich and L. Newkirk, "Corrugated Surface Antennas," Convention Record of the I.R.E., Part 2—Antennas and Communications, pp. 18–33; 1953.

tions by some sacrifice of the match. An optimum compromise can be determined by experiment. The remaining feed radiation can be phased to improve the over-all radiation pattern. Assuming a suitable design, the radiation pattern is then contributed to chiefly by the corrugated surface and its ground plane and is characterized by an endfire main beam tilted up somewhat from the plane of the surface. An approximate theory is derived which permits an estimation of the pattern in terms of the corrugation geometry and the lengths of the corrugated surface and its ground plane. Curves of maximum tilt angle and minimum beamwidth as functions of these parameters are presented. The effect on the radiation pattern of the presence of higher order surface modes is found to be slight. Their presence would appear to be objectionable only when the corrugated surface is being used as a transmission line. They may always be suppressed simply by narrowing the teeth.

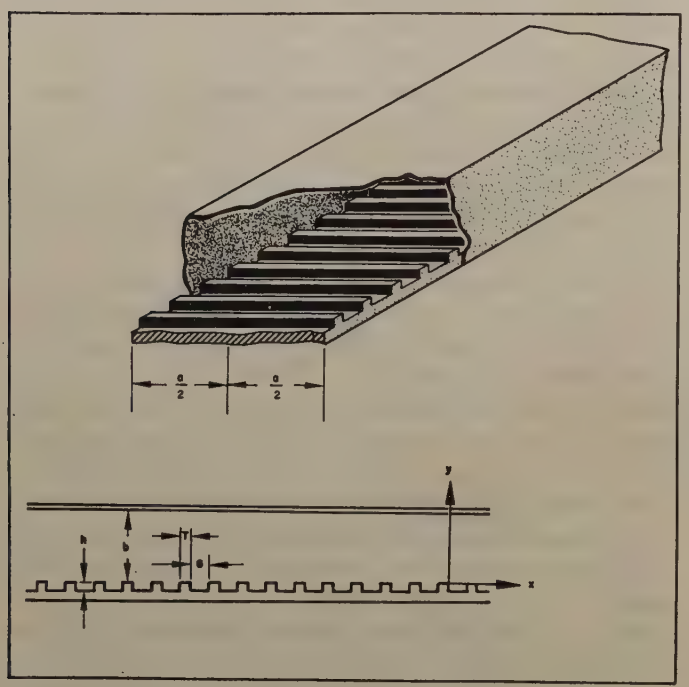

Fig. 1—Corrugated rectangular waveguide.

The Corrugated Waveguide

As a starting point for the analysis, assume an infinitely long rectangular waveguide whose bottom wall is uniformly corrugated as shown in Fig. 1. It is desired to find the field configurations which can exist inside this structure. If T is the width of a tooth and G the width of a gap, the structure is periodic in units of $(T+G)$. Hence if $F(x_o, y, z)e^{j\omega t}$ is the distribution of a field component in the plane $x=x_o$ (for $O \leqq y \leqq b$, $-\lambda/2 \leqq z \leqq \frac{a}{2}$), then $F(x_o+[T+G], y, z)e^{j\omega t} = F(x_o, y, z)$ $e^{-j\beta_o(T+G)}e^{j\omega t}$ is the distribution one period further down the guide. β_o is a complex constant whose value depends on the geometry. Since the only function which satisfies this requirement for all x_o is $e^{-j\beta_o x}$ we have

$$F(x, y, z) = f(x, y, z)e^{-j\beta_o x}. \tag{1}$$

Further, $f(x, y, z)$ must be periodic in x in the interval $(T+G)$ or

$$f(x, y, z) = g(y, z) \sum_{n=-\infty}^{\infty} a_n e^{-j(2\pi n x)/(T+G)}. \tag{2}$$

Thus each field component may be written in the form

$$\sum_{n=-\infty}^{\infty} g(y, z)e^{j\omega t - j\beta_n x} \tag{3}$$

in which

$$\beta_n = \beta_o + \frac{2\pi n}{T+G} \tag{4}$$

is a complex constant to be determined by the geometry. This is Floquet's theorem.

We shall assume that the structure is to be excited by a TE_{01} mode incident from a tandem section of regular guide. The allowable modes in the region above the corrugations are then hybrid, characterized by the absence of an E_z component, and given by

$$\begin{aligned}
E_x &= \sum_{n=-\infty}^{\infty} A_n \sinh \alpha_n(y-b)\cdot\cos\frac{\pi z}{a}\cdot e^{j(\omega t-\beta_n x)} \\
E_y &= \sum_{n=-\infty}^{\infty} \frac{j\beta_r A_n}{\alpha_n}\cosh \alpha_n(y-b)\cdot\cos\frac{\pi z}{a}\cdot e^{j(\omega t-\beta_n x)} \\
H_x &= \sum_{n=-\infty}^{\infty} \frac{-j\beta_n\pi}{j\omega\mu\alpha_n a} A_n \cosh \alpha_n(y-b)\cdot\sin\frac{\pi z}{a}\cdot e^{j(\omega t-\beta_n x)} \\
H_y &= \sum_{n=-\infty}^{\infty} \frac{\frac{\pi}{a}\cdot A_n}{j\omega\mu}\sinh \alpha_n(y-b)\cdot\sin\frac{\pi z}{a}\cdot e^{j(\omega t-\beta_n x)} \\
H_z &= \sum_{n=-\infty}^{\infty} \frac{-K^2}{j\omega\mu\alpha_n} A_n \cosh \alpha_n(y-b)\cdot\cos\frac{\pi z}{a}\cdot e^{j(\omega t-\beta_n x)}
\end{aligned} \tag{5}$$

where

$$\alpha_n = \sqrt{\beta_n^2 - K^2}, \qquad K = \sqrt{k^2 - \left(\frac{\pi}{a}\right)^2}. \tag{6}$$

With the origin of co-ordinates chosen as shown in Fig. 1, the field distribution in the gap beneath the origin may be written

$$\begin{aligned}
E_x &= -j\omega\mu\cdot B_o \sin K(y+h)\cos\frac{\pi z}{a}\cdot e^{j\omega t} \\
&\quad + \sum_{m=1}^{\infty} B_m \cos\frac{m\pi x}{G}\cdot\cos\frac{\pi z}{a}\cdot e^{j\omega t+\gamma_m y} \\
E_y &= \sum_{m=1}^{\infty} \frac{m\pi}{\gamma_m G} B_m \sin\frac{m\pi x}{G}\cos\frac{\pi z}{a}\cdot e^{j\omega t+\gamma_m y} \\
H_x &= -\sum_{m=1}^{\infty} \frac{\pi}{j\omega\mu\gamma_m a}\cdot\frac{m\pi}{G}\cdot B_m\cdot\sin\frac{m\pi x}{G}\cdot\sin\frac{\pi z}{a}\cdot e^{j\omega t+\gamma_m y} \\
H_y &= -\frac{\pi}{a}\cdot B_o\cdot\sin K(y+h)\cdot\sin\frac{\pi z}{a}\cdot e^{j\omega t}
\end{aligned}$$

$$+\sum_{m=1}^{\infty}\frac{1}{j\omega\mu}\cdot\frac{\pi}{a}\cdot B_m\cdot\cos\frac{m\pi x}{G}\cdot\sin\frac{\pi z}{a}\cdot e^{j\omega t+\gamma_m y}$$

$$H_z=-KB_o\cos K(y+h)\cdot\cos\frac{\pi z}{a}\cdot e^{j\omega t}$$

$$-\sum_{m=1}^{\infty}\frac{K^2}{j\omega\mu\gamma_m}B_m\cos\frac{m\pi x}{G}\cdot\cos\frac{\pi z}{a}\cdot e^{j\omega t+\gamma_m y} \tag{7}$$

in which

$$\sqrt{m}=\sqrt{\left(\frac{m\pi}{G}\right)^2-K^2}. \tag{8}$$

Implicit in (7) is the concept that each slot is a short-circuited waveguide of length h. The m series represents that combination of TM and TE modes, all beyond cutoff, which together satisfy the requirement that $E_z\equiv O$. It is assumed that the slot width G is so small compared to the free space wavelength that all of these modes are attenuated to a negligible amplitude before they reach the bottom of the slot and hence have no reflected component. The one propagating mode is represented by the standing wave terms, written separately in (7). Thus K and $\sqrt{m}$, given by (8), are positive real quantities determined solely by the geometry.

Since the tangential fields must be continuous across the boundary between the two regions, that is, across the plane $y=O$, one may equate the integrals

$$\int_{-a/2}^{+a/2}\int_0^{G+T}\vec{E}_1\times\vec{H}_1^*\cdot\vec{u}_y dxdz$$

$$\equiv\int_{-a/2}^{+a/2}\int_0^{G}\vec{\mathcal{E}}_1\times\vec{\mathcal{H}}_1^*\cdot\vec{u}_y dxdz \tag{9}$$

in which $\vec{E}_1$, $\vec{H}_1$ are the unknown fields expressed in terms of (5) and $\vec{\mathcal{E}}_1$, $\vec{\mathcal{H}}_1$ are the unknown fields expressed in terms of (7). All terms of the integrands of (9) contain z only in the factor $\cos\pi z/a$. Hence (9) reduces to

$$\int_0^{G+T}EH^*dx=\int_0^{G}\mathcal{E}\mathcal{H}^*dx \tag{10}$$

where

$$E=-\sum_{n=-\infty}^{\infty}A_n\sinh\alpha_n b\cdot e^{j(\omega t-\beta_n x)} \tag{11a}$$

$$H=-\sum_{n=-\infty}^{\infty}\frac{K^2}{j\omega\mu\alpha_n}A_n\cosh\alpha_n b\cdot e^{j(\omega t-\beta_n x)} \tag{11b}$$

$$\mathcal{E}=-j\omega\mu B_o\sin Kh\cdot e^{j\omega t}+\sum_{m=1}^{\infty}B_m\cos\frac{m\pi x}{G}\cdot e^{j\omega t} \tag{11c}$$

$$\mathcal{H}=-KB_o\cos Kh\cdot e^{j\omega t}-\sum_{m=1}^{\infty}\frac{K^2}{j\omega\mu\gamma_m}\cdot B_m\cos\frac{m\pi x}{G}\cdot e^{j\omega t} \tag{11d}$$

and

$$E\equiv\mathcal{E},\qquad H\equiv\mathcal{H}. \tag{12}$$

The Fourier coefficients A_n and B_m may be expressed in terms of integrals of the unknown electric field, i.e.,

$$A_n^*=-\frac{1}{(G+T)\sinh\alpha_n b}\int_0^{G+T}E^*e^{j(\omega t-\beta_n x)}dx \tag{13}$$

$$B_o^*=\frac{1}{j\omega\mu G\sin Kh}\int_0^{G}\mathcal{E}^*e^{j\omega t}dx \tag{14}$$

$$B_m^*=\frac{2}{G}\int_0^{G}\mathcal{E}^*\cos\frac{m\pi x}{G}\cdot e^{j\omega t}dx \tag{15}$$

and when these relations are substituted in (11b) and (11d) the magnetic field is given in terms of the electric field. Upon inserting the resulting expressions for the magnetic field in (10), making use of (12), and rearranging terms, one obtains

$$\cot Kh=\frac{\sum_{n=-\infty}^{\infty}\frac{G}{G+T}\cdot\frac{K}{\alpha_n}\cdot\coth\alpha_n b\int_0^{G+T}Ee^{j\beta_n x}dx\int_0^{G+T}E^*e^{-j\beta_n x}dx+\sum_{m=1}^{\infty}\frac{2K}{\gamma_m}\int_0^{G}E\cos\frac{m\pi x}{G}dx\int_0^{G}E^*\cos\frac{m\pi x}{G}dx}{\int_0^{G}Edx\int_0^{G}E^*dx} \tag{16}$$

By a similar procedure, (12) can be expressed entirely in terms of the unknown field H, giving

$$\frac{1}{\cot Kh}=\frac{\sum_{n=-\infty}^{\infty}\frac{G}{G+T}\cdot\frac{\alpha_n}{K}\cdot\tanh\alpha_n b\int_0^{G+T}He^{j\beta_n x}dx\int_0^{G+T}H^*e^{-j\beta_n x}dx+\sum_{m=1}^{\infty}\frac{2\gamma_m}{K}\int_0^{G}H\cos\frac{m\pi x}{G}dx\int_0^{G}H^*\cos\frac{m\pi x}{G}dx}{\int_0^{G}Hdx\int_0^{G}H^*dx} \tag{17}$$

Equations (16) and (17) are suggestive of Schwinger's variational form but investigation discloses that only (17) is stationary about the true fields.[14] However, both must be *satisfied* by the true fields and from this fact

[14] R. S. Elliott, "On the Theory of Corrugated Plane Surfaces," Hughes Research and Development Labs., Technical Memorandum No. 317; October, 1953. (Revised.)

one can derive useful information. To see how good an approximation the fundamental mode is, we insert the trial function $E=-A_0 \sinh \alpha_o b \cdot e^{j(\omega t-\beta_o x)}$ in (16) and obtain the asymptotic formula

$$\cot Kh = \frac{G+T}{G}\cdot\frac{K}{\alpha_o}\coth \alpha_o b \tag{18}$$

as $G+T\to O$. Similarly, when the companion trial function

$$H = -\frac{K^2}{j\omega\mu\alpha_o} A_o \cosh \alpha_o b \cdot e^{j(\omega t-\beta_o x)}$$

is inserted in (17), the asymptotic formula

$$\cot Kh = \frac{G}{G+T}\cdot\frac{K}{\alpha_o}\cdot\coth \alpha_o b \tag{19}$$

results when $G+T\to O$. Previous work by the Stanford group on a similar problem[11] indicates that these formulas are good representations for $(\lambda_o/G+T)\geqq 10$.

It is interesting to note that only for $T=O$ are the two formulas the same. This is reasonable when one recalls that $E_{\tan}\equiv O$ over each tooth and the trial function used to obtain (18) does not satisfy this requirement if $T>O$. Hence, we conclude that only if (a) the number of corrugations/wavelength is large, and (b) tooth width/gap width is small, does the field distribution above the corrugations consist essentially of the fundamental mode. Point (b) seems previously to have been overlooked and it can have important bearing on the impedance concept when corrugated surfaces are used as transmission lines. This shall be discussed further in a later section.

The question still remains as to which formula, (18) or (19), is more accurate when $T>O$. One would suspect (19) is, because of its stationary character, and because of the severe requirement on $E_{\tan}$. Support for this belief arises when any more general trial function is substituted in (16) and (17). The variation in (16) is always greater than the corresponding variation in (17).

Henceforth we shall assume that there are at least ten corrugations per wavelength and that the teeth are narrow compared to the gaps. Then to a good approximation the field above the corrugations is given by

$$E_x = A_o \sinh \alpha_o(y-b)\cdot\cos\frac{\pi z}{a}\cdot e^{j(\omega t-\beta_o x)}$$

$$E_y = \frac{j\beta_o}{\alpha_o} A_o \cosh \alpha_o(y-b)\cdot\cos\frac{\pi z}{a}\cdot e^{j(\omega t-\beta_o x)}$$

$$H_x = -\frac{j\beta_o\pi}{j\omega\mu\alpha_o a} A_o \cosh \alpha_o(y-b)\cdot\sin\frac{\pi z}{a}\cdot e^{j(\omega t-\beta_o x)}$$

$$H_y = \frac{\pi}{j\omega\mu a} A_o \sinh \alpha_o(y-b)\cdot\sin\frac{\pi z}{a}\cdot e^{j(\omega t-\beta_o x)}$$

$$H_z = -\frac{K^2}{j\omega\mu\alpha_o} A_o \cosh \alpha_o(y-b)\cdot\cos\frac{\pi z}{a}\cdot e^{j(\omega t-\beta_o x)}$$

$$\alpha_o = \sqrt{\beta_o^2 - K^2}$$

$$\cot Kh = \frac{G}{G+T}\cdot\frac{K}{\alpha_o}\cdot\coth \alpha_o b$$

$$K = \sqrt{k^2-\left(\frac{\pi}{a}\right)^2}. \tag{20}$$

We notice that if $O\leqq Kh\leqq(\pi/2)$ then β_o and α_o are both real and $\beta_o>K$ so that wave propagation is slower than it would be in uncorrugated guide.

If the side walls are allowed to recede to infinity, the solution for a corrugated parallel plate transmission line is obtained. Namely,

$$E_x = A_o \sinh \alpha_o(y-b)e^{j(\omega t-\beta_o x)}$$

$$E_y = \frac{j\beta_o}{\alpha_o} A_o \cosh \alpha_o(y-b)e^{j(\omega t-\beta_o x)}$$

$$H_z = \frac{j\omega\epsilon}{\alpha_o} A_o \cosh \alpha_o(y-b)e^{j(\omega t-\beta_o x)}$$

$$\alpha_o = \sqrt{\beta_o^2 - k^2}$$

$$\cot kh = \frac{G}{G+T}\cdot\frac{\coth \alpha_o b}{\sqrt{(\beta_o/k)^2-1}}. \tag{21}$$

If the spacing b becomes indefinitely large, the solution for a single flat corrugated surface results:

$$E_x = Ae^{j\omega t-j\beta_o x-\alpha_o y}$$

$$E_y = -\frac{j\beta_o}{\alpha_o} Ae^{j\omega t-j\beta_o x-\alpha_o y}$$

$$H_z = \frac{-j\omega\epsilon}{\alpha_o} Ae^{j\omega t-j\beta_o x-\alpha_o y}$$

$$\alpha_o = \sqrt{\beta_o^2 - k^2}$$

$$\cot kh = \frac{G}{G+T}\cdot\frac{1}{\sqrt{(\beta_o/k)^2-1}}$$

in which

$$A = \lim_{b\to\infty}\left[-\frac{A_o}{2}e^{\alpha_o b}\right]. \tag{22}$$

Thus we conclude that if the side and top walls of a corrugated waveguide are gradually flared out and then terminated, a surface wave may be satisfactorily launched on the extended bottom wall with the expectation of a good match. If at the other end of the corrugated waveguide the depth of corrugations is gradually tapered to zero, a good match to regular guide can be achieved[13] and the resulting system can be efficiently excited by a TE_{01} mode.[15]

Radiation from Corrugated Surfaces

A problem of considerable practical interest is the computation of the radiation pattern of the system of

[15] As with any horn, there are space limitations to such a system and for wide surfaces, line feeds (such as pill boxes, hog horns, etc.) are more desirable. In such cases, flaring of the top wall is still helpful to the match.

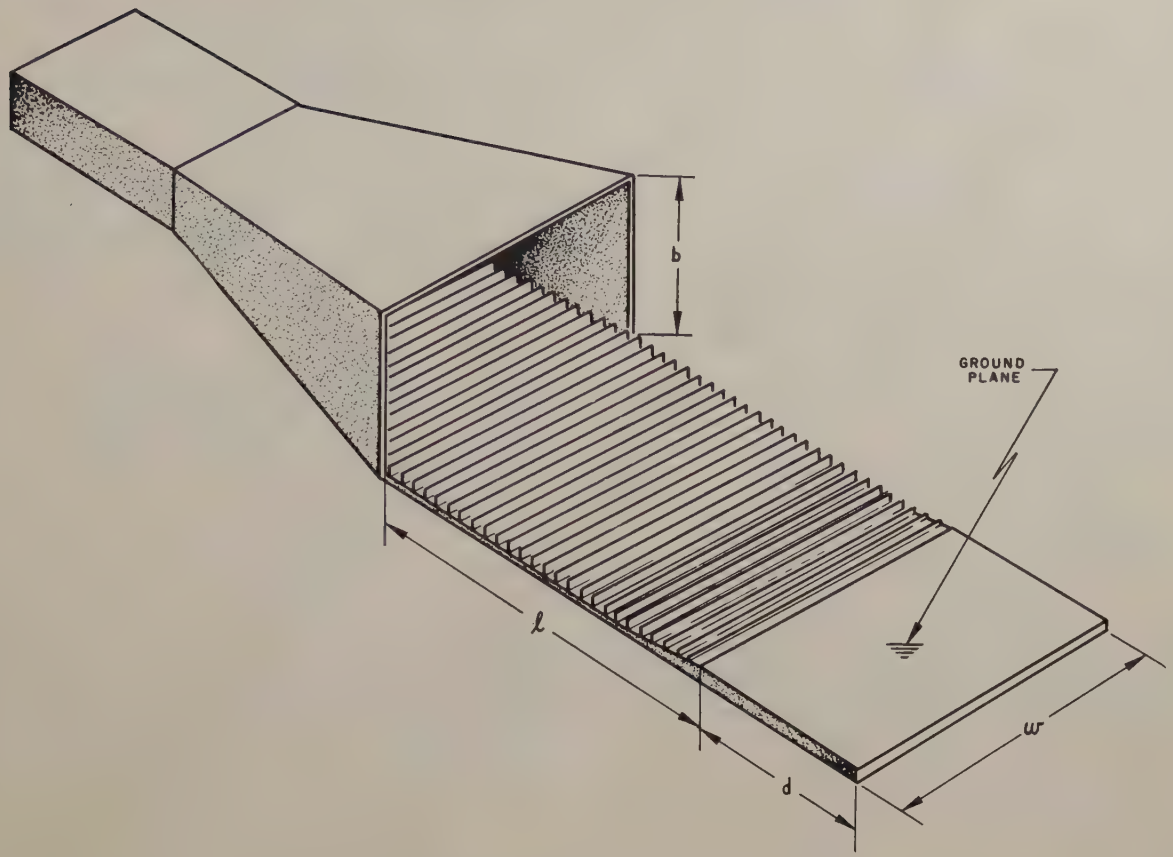

Fig. 2—Corrugated surface antenna.

Fig. 2. We shall assume all the requirements for a good match are met, i.e., tapered corrugations in the wave guide and gentle flare angles for the horn to a large aperture $b \times w$. It is then reasonable to expect that most of the power incident in a TE_{01} mode is transformed to a surface mode as given by (22).

Since the chief effect of the finite width w is to alter the horizontal beamwidth, we shall infer the solution of this problem from the similar but simpler problem of an infinitely wide parallel plate transmission line whose lower plate is corrugated and extended out to form a single surface, as shown in Fig. 3. For the present, we shall assume the surface to be terminated by an infinite ground plane, deferring to the next section a discussion of the effect of a finite ground plane. The radiation pattern of the system of Fig. 3 is contributed to by the secondary source distribution across the mouth of the aperture, the current distribution in the corrugated section of length l, and the current distribution in the infinite ground plane. (The assumption of a good match implies that the currents which leak back over the outside of the upper plate are negligible. If $f \ll l$ it may be ignored. If not, the effective length l' can be taken as some reasonable compromise, such as $l' = l + \frac{1}{2}f$.)

Lucke has shown[16] that for $f = O$ the reflection coefficient for a surface wave of the form (22), incident at the junction of the corrugated surface and its infinite ground plane, is given in magnitude by

$$|R| = \frac{\beta_o - k}{\beta_o}. \tag{23}$$

We shall see shortly that maximum gain results for the corrugated surface of Fig. 3 if $(\beta_o - k)l = \pi$ (the Hansen-Woodyard relation). Hence for practical systems $\beta_o/k - 1$ is small and likewise $|R|$ is small. The tapered section f tends to reduce $|R|$ still further so we shall assume no reflection at all.

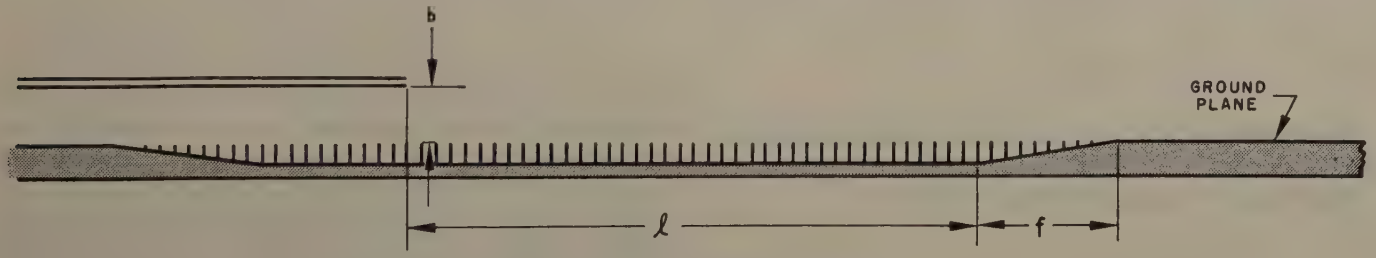

Fig. 3—Simplified antenna system.

[16] Third Quarterly Progress Report, "Ridge and Corrugated Antenna Studies," Stanford Research Inst.; April, 1950.

The field distribution over the corrugated surface is then given by (22). If this field is terminated by the electric and magnetic current sheets

$$\vec{J} = -\vec{u}_x \frac{j\omega\epsilon}{\alpha_o^s} A e^{j(\omega t-\beta_o^s x)} \tag{24}$$

$$\vec{J}_m = \vec{u}_z A e^{j(\omega t-\beta_o^s x)} \tag{25}$$

the corrugated surface may be removed and the ground plane extended back to the mouth of the feed. The effect of the ground plane can then be accounted for by the method of images.

Referring to (21), the field at the mouth of the feed can be terminated by the sheets

$$\vec{J} = -\vec{u}_y \frac{j\omega\epsilon}{\alpha_o^F} A_o \cosh \alpha_o^F(y-b) e^{j(\omega t-\beta_o^F x_o)} \tag{26}$$

$$\vec{J}_m = -\vec{u}_z \frac{j\beta_o^F}{\alpha_o^F} A_o \cosh \alpha_o^F(y-b) e^{j(\omega t-\beta_o^F x_o)} \tag{27}$$

in which x_o is the x-co-ordinate of the aperture. (The superscripts s and F are employed as mnemonic devices for the surface and feed respectively.) The images of (24)–(27) are

$$\vec{J} = \vec{u}_x \frac{j\omega\epsilon}{\alpha_o^s} A e^{j(\omega t-\beta_o^s x)} \tag{24a}$$

$$\vec{J}_m = \vec{u}_z A e^{j(\omega t-\beta_o^s x)} \tag{25a}$$

$$\vec{J} = -\vec{u}_y \frac{j\omega\epsilon}{\alpha_o^F} A_o \cosh \alpha_o^F(|y|-b) e^{j(\omega t-\beta_o^F x_o)} \tag{26a}$$

$$\vec{J}_m = -\vec{u}_z \frac{j\beta_o^F}{\alpha_o^F} A_o \cosh \alpha_o^F(|y|-b) e^{j(\omega t-\beta_o^F x_o)} \tag{27a}$$

so that the original system is equivalent to a magnetic current sheet

$$\vec{J}_m = \vec{U}_z 2A e^{j(\omega t-\beta_o^s x)} \tag{28}$$

occupying the same position as the corrugated surface, and a double sheet

$$\vec{J} = -\vec{u}_y \frac{j\omega\epsilon}{\alpha_o^F} A_o \cosh \alpha_o^F(|y|-b) e^{j(\omega t-\beta_o^F x_o)} \tag{29}$$

$$\vec{J}_m = -\vec{u}_z \frac{f\beta_o^F}{\alpha_o^F} A_o \cosh \alpha_o^F(|y|-b) e^{j(\omega t-\beta_o^F x_o)} \tag{30}$$

extending from $-b$ to $+b$ in the plane of the feed mouth ($x=x_o$).

The radiation patterns of these sources are

$$H_z^s = -\frac{\omega\epsilon}{2} lA\sqrt{\frac{2}{\pi k\rho_0}} \cdot e^{j(\omega t-k\rho_0+\pi/4)} \frac{\sin\frac{\pi l}{\lambda}\left[\frac{\beta_o^s}{k}-\cos\theta\right]}{\frac{\pi l}{\lambda}\cdot\left[\frac{\beta_o^s}{k}-\cos\theta\right]} = \tag{31}$$

$$H_z^F = j\omega\epsilon A_o \frac{\beta_o^F + k\cos\theta}{2\alpha_o^F}\sqrt{\frac{2}{\pi k\rho_o}} \cdot e^{j(\omega t-k\rho_o+\pi/4)} e^{j(\pi l/\lambda)(\beta_o^F/k-\cos\theta)} \times \frac{k\sin\theta\cdot\sin[kb\sin\theta] + \alpha_o^F \sinh \alpha_o^F b}{(\alpha_o^F)^2 + k^2\sin^2\theta} \tag{32}$$

in which the center of the corrugated surface has been chosen as origin (making $x_o=-l/2$). The corrugated surface is seen to give a conventional endfire pattern which can be maximized by setting

$$(\beta_o^s - k)l = \pi. \tag{33}$$

This is the Hansen-Woodyard relation mentioned previously.

Although there is considerable turbulence in the region of the mouth, if the guide and surface modes are extrapolated to the position $x=-l/2$, we can write

$$\frac{-A_o \sinh \alpha_o^F b\cdot e^{j(\beta_o^F l)/2}}{Ae^{j(\beta_o^s l)/2}} = Ce^{j\psi} \tag{34}$$

in which C and ψ are positive real numbers which depend on the corrugation geometry and the mouth height, b, but *not* on length of corrugated surface, l, since it is assumed there are no reflections. The quantity

$$\frac{C^2}{\sinh^2 \alpha_o^F b} = \left|\frac{A_o}{A}\right|^2 \tag{35}$$

can be found by equating the power in the guide and surface modes, which gives

$$\left|\frac{A_o}{A}\right|^2 = \frac{\beta_o^s}{\beta_o^F}\left(\frac{\alpha_o^F}{\alpha_o^s}\right)^3 \frac{1}{\alpha_o^F b + \sinh \alpha_o^F b\cdot\cosh \alpha_o^F b}. \tag{36}$$

Both fields (31) and (32) have their maxima in the direction $\theta=0$ degrees. Making the substitutions (33) and (34), the ratio of these maxima is

$$\frac{H_z^s}{H_z^F} = -\frac{2l(\beta_o^F - k)}{\pi Ce^{j\psi}} \tag{37}$$

and the corresponding power ratio is

$$\frac{P^s}{P^F}(\theta = 0°) = \frac{4l^2(\beta_o^F - k)^2}{\pi^2 C^2}. \tag{38}$$

This relationship is plotted in Fig. 4 for several lengths of corrugated surface. It is seen that the mouth must be made quite small to effect satisfactory feed suppression. This is going contrary to the requirements for a good match, and the analysis breaks down when the match is poor enough that it is no longer proper to equate the powers in the two modes. Hence, some optimum height b exists, which for practical systems probably will not yield more than 10 to 15 db of suppression. This optimum height will be a function of β_o^s and l and can best be determined by experiment.

It is observed from (37) that if ψ is small (which seems reasonable) the two fields are essentially out of phase in the forward direction. Since the feed pattern is broad, this tends to sharpen the main beam. As an illustration of this, Fig. 5 shows the experimental pattern of a 7.33λ corrugated surface as measured by Ehrlich. β_o^s was adjusted to give maximum gain, i.e., $(\beta_o^s-k)l=\pi$. For

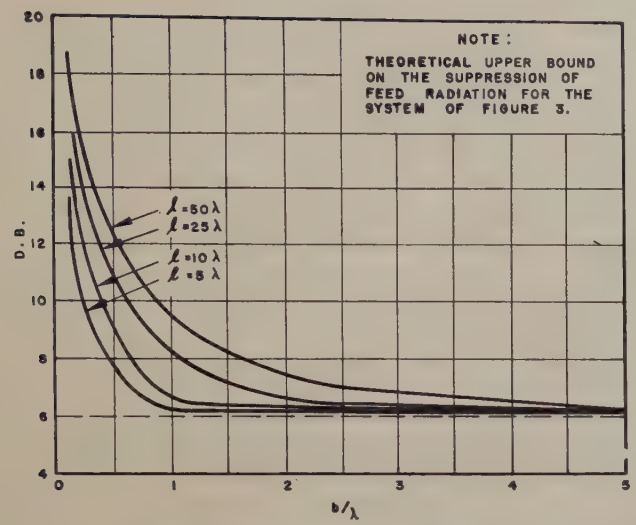

Fig. 4—Feed suppression in db.

comparison, the theoretical patterns for the corrugated surface alone, and for the surface plus feed with $\psi = O$, π are plotted. It is seen that the case $\psi = O$ corresponds most closely to experiment. Thus it is wise to use the Hansen-Woodyard relation even when the feed radiation is considered, for the phasing is then proper to provide additional beam sharpening. This will also be seen to be true in the presence of finite ground planes.

The Effect of a Finite Ground Plane

Thus far the corrugated surface has been assumed to be terminated by an infinite ground plane which permits the use of the image principle and greatly simplifies the analysis. A reasonable approximation to the pattern for the case of a finite ground plane can be obtained by assuming the dominant mode to be present over the corrugations and by assuming the same current distribution to exist in the finite ground plane as would exist in the same portion of an infinite ground plane.

For the case of no ground plane at all, this implies the radiation pattern arises essentially from the double sheet (24) and (25). (We assume feed radiation is sufficiently suppressed as to be only a minor perturbation on results following.) This radiation pattern is given by

$$H_z = -(\alpha_o^s + jk\sin\theta)\frac{\omega\epsilon l A}{4\alpha_o^s}\sqrt{\frac{2}{\pi k\rho_o}}\,e^{j(\omega t - k\rho_o + \pi/4)} \cdot \frac{\sin\frac{\pi l}{\lambda}\left[\frac{\beta_o^s}{k} - \cos\theta\right]}{\frac{\pi l}{\lambda}\cdot\left[\frac{\beta_o^s}{k} - \cos\theta\right]}; \qquad 0 < \theta < \pi \tag{39}$$

and is an approximation which is valid only for $(\beta_o^s - k)l$ small. A plot of (39) is characterized by a main beam tilted up from the endfire position and slightly broadened with respect to the infinite ground plane case. These results are consistent with experiment. The tilt angle of the main beam is given by

$$\frac{\tan\frac{\pi l}{\lambda}\left[\frac{\beta_o^s}{k} - \cos\theta_T\right]}{\frac{\pi l}{\lambda}\cdot\left[\frac{\beta_o^s}{k} - \cos\theta_T\right]} = 1 + \frac{k}{\beta_o^s}\cos\theta_T. \tag{40}$$

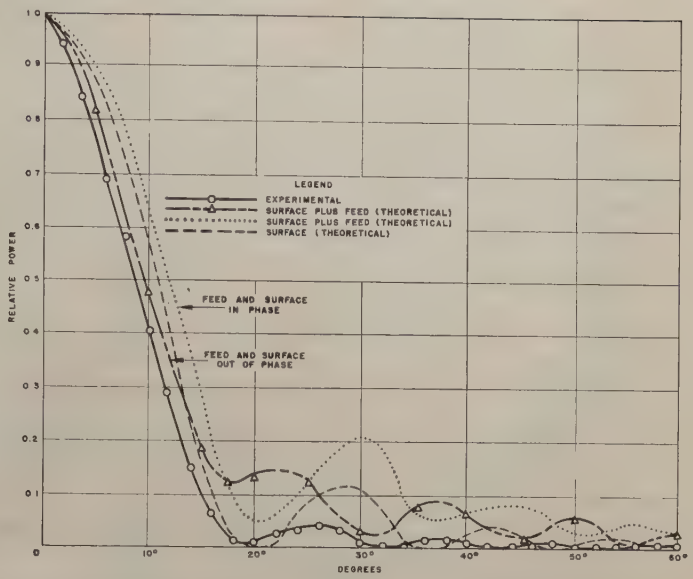

Fig. 5—Theoretical and experimental radiation patterns for a corrugated surface of length 7.33λ excited by a waveguide.

This tilt angle is a decreasing function of β_o^s/k for all lengths l and thus has an upper bound for $\beta_o^s/k = 1$. This is fortunate, for the approximation is most accurate for this minimum value of β_o^s/k. A plot of the upper bound is shown in Fig. 6, on following page.

To see what happens as ground plane is added, we first must find the current distribution in the infinite ground plane. Using the source system (28), we find

$$J_x = H_z = -\frac{\omega\epsilon A}{2}e^{j\omega t}\int_{-l/2}^{l/2} H_o^{(2)}[k(x-x')]e^{-j\beta_o^s x'}dx' \qquad \frac{l}{2} \leqq x < \infty. \tag{41}$$

This may be converted to

$$J_x = -\frac{\omega\epsilon A}{2k}e^{j(\omega t - \beta_o^s x)}\int_{k(x-l/2)}^{k(x+l/2)} H_o^{(2)}(u)e^{j(\beta_o^s/k)u}du \tag{42}$$

in which $u = k(x - x')$. When the Hansen-Woodyard relation, $(\beta_o^s - k)l = \pi$, is satisfied, the phase change of the integrand of (42) over the interval $k(x - l/2) \leqq u \leqq k(x + l/2)$ is approximately π radians for all x. Thus the integrated error accruing from the substitution

$$H_o^{(2)}(u) = \sqrt{\frac{2}{\pi u}}\,e^{-iu}e^{j(\pi/4)} \tag{43}$$

is negligible for all x in the range

$$\frac{\lambda}{2} \leqq x - \frac{l}{2} < \infty. \tag{44}$$

Then

$$J_x = -\frac{\omega\epsilon A}{k\sqrt{2\pi}}e^{j(\omega t - \beta_o^s x + \pi/4)}\int_{k(x-l/2)}^{k(x+l/2)}\frac{e^{j(\beta_o^s/k - 1)u}}{\sqrt{u}}du \qquad \frac{l}{2} + \frac{\lambda}{2} \leqq x < \infty. \tag{45}$$

Equation (45) may be solved in terms of Fresnel integrals through the substitution

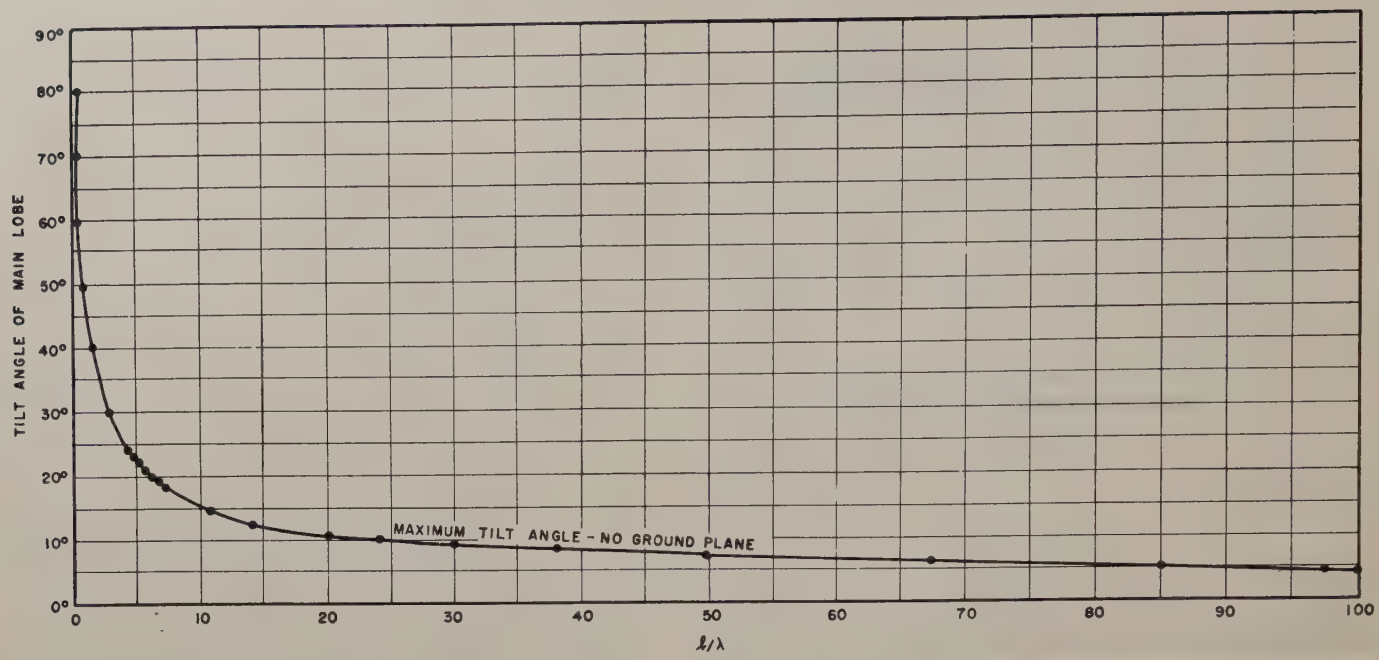

Fig. 6—Theoretical upper bound on the main beam-tilt angle for the radiation pattern of a flat corrugated surface with no ground plane.

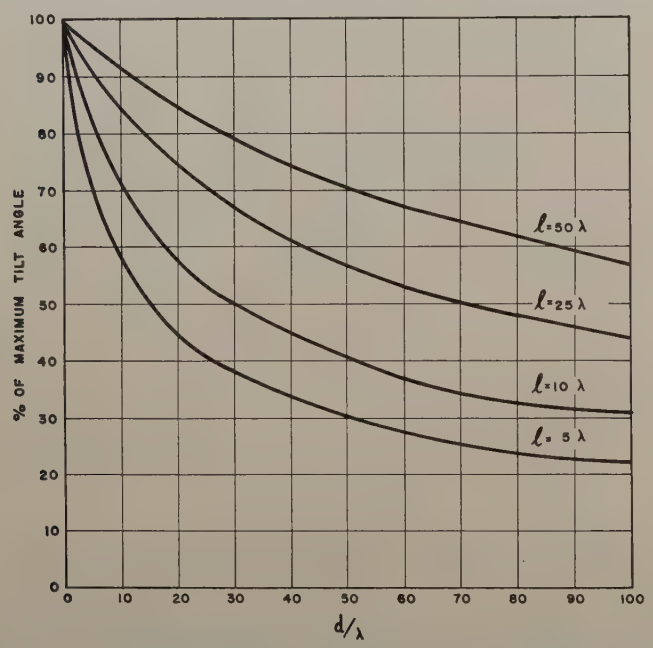

Fig. 7—Theoretical upper bound on the main beam-tilt angle of the radiation pattern for a flat corrugated surface as a function of the lengths of the surface and its ground plane.

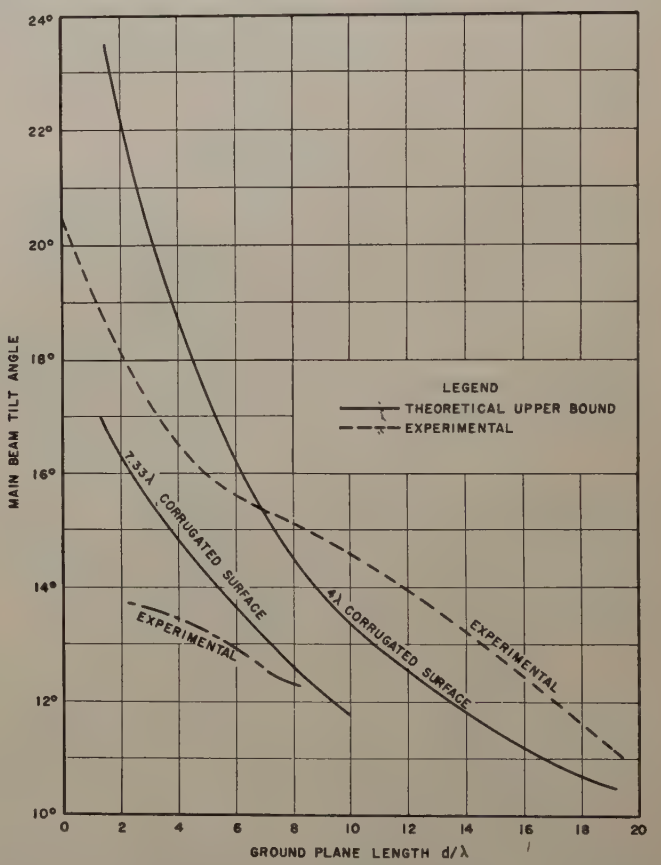

Fig. 8—Comparison between theory and experiment for two corrgugated surfaces obeying the Hansen-Woodyard relation, one 7.33λ long and the other 4λ long.

$$\sqrt{\frac{\pi}{2}}\,v = \sqrt{\left(\frac{\beta_o{}^s}{k} - 1\right)}u \tag{46}$$

with the result

$$J_x = -\frac{\omega\epsilon A}{\sqrt{k(\beta_o{}^s - k)}} \cdot e^{j(\omega t - \beta_o{}^s x + \pi/4)}\left[C(v) + jS(v)\right]_{\sqrt{2(\beta_o{}^s - k)}\,x - \pi}^{\sqrt{2(\beta_o{}^s - k)}\,x + \pi}$$

$$\frac{l}{2} + \frac{\lambda}{2} \leqq x < \infty. \tag{47}$$

Since the value of J_x is also known at $x = l/2$, the current distribution in the intervening half-wavelength can be inferred by extrapolation. Equation (47) indicates that for a given x, the current density is a decreasing function of $\beta_o{}^s/k$. Thus for a finite ground plane of length d, with the assumed current distribution (47), the larger the value of $\beta_o{}^s/k$, the smaller the end disturbance and the smaller the tilt angle. Therefore the tilt angle is a decreasing function of d for all $\beta_o{}^s/k$, with the rate of decrease least for $\beta_o{}^s/k = 1$. But for the case $\beta_o{}^s/k = 1$, the corrugated surface of length l, and its ground plane of

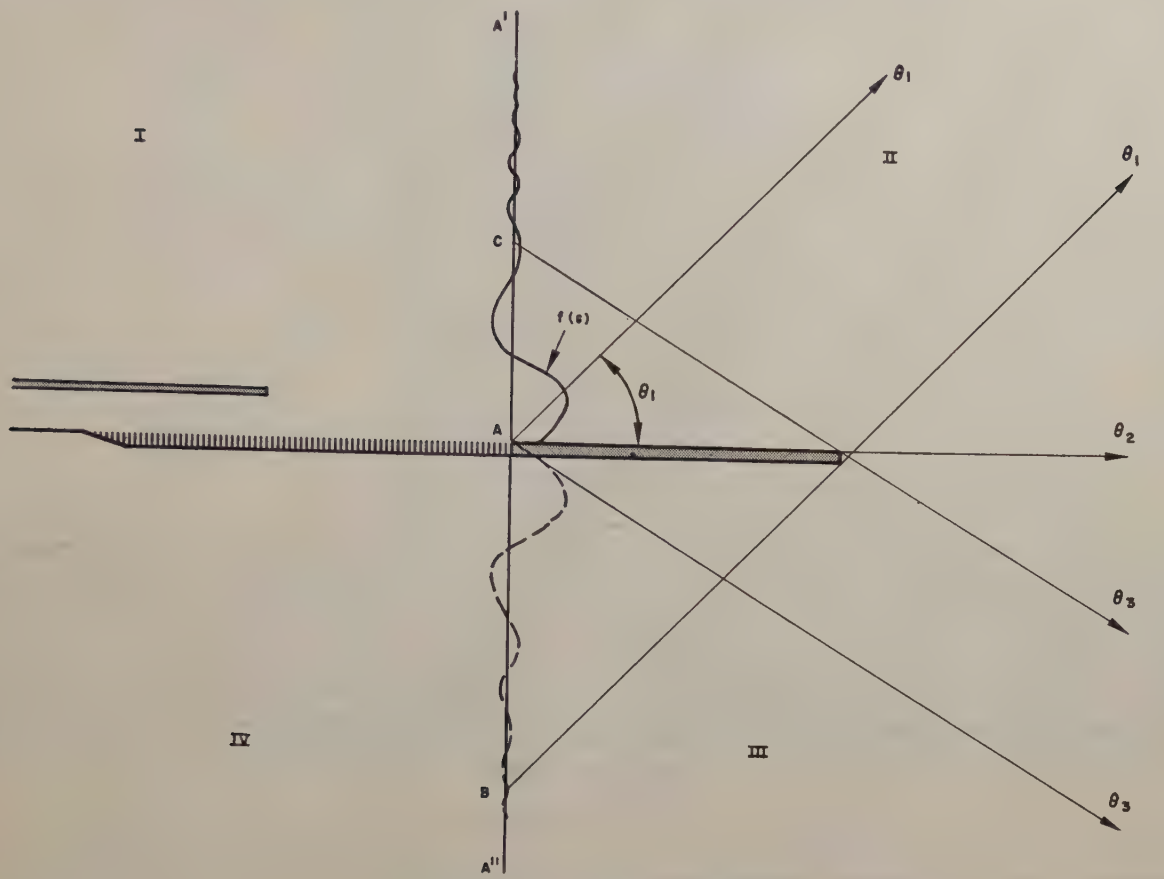

Fig. 9—Geometrical optics formulation.

length d are electrically indistinguishable, and Fig. 6 becomes the upper bound when $(l+d)/\lambda$ is substituted for l/λ as the abscissa scale. This information can be plotted in an alternative way as shown in Fig. 7, left.

To check this theory, a series of ground planes of length 0λ to 19λ were added to a 4λ corrugated surface and the tilt angles measured. In a second experiment, ground planes ranging from 2λ to 8λ were attached to a 7.33λ corrugated surface and the measurements repeated. The results are shown in Fig. 8, page 78. The agreement with theory is fair, with the greatest departure occurring for long ground planes.

A satisfactory picture of the general nature of the four-quadrant radiation pattern can be gleaned from a geometrical optics argument.

Referring to Fig. 9, (shown above) if we neglect the feed radiation and assume that the current distribution in the ground plane does not radiate in the backward direction, the radiation field along the half-plane $A-A'$ is given by (39) and if this field is terminated by the proper double sheet the radiation field in quadrants II, III, and IV is approximately determined by this double sheet in the presence of the ground plane as an obstacle. The amplitude distribution of the source system along $A-A'$ is suggested by the curve $f(s)$ and serves to explain many of the features of the pattern.

For an angle θ_1 in quadrant II, the radiation is computed from the sources along $A-A'$ plus the image sources from B to A. As θ_1 approaches 90 degrees, the radiation approaches the value computed for an infinite ground plane, and throughout quadrant I we assume that the radiation pattern does correspond to this infinite case. As θ_1 approaches 0 degrees, fewer of the image sources contribute, and in the position θ_2, the field strength is down to one-half the value found for the infinite case. At any angle θ_1, the radiation approaches more nearly to the infinite case as the ground plane is lengthened.

For an angle θ_3 in quadrant III, only the sources from C to A' contribute and as θ_3 approaches -90 degrees, field decreases to zero, oscillating slightly as changing source system phases in and out. Under this geometrical argument, no energy is found in quadrant IV.

Using the above model, a sketchy picture of the radiation pattern may be synthesized as follows: For the lengths l and d of surface and ground plane being considered, determine from Figs. 6 and 7 the approximate tilt angle, θ_T, of the main beam. Use the field distribution (31) for the region $\theta_T \leqq \theta \leqq 180$ degrees, assuming the null positions are undisturbed. For the region -90 degrees $\leqq \theta \leqq \theta_T$ sketch in a smoothly decreasing field approximately 6 db down at $\theta = 0$ degrees. Result for a 7.33λ surface with a $\frac{1}{2}\lambda$ ground plane is in Fig. 10, page 80. This pattern agrees in its general shape with measured patterns, two examples of which are given in Fig. 11, on page 81.

Beamwidth

The geometrical optics picture just outlined suggests that for a corrugated surface of given length "l," as the ground plane length "d" is increased, the main beam not

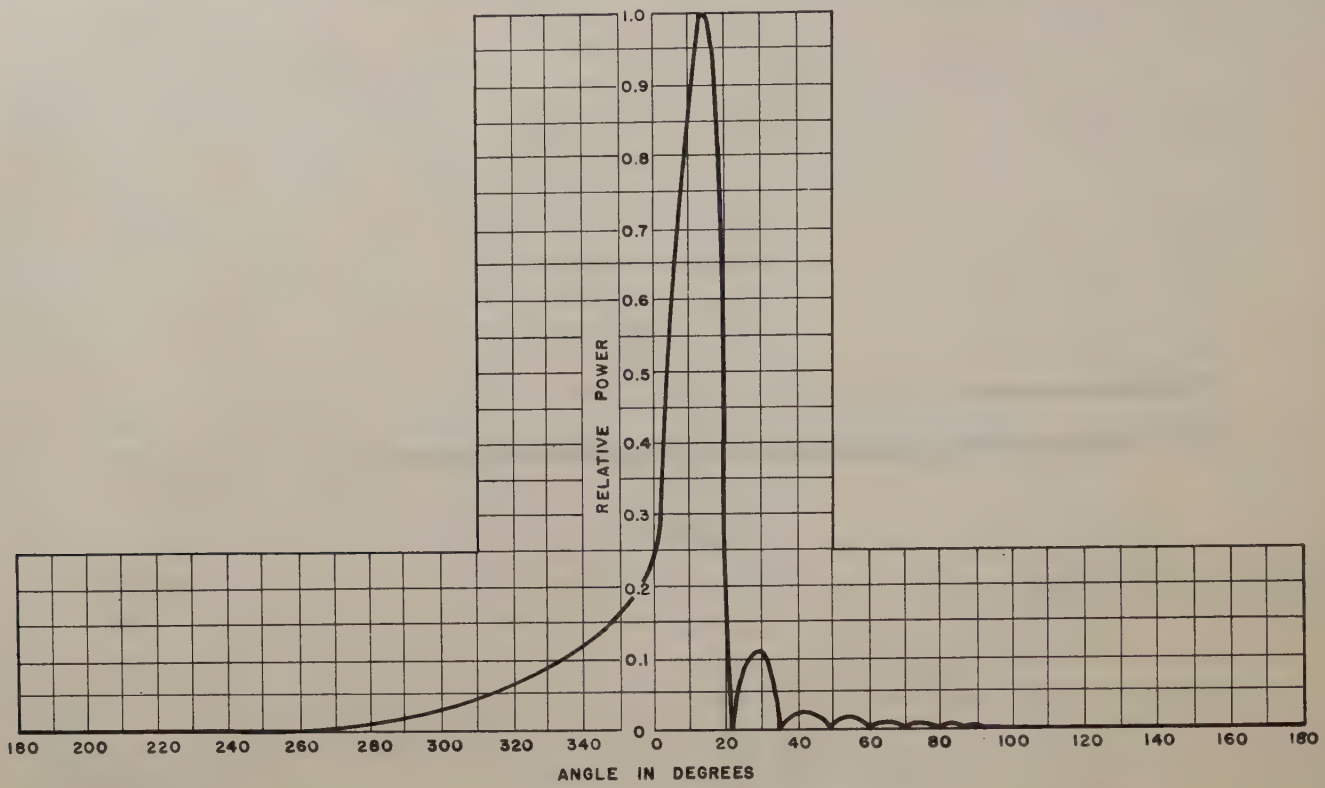

Fig. 10—Empirical radiation pattern for a 7.33λ corrugated surface with a λ/2 ground plane.

only tilts down closer to the plane, but the beamwidth narrows, approaching the infinite plane value as a limit. Plotted in Fig. 12, on following page, are the results of beamwidth measurements for a 7.33λ surface and a variety of ground planes. As can be observed, the pattern actually narrows as the endfire position is approached.

A lower bound on the beamwidth can thus be found from (31). A plot of this lower bound as a function of $1/\lambda$ is shown in Fig. 13 for $(\beta_o{}^s - k)l = \pi$ on the following page.

The Effect of Finite Tooth Width

We have already observed that unless the teeth are extremely narrow, the dominant mode cannot adequately satisfy (16) and (17) and that the wider the teeth, the more the higher order modes are excited. Referring to (4), if there are twenty corrugations per wavelength,

$$\frac{\beta_1}{k} \cong 21, \quad \frac{\beta_2}{k} \cong 41, \quad \text{etc.} \tag{48}$$

and if these modes are excited, they will have radiation patterns expressed in the form of (39), with appropriate substitutions for α, β, and A. The factor

$$(\alpha_n{}^s + jk \sin \theta) \tag{49}$$

is practically insensitive to θ. The factor

$$\frac{\sin \frac{\pi l}{\lambda}\left[\frac{\beta_n{}^s}{k} - \cos\theta\right]}{\frac{\pi l}{\lambda}\left[\frac{\beta_n{}^s}{k} - \cos\theta\right]} \tag{50}$$

gives essentially the same pattern for all higher modes, i.e., $2l/\lambda$ equal lobes with the nulls occurring at different angles for different modes. The fields of these higher modes will have phase relationships which depend on the complex constants A_n.

An effort was made to excite these modes by constructing a corrugated surface with twenty teeth per wavelength and teeth three times as wide as the gaps. Its radiation pattern was compared with that of a similar surface in which the gaps were three times as wide as the teeth. The slot depths of the two surfaces differed by the amount necessary to establish the same value of $\beta_o{}^s/k$, a value chosen to satisfy the Hansen-Woodyard relation. Two typical patterns are shown for comparison in Fig. 11. No essential differences were observed. Though not reported here, this experiment was performed over a range of frequencies, for several ground plane lengths, including an effectively "infinite" ground plane, and for tooth width/gap width ratios of 3:1, 1:1, and 1:3. In no case were there any significant differences in the patterns. The conclusion appears that the higher order modes are excited when the teeth are wide but that their amplitudes are comparable and phases random so that their net effect on the radiation pattern is small.

It should be emphasized that this does not mean that the effect of the presence of higher order modes is negligible when the corrugated surface is being used as a transmission line. In that case, the impedance concept is vastly complicated by their presence and it would seem advisable to use narrow teeth in an effort to obtain an uncontaminated dominant mode.

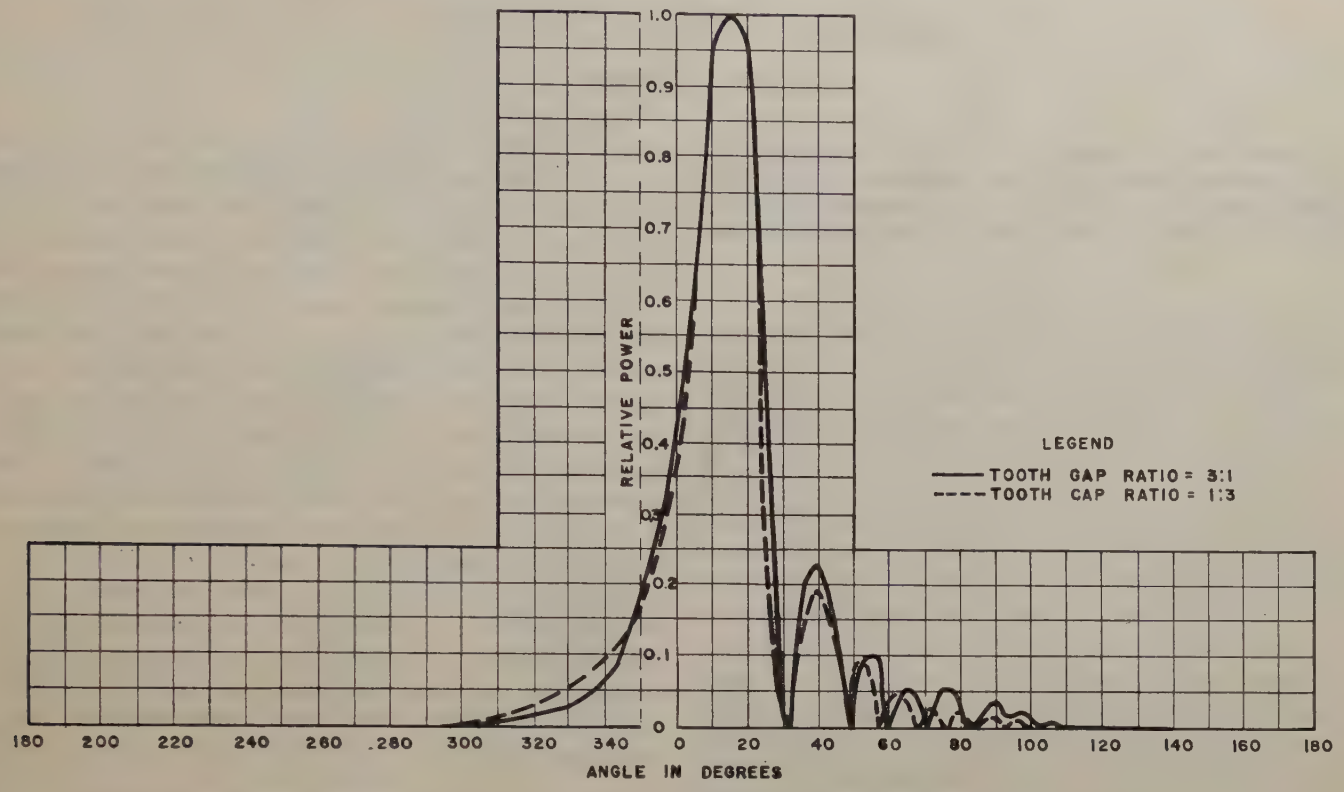

Fig. 11—Experimental radiation patterns for two corrugated surfaces 7.33λ long, one having a tooth to gap ratio of 3:1 and the other a tooth to gap ratio of 1:3, each terminated by a λ/2 ground plane.

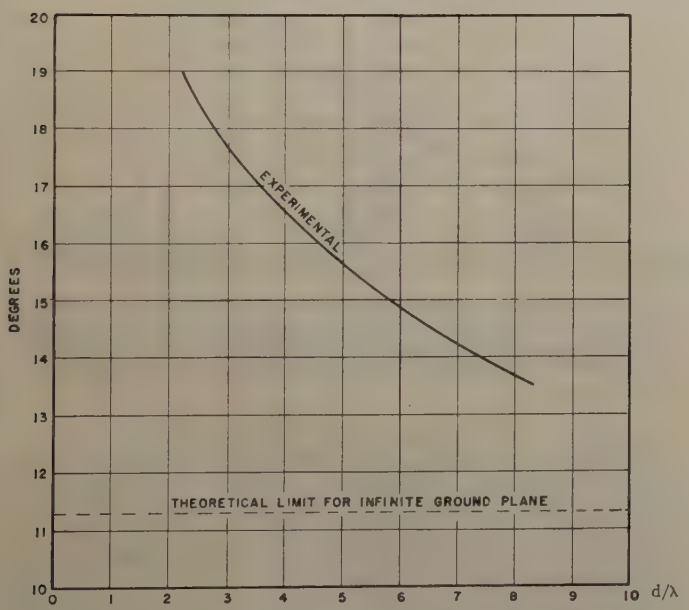

Fig. 12—Beamwidth versus ground plane length for a 7.33λ corrugated surface.

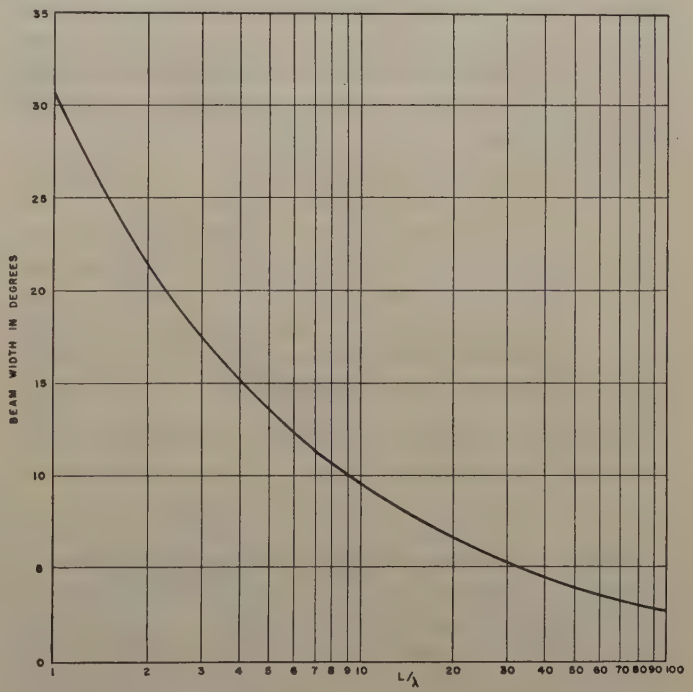

Fig. 13—Theoretical lower bound on beamwidth as a function of length of corrugated surface when Hansen-Woodyard relation is obeyed.

Conclusions

The analysis of a flat corrugated surface appears to be strengthened by a Floquet-Lucke method of field determination. Consideration of feed radiation gives better correlation between theory and experiment. Effect of a finite ground plane can be explained approximately by classic assumption of current distribution. Effect of finite tooth width, though it complicates transmission line analysis, apparently has no influence on radiation pattern when corrugated surface is used as an antenna.

Acknowledgment

The author is indebted to I. K. Williams for many stimulating discussions, Mrs. A. Cordova who did most of the computations, and E. N. Rodda who assisted in the experiments and the preparation of this report.

Meteoric Radio Echoes*

LAURENCE A. MANNING†

Summary—**Study of meteoric effects by radio methods has resulted in gain to three fields—astronomy, upper atmosphere physics, and radio propagation. In each of these fields progress is surveyed, and some of the more important unsolved problems are pointed out.**

Introduction

METEORS have been seen for centuries, photographed for decades. Only since World War II have they been extensively studied by radio echo methods. In these past few years, though, the rate at which facts have been gathered about meteoric effects has been the greatest in history. It is already time to appraise how far we have gone, and to ask what has been neglected in our haste. This paper, then, is a summary of progress in radio meteoric detection; but it tries to be more—it tries to classify work done to date, so as to make evident what is yet undone.

Meteoric studies can be placed in one of three groups. In group one are studies of the meteoric particles, treated as astronomical bodies; size, mass, velocity, orbit, composition are unknown. In group two are studies of the upper atmosphere; meteors are tools used to tickle the air, excite a response. In group three are studies of the influence of meteoric reflections on the propagation of radio signals. As a guide to the discussions which follow, we may list under these three groups the main fields of past and foreseeable future interest to the radio worker:

(a) Astronomical properties of meteors—1. Radiants. 2. Velocities. 3. Size and rate of arrival.

(b) Meteoric effects as a tool in finding atmospheric properties—1. Ion production, diffusion, recombination, composition. 2. Winds.

(c) Meteoric contributions to propagation—1. Obliquely propagated high frequency signals. 2. Ambient ionization and low frequency reflections.

In each of the fields above, some work has been done. How much?

Study of Meteoric Radiants

Meteoric radiants are found using only the simplest property of meteoric ionization trails—their shape. A typical meteor leaves a trail of ionization along its path that is about 25 kilometers long and but a few meters in diameter. Pierce, working at Harvard, was the first to point out that the very small ratio of diameter to length of these trails requires that a normal from the observatory strike the ionized part of the path, if a strong echo is to be received.[1] The reason for this behavior may be seen from the geometry of Fig. 1. The circular arcs of the figure represent equiphase surfaces of the incident wave. Assume that the surfaces are one-quarter of a wavelength apart; energy returned to the transmitter from point P_0 will clearly differ in phase by one-half cycle from that returned from P_1, but be in phase again with that from P_2, P_4, P_{2n}, etc. The part of the trail from P_{-1} to P_1 is called the first Fresnel zone. It is longer and returns a stronger signal than does the part from P_1 to P_2, or any of the higher order zones. Since the phase of signals returned from the higher zones alternates in sign, their contributions largely annul themselves. It is only when the first zone (centered about the normal reflection point) is ionized, that a strong signal is returned; conversely the presence of a reflected signal is an indication of normal reflection in the high majority of cases. The main exceptions occur for large meteors, and the lower frequencies; they seem to go with ionization distributed in other than the usual linear model.

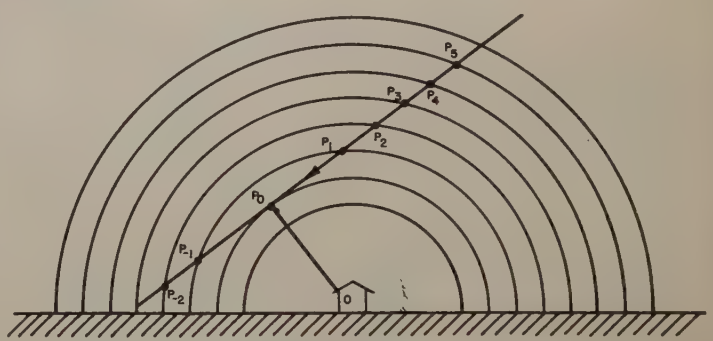

Fig. 1—The normal reflection condition for a meteoric ionization column. The circular arcs represent spherical wavefronts spaced by one-quarter wavelength. The scale is of course exaggerated; the first Fresnel zone $P_{-1}-P_1$ should be only about 1 per cent of the range OP_0.

A number of ways have been developed to use the normal reflection property in finding radiants. As is indicated in Fig. 2, it is assumed that an echo will occur only when the reflection point is within a height region of relatively narrow bounds. Let h_1 and h_2 be those bounds. The intersection of the plane p perpendicular to the radiant direction, with the region between heights h_1 and h_2, is drawn as the vertical hatched band in the plan view of the figure. All reflection points must lie in this band for a given radiant position, and so the position and orientation of this band serve to fix the coordinates of the radiant.

Clegg has made use of the localization of the reflecting regions to find radiants by setting up a highly directive antenna beam.[2] This beam is shown in the plan view of

* Manuscript received by PGAP, September 24, 1953. Jointly supported by the U. S. Army Signal Corps, the U. S. Air Force, and the U. S. Navy (Office of Naval Research).

† Electronics Research Lab., Dept. of Electrical Engineering, Stanford Univ., Stanford, Calif.

[1] J. A. Pierce, "Abnormal ionization in the *E*-region of the ionosphere," Proc. I.R.E., vol. 26, pp. 892–902; 1938.

[2] J. A. Clegg, "Determination of meteor radiants by observation of radio echoes from meteor trails," *Phil. Mag.*, vol. 39, pp. 577–594; 1948.

Fig. 2. Over a span of time, earth rotation causes a change in radiant direction, and so of the position of the reflection point band. By measuring range to that part of the band in the beam *versus* time, Clegg is able to locate the meteoric radiants. He has reported precision of about two degrees in the description of radiant direction. Comparable beam widths are not needed in the directive antennas.

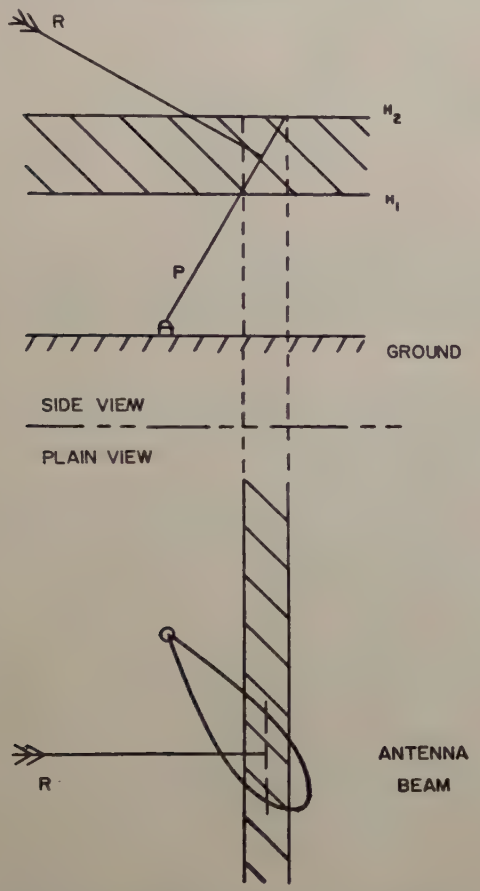

Fig. 2—The location of reflection points for meteors of radiant R. Ionization is assumed formed only between heights H_1 and H_2. The reflection point must lie in the plane P perpendicular to the trail direction.

It is clear that many other arrangements of antenna beams could be used to get the same result—the location of the band of possible reflection points. For example, an automatic scanning direction finder has been used in conjunction with range information at Stanford; in this way the position of the band can be plotted directly, without awaiting earth rotation. Variations of these techniques have been used by other workers.[3]

The methods of radiant determination which have been described have one main drawback; they are based upon analysis of a large number of meteoric echoes. Attempts have also been made to find radiants of single meteors by radio methods. The writer suggested the use of a triangulation technique in an early discussion of the problem.[4] In this way, it was shown that if the ranges and relative times of echo arrival were determined for three ground stations, the perpendicularity of the reflection process could be used to locate both the direction in space from which the particle came, and the point on the ground met by the extension of the trail. The differences in echo starting times are a measure of the relative distances along the trail to the intersections of the normal rays from the observing stations; this follows because a strong echo is not received until ionization is created at the perpendicular point. Application of the technique has been made by Millman and McKinley, but with the use of range-time plots to determine when the particle and its wake of ionization reach the nearest (the normal) point on the trail.[5] The triangulation technique has the disadvantage, in addition to the need for three isolated installations, of a relatively low rate of coincident meteor detection. There are not many orientations of a line 25 km long and 100 km in altitude which permit a normal from each of three stations separated the order of 40 km.

At present it seems that the most promising lines for future development of methods for finding the radiants of single meteors lie in the utilization of either fading or polarization effects. The use of fading properties would depend on the observed fact that certain trails break up, causing an uneven reflection coefficient along the length of the column. The simple Fresnel theory does not then apply; wind drift causes the signals of irregular strength scattered from parts of the trail of different range to beat together to form a fluctuating received signal. It can be shown that under certain conditions, by noting the phase of the fading envelope at three stations separated a kilometer or so apart, the horizontal projection of the trail direction can be obtained. In combination with horizontal and vertical elevation angle recording, it may be possible to use this effect for radiant fixes. The use of polarization properties for finding radiants also shows promise. The signals reflected when the transmitted electric field vectors are parallel and perpendicular to the trail are not equal during the early phase of an echo. Fig. 3 shows the amplitudes ob-

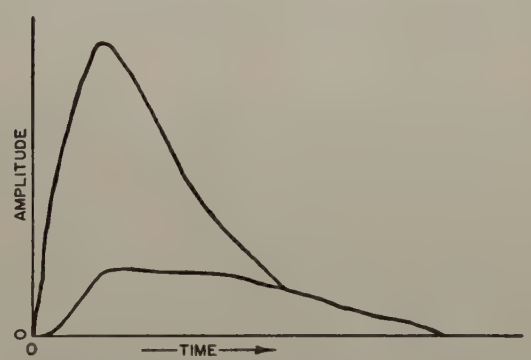

Fig. 3—Reflected signal strength versus time for the two characteristic polarizations of a typical meteor echo, observed on 23.1 mc at Stanford University by Van Valkenberg, using the two helix technique.

[3] J. S. Hey and G. D. Stewart, "Derivation of meteor stream radiants by radio reflection methods," *Nature*, vol. 158, p. 481; 1946.

[4] L. A. Manning, "The theory of the radio detection of meteors," *Jour. Appl. Phy.*, vol. 19, pp. 689–699; 1948.

[5] P. M. Millman and D. W. R. McKinley, "Three-station radar and visual triangulation of meteors," *Sky and Telescope*, vol. 8, p. 114; 1949.

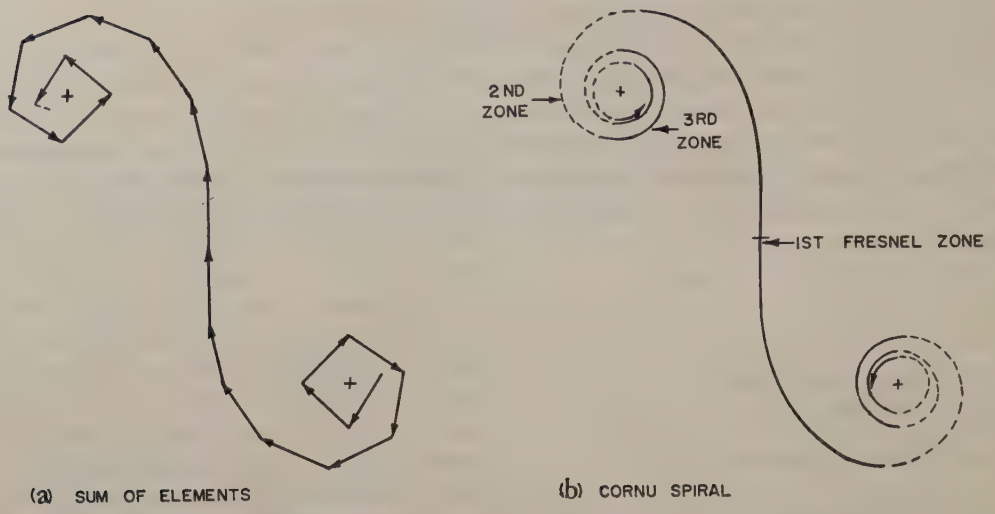

Fig. 4—The way in which the vector signals returned from the successive elementary lengths of the trail combine at the receiver: (a) Each vector represents the signal returned from a unit length of the trail; the phase of the vector depends upon the two-way path-length from the element to the receiver; (b) As the element length approaches zero, a Cornu spiral is obtained in the limit. Arc length corresponds to trail length.

served for the two polarization components of a typical echo. Again in combination with directional information, the polarization effect may be useful for finding individual radiants. However phase shifts may exist between the parallel and perpendicular reflection coefficients; the direction of the major axis of the reflection coefficient ellipse would then be skewed with respect to the trail. This effect would need to be looked into.[6,7]

Study of Meteoric Velocities

Three ways of measuring velocities are of importance. In order of their usefulness, they are—1. The Doppler meteor-whistle technique; 2. The diffraction technique; and 3. The change of range technique. All three methods are based upon the same properties of the ionization columns. In each case it is assumed that the ionization is created at once upon the arrival of the meteor. Thus, at any moment during the formation of the trail the ionization exists along a half-infinite line.

In the change of range technique, the slant range to the nearest part of the ionization column is plotted *versus* time during the column formation.[8] From analysis of the observed hyperbolic relationship velocity is deduced.[9] The main trouble is the small percentage of echoes for which it is possible to follow the range variation very far from the perpendicular reflection point. When the trail is in formation, only the short weakly reflecting high order Fresnel zones are effective. To get enough range difference to resolve the hyperbolic constants, the echo must be observed for a long period of time, with the resulting high order Fresnel zones and weak echoes. Associated with the small rate of detection of usable meteors is a relatively low accuracy on all except the largest echoes.

The Doppler whistle and the diffraction techniques are very close cousins theoretically.[10] However, they involve different observing techniques, and lead to rather different sensitivities and accuracies. It will be well to analyze them both from the same general viewpoint. Consider the trail to be divided into many elements of differential length. Assume also a uniform and not too dense ionization distribution along the trail. Then each of the elemental lengths of trail will return a component of reflected signal. It may be described by a vector with magnitude proportional to the length of the element, and with a relative phase determined by its position in one of the Fresnel zones. The total signal strength returned from the trail at any time during its formation is then found by adding up the vectors corresponding to each element of trail, all in correct phase relation. In Fig. 4(a) the manner in which these elementary signals add up is shown. Fig. 4(b) shows the theoretical Cornu spiral which is obtained by letting the length of the elements approach zero. In Fig. 5(a) is shown the way in which the amplitude of the reflected signal vector increases with time. The oscillation of amplitude following the initial build-up is the "diffraction fluctuation" utilized to measure velocity in the diffraction technique.[11] As can be seen by comparing Figs. 4 and 5, the period of the fluctuations is related to the rate at which the trail is formed beyond the perpendicular point, and corresponds to the revolutions in the upper turns of the Cornu spiral.

In the Doppler meteor-whistle technique, a fixed sig-

[6] J. A. Clegg and R. L. Closs, "Plasma oscillations in meteor trails," *Phil. Mag.*, vol. 39, p. 577; 1948.

[7] M. E. Van Valkenburg, "Polarization and Fading Studies of Meteoric Echoes," Ph.D. Dissertation, Stanford Univ., Stanford, Calif.; 1952.

[8] J. S. Hey, "The Giacobinid meteor shower, 1946," *Nature*, vol. 159, pp. 119-121; 1947.

[9] D. W. R. McKinley and P. M. Millman, "Determination of the elements of meteor paths from radar observations," *Canad. Jour. Res.*, vol. A27, p. 53; 1949.

[10] L. A. Manning, O. G. Villard, Jr., and A. M. Peterson, "Double Doppler study of meteoric echoes," *Jour. Geophys. Res.*, vol. 57, pp. 387–403; 1952.

[11] C. D. Ellyett and J. G. Davies, "Velocity of meteors measured by diffraction of radio waves from trails during formation," *Nature*, vol. 161, pp. 596–597; 1948.

nal of large amplitude is added to the received signal, so that a large signal is in the receiver at all times.[12] When an echo is received with a beating voltage present, it is possible to identify both spiral arms of Fig. 4(b) as an amplitude fluctuation. The first oscillation is used the most in the Doppler system. Among the merits of this method note that cross-correlation or coherent detection is naturally used, thereby improving the weak signal sensitivity.

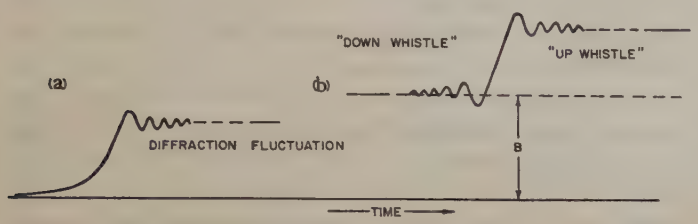

Fig. 5—The theoretical variation of received signal strength during trail formation. In (b) a beating voltage of magnitude B has been added to the returned signal of (a).

Ellyett and Davies first described the diffraction technique for velocity determination.[11] Following a suggestion of Herlofson they were the first to recognize the importance of the Fresnel approach. The observation of the Doppler effect had been made many years before by Chamanlal and Venkatamaran.[13] It was later independently noted by Villard.[14] The first theoretical treatments of the Doppler whistles were by Appleton and Naismith[15] and by Manning.[4] Later Manning, Villard, and Peterson verified the accuracy of the technique experimentally, using the Perseid shower as a source of meteors of known velocity.[12] McKinley has measured the velocities of thousands of meteors by the Doppler method. He firmly established the usefulness of the technique by showing that no appreciable fraction of radio meteors have velocities corresponding to hyperbolic orbits.[16] They are therefore members of our own solar system.

In addition to higher sensitivity, the Doppler technique has an advantage accruing from the experimental observation that the diffraction fluctuation of many observed meteor echoes is weaker, and contains fewer cycles, than the preceding "down" whistle. As many as three or four hundred cycles of down-whistle oscillation have been recorded; the up-whistle or "diffraction effect" rarely can be followed so long. The explanation of this effect has never been properly sought, although it is known that the ratio of down- to up-whistle amplitude increases with echo size.

[12] L. A. Manning, O. G. Villard, Jr., and A. M. Peterson, "Radio Doppler investigation of meteoric heights and velocities," *Jour. Appl. Phys.*, vol. 20, pp. 475–479; 1949.
[13] C. Chamanlal and K. Venkatamaran, "Whistling meteors—Doppler effect produced by meteors entering the ionosphere," *Electrotechnics*, vol. 14, p. 28; 1941.
[14] O. G. Villard, Jr., "Listening in on the stars," *QST*, vol. 30, p. 59; January, 1946.
[15] E. V. Appleton and R. Naismith, "The radio detection of meteors and applied phenomena," *Proc. Phys. Soc.*, vol. 59, p. 461; 1947.
[16] D. W. R. McKinley, "Meteor velocities determined by radio observations," *Astrophys. Jour.*, vol. 113, pp. 225–267; 1951.

The Rates of Meteoric Arrival

To the astronomer, the rate of occurrence and distribution in size of meteoric particles is of great importance. But it is not as easy to count meteors of a given size as it is to measure speed or direction. The trouble is twofold: observed counts are less than the true rate because of aspect, range and other effects; particle size can be found from echo amplitude or duration only with the aid of very shaky theory.

In his 1938 paper,[1] Pierce made an important contribution to the theory of meteor counting. Based upon the aspect sensitivity inherent in his normal reflection hypothesis, he was able to show that only a fraction of those meteors entering the atmosphere within normally detectable ranges (from a random radiant) would actually be detected. For example, trails directed straight at the observer do not have a normal for reflection within the 80–120 km height range, and so will not usually give an echo. Manning extended Pierce's calculations to the case of shower meteors from point radiants.[4] The same type of effect occurs; commonly the observed meteor count using nondirective antennas may be only 10 per cent of the true rate of arrival. It is therefore necessary to correct the observed rate. The actual size of the correction is hard to fix, since it depends on such usually unknown quantities as radiant distribution and trail length. Manning, Villard and Peterson have evolved a method for getting values of trail length; if applied more generally it would reduce some of the uncertainty.[17] If the rate is to be found for shower meteors from a known radiant, directive antennas may be used. Range data will then reduce much of the uncertainty about the fraction detected in the most favored direction.

Harder yet is the association of a known particle mass with a given echo. It is only quite recently that a sound theory of radio reflections from meteoric ionization trails has been available, from which even the relationship between ionization production and echo strength could be reliably inferred.[18] No reliable theory is yet available to relate meteoric mass and ionization production. When such a theory is at hand, however, it seems certain that radio methods will be able to augment with precision the existing knowledge, particularly with respect to the distributions of the smaller meteoric masses.

Processes in the Ionization Trail

Meteors are of use in finding the physical properties of the upper atmosphere because they produce a transient increase in ionization; the resulting time response of the medium may be easily observed. The details of the ionizing process are not understood; however, the way in which the ionization is distributed about the

[17] L. A. Manning, O. G. Villard, Jr., and A. M. Peterson, "The length of ionized meteor trails," *Trans. Amer. Geophys. Union*, vol. 34, pp. 16–21; 1953.
[18] V. R. Eshleman, "The Mechanism of Radio Reflections from Meteoric Ionization," Ph.D. Dissertation, Stanford Univ., Stanford, Calif.; 1952.

meteoric path, and the type of reflection which then results, are subjects that are finally yielding to experiment and analysis. The early ideas about the amount of ionization were those of Skellet[19] and of Pierce.[20] They postulated that the ionization surrounding the meteoric path extended, at least in the case of large meteors, to radial distances of up to a kilometer. These ideas of size were based in part on analogy with the glowing trains which are sometimes seen visually and telescopically.[21] Justification for the amount of ionization was given by assuming that nearly all of the energy of the meteor went to ionize the surrounding air. Most experiments at high frequencies are not consistent with the assumption of columns of the breadth assumed in the early work. Perhaps at the frequencies of 3.5 mc or so used by Pierce it may be possible to detect low ionization densities at such great radii; it is certainly unsafe to assume on the basis of present evidence that those meteors with large diameter glowing trains may not also exhibit ionization columns of comparable size.[22]

The contrary tack was taken by the investigators at the University of Manchester. In reviewing the theory of meteoric ionization, Herlofson was led to estimate that the energy available for the production of ionization would be of the order of 10^{-4} of the total available kinetic energy.[23] On the basis of these figures, and assuming the ionized molecules were those of atmospheric air, he gave a tentative estimate of the relationship between visual meteoric magnitude and line density of ionization along the trail. A 6th magnitude meteor was assumed to produce 10^{10} electrons per centimeter of path, and a +1 magnitude meteor 10^{12} electrons per cm. The electron densities resulting from Herlofson's estimate are so low that an incident wave will not be appreciably attenuated by the charges; the received signal strength is that caused by Thompson scattering of the individual electrons in the trail. A scattering formula expressing these relations was given by Lovell and Clegg who used it to estimate electron densities from received signal strengths.[24] They reported a confirmation of the electron density-magnitude relations predicted by Herlofson, but it appears that something was wrong with the results. More recent signal strength measurements, both of the Manchester and Stanford groups have shown that the electron densities are many orders of magnitude greater than those given by Lovell and his co-workers.[18,25] It now seems that the experiments of Lovell were in error. In addition it seems that the tentative estimates of Herlofson, with which the experiments were purported to be in agreement, were based on rather a weak foundation. They should be revised using further knowledge of the processes involved.

What we now know of the structure of meteoric ionization columns depends on combined inference from polarization, reflected signal strength, and duration data. Polarization studies show unequal reflection coefficients for parallel and transverse polarization during the early part of the echo, as in Fig. 3. No polarization effect is ordinarily observed at the end of the echo. Two ways of measuring polarization have been used. Clegg and Closs transmitted energy with the electric field both parallel and perpendicular to the trails of shower meteors of known orientations, and measured the two reflection coefficients directly.[6] Van Valkenberg of the Stanford group employed circularly polarized transmitting and receiving antennas and measured the ellipticity of the received echo when the trail was excited with circular polarization.[7] The method used at Manchester has the advantage of identifying the two polarizations with the trail axis; the method employed at Stanford enables the relative magnitudes of the reflected polarized components to be found for meteors of unknown orientation.

Herlofson was the first to suggest that the cause of the polarization effect was a plasma resonance phenomenon;[26] the resonance takes place when a trail with dielectric constant about minus one is excited crosswise. The high electron concentration required to support plasma resonance is a first clue to the state of the trail. A second is that the breadth of the trail must be small in wavelengths for plasma resonance to occur; otherwise the time lag across the column results in out-of-phase excitation of the effect.

A general theory for the reflection of radio waves from meteoric ionization may well start with the assumption that the ionization is initially confined within a radial region whose scale is determined by the mean free path of the air—10 cm or so. If the ionization is assumed formed either of air by collision, or of meteoric molecules, such a distribution would be expected on theoretical grounds. The values of the mean free path are consistent with the small size demanded for the polarization effect. Both Kaiser and Closs,[27] and Eshleman[18] have worked out the reflection coefficient to be expected from such a column, assuming an initial Gaussian distribution of ionization, and subsequent growth of the trail by diffusion. Fig. 6 shows how a Gaussian distribution expands due to diffusion alone. Eshleman has considered the effect on the column growth of a number of values of recombination coefficient, as well as of diffu-

[19] A. M. Skellet, "The ionizing effects of meteors," PROC. I.R.E., vol. 23, pp. 132–149; 1935.
[20] J. A. Pierce, "A note on ionization by meteors," *Phys. Rev.*, vol. 59, pp. 625–626; 1941.
[21] C. C. Trowbridge, "Physical nature of meteor trains," *Astrophys. Jour.*, vol. 26, pp. 95–116; 1907.
[22] E. W. Allen, Jr., "Reflection of very-high-frequency radio waves from meteor ionization," PROC. I.R.E., vol. 36, pp. 346–353; 1948. (See also discussion of this paper by L. A. Manning and O. G. Villard, Jr., PROC. I.R.E., vol. 36, pp. 1255–1257; 1948.)
[23] J. Herlofson, "The theory of meteor ionization," *Phys. Soc. Rep. Prog., Phys.*, vol. 11, pp. 444–454; 1948.
[24] A. C. B. Lovell and J. A. Clegg, "Characteristics of radio echoes from meteor trails: I. The intensity of the radio reflections and electron density in the trails," *Proc. Phys. Soc. A*, vol. 60, p. 491; 1948.
[25] J. R. Greenhow and G. S. Hawkins, "Ionizing and luminous efficiencies of meteors," *Nature*, vol. 170, pp. 355–357; 1952.
[26] N. Herlofson, *Observatory*, vol. 68, p. 230; 1948.
[27] T. R. Kaiser and R. L. Closs, "Theory of radio reflections from meteor trails: I," *Phil. Mag.*, vol. 43, p. 1; 1952.

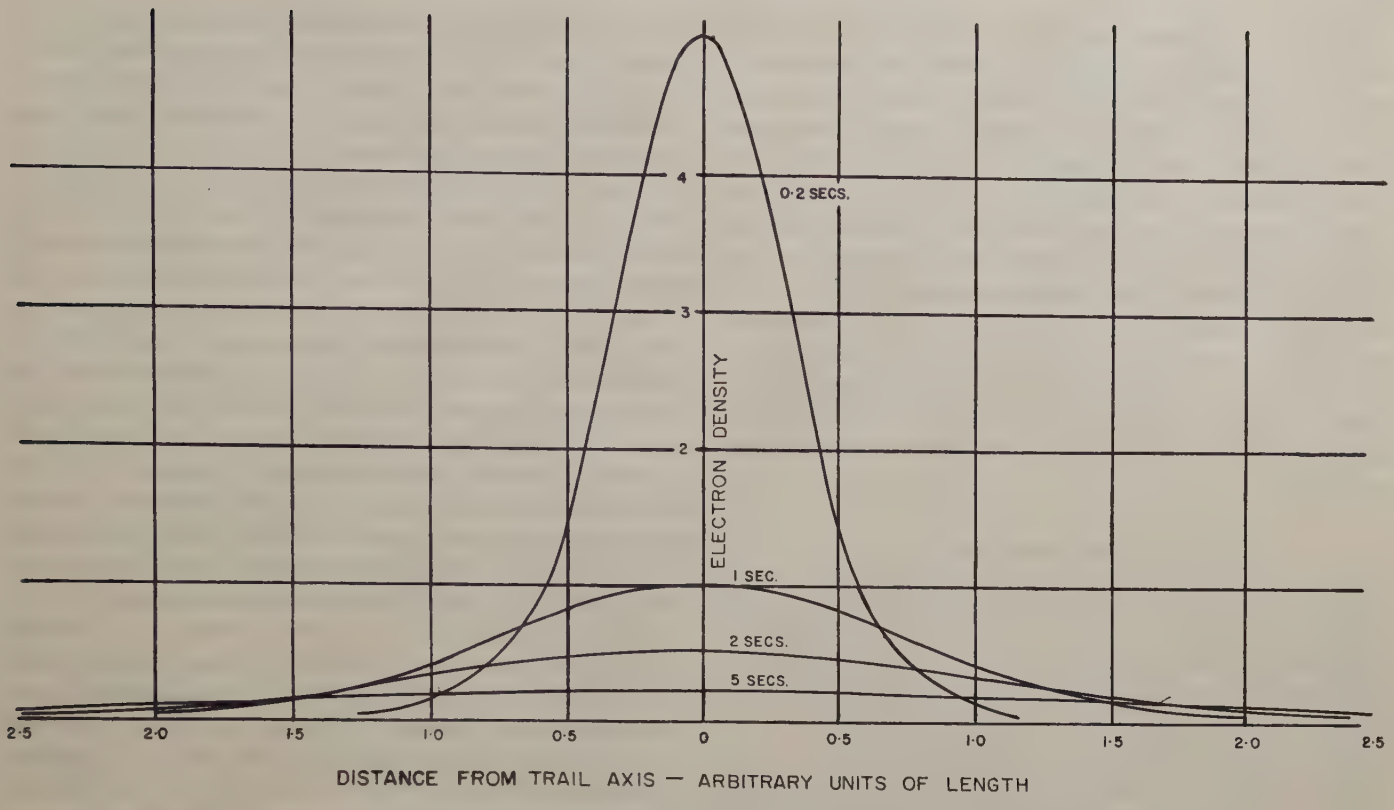

Fig. 6—The effect of diffusion upon an initially Gaussian distribution of electrons. When first formed, most of the ionization is found within 10 cm or so of the axis.

sion coefficient. In both cases the calculations were carried out by finding approximate expressions valid in limited size and line density regions. Feinstein[28] and Herlofson[29] had both previously considered the small radius low density trail, but they were misled by Lovell's erroneous experimental results into believing that no need existed for a theory involving greater line densities. Herlofson was able to show that in the low density region, where no more than 10^{12} electrons exist per cm of path, the echo strength would decay exponentially, with a time constant determined by the value of the diffusion coefficient and the square of the wavelength. Such a behavior agrees with the observed characteristics of many meteor echoes. The mean rate of decay of echo strength suggests a diffusion coefficient of about 3 meters^2 per second for the heights near 95 kilometers. At Stanford for frequencies of 6 to 30 mc, and elsewhere for higher frequencies, the dependence of echo duration on the square of the wavelength has been checked.

Not all radio reflections have roughly exponential rates of signal strength decay; some show greatly increased durations and slow loss of signal strength (but with violent fading). It has long been realized that the great durations could be explained by large meteors with great ionization productions, if only recombination effects could be neglected. However, it has also long been recognized that the recombination coefficient of 10^{-8} cm^{-3} sec^{-1} which is appropriate for the *E*-region would quickly reduce even an infinite initial electron density to a very low value; the increased durations would no longer be possible.[30] Computation of the reflections from large highly ionized trails has been carried out by assuming that the trails are equivalent to metallic cylinders; their radius is equal to the radius at which the dielectric constant of the actual trail is zero. As has been shown by Kaiser and Closs, and by Eshleman, the behavior of the echoes computed in this way is quite consistent with the observed phenomena of radio reflection if recombination is small, and neglecting for the present the fading effects.

When recombination is included, Eshleman has shown in detail the effect of variation of recombination coefficient upon line density.[18] From his results it follows that the maximum coefficient consistent with the longer duration echoes is of the order 10^{-10} cm^{-3} sec^{-1}. Since the *E*-region recombinaton coefficient is 100 times greater than this, it may be supposed either that as suggested by Eshleman, the greatly increased temperature along the trail reduces the recombination coefficient of air during the initial expansion, or else that in meteoric columns it is not mainly the oxygen which is ionized. The latter possibility is of especial interest. The resulting recombination coefficient would be determined by the meteoric elements, and since we don't know what their coefficients are, we may speculate that they are

[28] J. Feinstein, "The interpretation of radar echoes from meteor trails," *Jour. Geophys. Res.*, vol. 56, p. 37; 1951.

[29] N. Herlofson, "Plasma resonance in ionospheric irregularities," *Arkiv för Fysik*, vol. 3, p. 247; 1951.

[30] J. Feinstein, "On the nature of the decay of a meteor trail," *Proc. Phys. Soc. B*, vol. 65, p. 741; 1952.

suitably low, at least for some constituents. Note that it is found spectroscopically that the lines observed in meteoric light are not those of air; indeed, concentrations of ionized calcium in particular are known to exist in roughly adequate amounts.[31]

Assumption of the ionization of meteoric molecules with lower energies of ionization than air may remove much of the difficulty in reconciling the kinetic energy of the particle with the fraction thereof which can be turned to ionization. There are amply enough molecules of meteoric material to supply the observed electron densities. It is clearly of great importance that experiments be devised to actually measure recombination in meteor trails, and to discover the nature of the ionized particles.

Wind Measurements

It is in the study of upper atmosphere winds that meteoric ionization trails are most nearly describable as tools used in the process of research. For purposes of wind measurement the ionization may be looked at as being a marker which makes it possible to follow the motions of the air in which it is imbedded.

The principal means of investigating wind motions makes use of a Doppler frequency shift called the "body Doppler",[32] it occurs after the down-whistle and diffraction fluctuation sketched in Fig. 5. Unlike the variable frequency and high pitched meteor whistle which ushers in the formation of a new trail, the body Doppler is of a low and constant frequency for the duration of the echo. Five cycles per second is a typical frequency on a 20 Mc carrier. By scaling the value of the body Doppler shift, it is possible to find the radial velocity component of the wind drift for a particular trail. It is necessary, as Manning, Villard, and Peterson described in the original paper,[32] to have a sense indicator which will indicate whether the motion of the reflector is toward or away from the observer, if maximum use is to be made of the effect.

With the aid of the body Doppler shift, it is possible to find several quantities descriptive of the wind. The speed and direction of the average translation of the air mass, including a vertical component if present, is one such quantity. This measure of the vector average of the individual motions which exist in a region will clearly be less than the peak wind speed found at any point or in any stratified layer included within the region. Another descriptive quantity is the root-mean-square wind speed for both horizontal and vertical components, as averaged over a height region.[33] This rms speed is a good measure of the rapidity with which the air is blowing, since air motions in different directions do not cancel in producing the final result.

Average winds are found by a sampling technique; the radial velocity component is measured for a large number of echoes distributed in azimuth about the observatory. In those directions from which the average wind is coming, the average radial velocity component will be towards the observer, and conversely in the opposite directions. By plotting the average Doppler shift *versus* the azimuthal direction from which the meteors are received a sine relationship is found, marred only by randon sampling errors. Careful statistical analysis shows that the amplitude and phase of the sine variation may be used to compute the magnitude and direction of the average wind with good accuracy. A sample of several hundred meteors must be employed; one or two hours of recording generally suffice to obtain a sample of this size if sensitive equipment is used in the vicinity of 20 mc. Velocities found by this means typically are of the order of 25 mc, when averaged for several consecutive hours over the 80–120 km height range. Great variability occurs in both the magnitude and direction of the velocity. Average vertical drift is no greater than 3 mc as observed at Stanford, and may be nonexistent.

Root-mean-square winds are best found by plotting the average square of measured radial velocity components versus the quantity $(h/R)^2$, where h is the height of the reflector, and R is its slant range. As has been shown by Manning, Peterson, and Villard,[34] when plotted in this way the resulting curve is straight, and a regression line is easily fitted. The rms horizontal and vertical velocities are then found as the $(h/R)^2=0$ and 1 ordinates. Experimental observations need only be taken in the middle range of elevation angles, not overhead or on the horizon. Typical horizontal rms velocities determined in this way are 50 mc; they exhibit much less variability than do the mean vector winds, which appear to be averages between large and opposing motions The vertical rms velocities are much less than the horizontal velocities. They are certainly less than 20 mc on ordinary occasions, and quite possibly much smaller. The resolution of the measurements has not been increased enough to give a more accurate answer.

One of the great advantages of the meteoric method for finding velocities is that the motions of discrete marked patches of air are examined. On theoretical grounds it has been concluded that there is little possibility that the ionization does not move with the air at meteoric heights. The collision frequencies for both electrons and ions are above their gyro-frequencies for most of the meteoric region. It is sufficient, however, that the ionic collision frequency be well above the ionic gyro-frequency in the region in order that the geomag-

[31] P. M. Millman, "Meteoric ionization," *Jour. R. Astr. Soc. Canad.*, vol. 44, pp. 209–220; 1950.

[32] L. A. Manning, O. G. Villard, Jr., and A. M. Peterson, "Meteoric echo study of upper atmosphere winds," Proc. I.R.E., vol. 38, pp. 877–883; 1950.

[33] L. A. Manning, "Recent advances in the study of ionospheric winds," *Bull. Amer. Met. Soc.* (in press), 1954.

[34] L. A. Manning, A. M. Peterson, and O. G. Villard, Jr., "Ionospheric Wind Analysis by Meteoric Echo Techniques," Tech. Rep. No. 60, Electronics Res. Lab., Stanford Univ., Stanford, Calif. *Jour. of Geophys. Res.* (in press).

netic field be unable to affect drift of the ionization with the wind. It may be noted here that in the related problem of the effect of the earth's magnetic field on the coefficient of diffusion, again no effect is anticipated. In the literature there is a supposed demonstration of such a variation of diffusion coefficient,[35] but close attention to the theory shows that the plotted results do not have the predicted form. Attempts to verify the effect have been made by McKinley, and by the Stanford group without success.

Further development of the Doppler method of wind measurement may well take advantage of the definite positions of meteoric reflectors in order to delineate the variations which exist in wind structure with height. The method has been adopted by Huxley's group in Adelaide, Australia; winds are being recorded automatically, with complete height information accompanying each record. From such work valuable results concerning the stratification of wind layers, and the variation of tidal motions with height, may be expected.

In addition to those simply described meteoric reflections which exhibit a single Doppler shifted spectral component, there are many received echoes which consist of two or more reflected waves. Beating of the separate frequency components causes them to fade in amplitude. It has been shown by Manning, Villard, and Peterson that analysis of these signals may advantageously be carried out by use of a "double Doppler" vector echo presentation.[10] By treating the received signal as a vector, spectrum analysis can be achieved by a process of double Fourier analysis of two Doppler channels in which the beating voltages differ by ninety degrees. In the case of the fading echoes, the fading rate is governed by the difference frequency between independent spectral components. To the extent that all spectral components are caused by different wind motions at separate points along the trail, analysis of fading rates can be used to find the difference in wind velocity between neighboring reflecting regions.[36] Investigations at Stanford have revealed in addition that in some cases it is possible to determine the displacement along the trail between the reflecting centers by noting the phase difference between the fading envelopes detected at separate ground stations. Analysis of fading characteristics to determine wind gradients suffers from the danger that some of the fading may not be caused by wind motions at all. Feinstein has shown that for sufficiently abruptly bounded electron distributions in an expanding trail, fading may occur as a result of a kind of beating of the waves scattered from the near and far boundaries of the column.[28] Eshleman has shown that such a fading effect can occur without introducing an unduly great increase in the rate of decay of echo amplitude from its maximum value.[18] In a number of cases meteoric echoes are found to fade with two independent and well defined fading rates, the lower frequency fading envelope limiting the amplitude of the faster fluctuations. It taxes one's credulity to believe that all echoes of this nature result from four discrete spectral components caused by wind motion, and neatly paired in amplitude. Further investigation of the reality of the Feinstein type of fading is definitely required.

[35] A. C. B. Lovell, "Meteoric ionization and ionospheric abnormalities," *The Phys. Soc.*, (reports on progress in physics), vol. 11, pp. 415–444; 1948.

[36] J. S. Greenhow, "A radio echo method for the investigation of atmospheric winds at altitudes of 80 to 100 km," *Jour. Atmos. Terr. Phys.*, vol. 2, pp. 282–291; 1952.

The Contribution of Meteors to Obliquely Propagated High Frequency Signals

Very little consideration had been given until recently to the possible use of meteoric reflections for the transmission of signals over an oblique path. Even the changes in the reflection characteristics exhibited at obliquely incidence by individual trails had received very little attention. One of the earliest studies of this problem was undertaken by Allen,[22] who recorded the bursts of signal strength received from very-high-frequency FM stations over an extended path. He noted the existence at times of received signal strengths for which the radius of the equivalent metallic reflector must have been several hundred meters. More recently, the problem has been attacked theoretically by Eshleman and Manning,[37] and experimentally by Villard, Peterson, Manning, and Eshleman.[38] The results of both theory and experiment indicate that meteors should not be neglected in considering possible transmission mechanisms at frequencies above the normal layer criticals.

The predominant effect of obliquity upon the nature of the reflected signal is to increase the echo duration by what may be a large ratio as compared with back reflection. In the case of back scattering, the factor which normally limits the echo duration is the phase opposition of energy scattered from electrons situated across the breadth of the trail. As the trail expands as a result of diffusion, the phase opposition becomes more and more pronounced, and the returned signal dies out. In the case of oblique reflection, the same process applies, but the geometry is now such that a separation of sec ϕ times that necessary in the back scatter case produces the same phase cancellation; ϕ is half the forward scattering angle. The effect upon phase cancellation is as though the wavelength of the incident wave were reduced by the factor cos ϕ. Since it has been demonstrated experimentally that the echo duration is proportional to the square of the effective wavelength, it follows that the effect of obliquity upon echo duration goes as the square of the secant of half the forward

[37] V. R. Eshleman and L. A. Manning, "Radio Communication by Scattering from Meteoric Ionization," Tech. Rep. No. 57, Electronics Res. Lab., Stanford Univ., Stanford,Calif. Proc. I.R.E., vol. 42, pp. 530–536; March, 1954.

[38] O. G. Villard, Jr., A. M. Peterson, L. A. Manning, and V. R. Eshleman, "Extended-range Radio Transmission by Oblique Reflection from Meteoric Ionization," Tech. Rep. No. 55, Electronics Res. Lab., Stanford Univ., Stanford, Calif.; *Jour. Geophys. Res.*, vol. 58, pp. 83–93; 1953.

scattering angle. This duration increase factor can quite easily be as large as ten or twenty times for meteors situated near the middle of a path of one or two thousand kilometers.

In assessing the importance of meteors to obliquely propagated signals, it is necessary to consider also the total number of meteors in the reflection process. Over an oblique path, a large area is available within which meteors may fall and produce usable signals. The same limitations as in the back scattering case apply to the fraction of meteors whose aspect is correct to reflect an echo to a given receiver. Although the total fraction of meteors effective for oblique transmission is not especially different from that for back reflection, the fraction effective is a marked function of the part of the region between the transmitter and the receiver in which the meteor falls. Since the duration increase factor is also a function of position, detailed consideration is needed in order to demonstrate the total magnitude of the integrated signal strength effect at the receiver. Also important in assessing the quality of meteor propagated signals is the probability that there will be at least one trail so situated as to propagate a signal at a given time. Statistical considerations based upon the above concepts lead to the conclusion that at frequencies of the order of 20 mc, meteoric signals will be present over an oblique path a very large fraction of the time. Experimental study of such paths has shown that useful signals are indeed present as a result of meteoric action in this frequency range. At the very high frequencies, however, it is doubtful that meteoric effects alone are capable of supporting a useful transmission.

The Contribution of Meteors to the Ambient Ionization of the *E*-Region

Theoretical study of the contribution of meteors to the ambient ionization level of the *E*-region is hampered by lack of accurate information on the correct value of recombination coefficient to be applied to meteoric ionization, and on the total number of electrons generated by meteors in the various magnitude ranges. It seems very improbable that the recombination coefficient for meteoric ionization could be greater than $10^{-8}/cm^3$ sec, and if molecules of meteoric matter are ionized, the recombination coefficient may be much smaller. Assume the largest reasonable value of recombination coefficient, and make very rough assumptions concerning the total number of electrons generated in the region; then we may estimate that an ambient level corresponding to a critical frequency of the order of several hundred kilocycles might result. With what we now know of recombination any such calculation will be crude, and has never been carried through with care. Nevertheless, meteoric effects clearly are of importance to low frequency propagation. In this field, it is important that further studies be made, but they will need to be based upon better knowledge of the numerical values of the constants involved in the ionization and recombination processes.

Conclusions

Since the first serious study of the subject was undertaken, the radio detection of meteors has made important contributions to our knowledge in the fields of meteoric astronomy, upper atmosphere physics, and radio propagation. The application of radio methods to find the orbital constants of the meteoric particles has been very successful. There is still much which needs to be done before an adequate knowledge of the size distribution of meteoric particles is available. Study of meteoric echoes has yielded dividends in the understanding of the nature of the atmosphere, and of its reaction to suddenly applied charge. An important problem remains in relation to the recombination coefficient applicable to meteoric ionization; is it that for air, or that applicable to the meteoric particles?

Of great value has been the use of meteoric techniques in the study of wind motions in the upper atmosphere. In this field important and detailed results can be obtained. With the aid of height finding apparatus, one may investigate the structure of the wind in height, and determine many statistical properties characteristic of its behavior.

Only recently have meteors been considered extensively from the point of view of their utility for communication purposes. It is found that at the high frequencies meteors can support useful transmissions at times when regular layer transmission is absent. However, in some situations the meteoric signals are unwanted, and constitute interference. Very little has yet been done to investigate the amount of ambient ionization below the *E*-region which is caused by meteors. It is to be hoped that future study will serve to resolve the remaining problems which have arisen in meteoric research, and to pose many new ones as well.

Acknowledgment

This paper is based upon a talk given by the writer at the Geophysical Institute of the University of Alaska, and at the Third Alaskan Science Conference. It was prepared in draft form while he was a guest of the Institute in October, 1952.

INSTITUTIONAL LISTINGS

The IRE Professional Group on Antennas and Propagation is grateful for the assistance given by the firms listed below, and invites application for Institutional Listing from other firms interested in the field of Antennas and Propagation.

THE GABRIEL LABORATORIES, 135 Crescent Road, Needham Heights, Massachusetts
Research and Design of Antenna Equipment for the Workshop Assoc. and Ward Products Div. of the Gabriel Co.

HUGHES AIRCRAFT COMPANY, Culver City, California
Research, Development, Manufacture: Radar, Guided Missiles, Tubes, Systems, Solid State Physics, Computers.

MARYLAND ELECTRONIC MANUFACTURING CORPORATION, College Park, Maryland
Antenna and System Development and Production for Civil and Military Requirements.

POLYTECHNIC RESEARCH AND DEVELOPMENT COMPANY, INC., 55 Johnson Street, Brooklyn 1, New Yo
Microwave Precision Test Equipment—Design, Development, Production.

WHEELER LABORATORIES, INC., 122 Cutter Mill Road, Great Neck, New York
Consulting Services, Research and Development, Microwave Antennas and Waveguide Components.

The charge for an Institutional Listing is $25.00 per issue or $75.00 for four consecutive issues. Application for listing may be made to the Technical Secretary, The Institute of Radio Engineers, 1 East 79th Street, New York 21, New York.